

Improving Energy Efficiency and Reducing Carbon Footprint for Lighting in Controlled Environment Agriculture

MPhil Thesis

Gulce Onbasili

Supervisors: Prof Simon Pearson & Prof Chris Bingham

Funded by the AHDB



Department of Engineering

University of Lincoln

UK

10.2021

Declaration

I confirm that this is my own work and any use of material from other sources has been fully acknowledged throughout.

- Gulce Onbasili

Acknowledgements

Firstly I would like to thank my supervisors Professor Simon Pearson and Professor Chris Bingham for assisting me in completing this research. Secondly, I would like to thank the AHDB for funding this research and sponsoring me to attend various beneficial events. I would also like to thank Keiri (Winnie) Swan from the University of Reading and Professor Leo Marcelis from Wageningen University & Research for giving me a tour of their respective greenhouse facilities.

I would also like to thank the people I worked beside at the University of Lincoln campus for their support and encouragement, particularly: Hadrien Dufour, Yangyan (Sally) Gao, Liana Cechladze, Dan Stones and Samuel Cruz Manzo. Finally I would like to thank my friends and family for their support throughout my studies.

Abstract

Artificial lighting for agriculture is a rapidly developing field, with energy efficiency and cost limiting widespread implementation. LEDs are the most efficient source of artificial lighting, allowing customisation of wavelength to suit plant responses. This project firstly conducts experiments to demonstrate the impact of six different LED wavebands at fixed input energy on the growth of Little Gem lettuce. These results are then combined with data from the literature, to create a large data-set from which a neural network model is developed to attempt to predict optimal plant spectral light recipes.

Secondly, a case study is conducted, looking at the setup and energy consumption of an LED lit strawberry greenhouse. Areas to increase efficiency are identified, these include opportunities to deploy specific LED devices, different optimal spectral recipes, adjusting LED efficacy with different electrical currents and evaluating energy saving from daylight dimming. Multiple strategies are assessed giving a combined total estimated energy saving of 47%; whilst maintaining constant photosynthetic photon flux density (PPFD) received by the plant.

Thirdly, we examined how LED modules in plant growth facilities supplied by AC grids could be driven through primary DC grids, since an increasing number of DC appliances and integrated DC renewable sources has put emphasis on research of DC grids, especially at local scales where loads are mainly DC. With AC grid supply, every appliance must have a double stage AC-DC and DC-DC conversion for the rating of the device, which decreases electrical efficiency. This project therefore outlines a proposed DC system setup for LED plant growth facilities, arguing that there would be increased energy efficiency when converting AC to DC at the whole plant power supply level; supplying LED modules with DC electricity.

Fourthly a primary disadvantage of controlled environment agriculture (CEA) is the high energy consumption, which carries a considerable carbon footprint. If renewable energy technologies could be integrated into CEA systems, they could become more sustainable and potentially cost saving. This project therefore investigates renewables for artificially lit greenhouses. The renewable technologies assessed include solar, wind, batteries and bio-fuel CHP. The HOMER software is used

to investigate feasibility for both small and large modelled systems to reduce carbon footprint and cost. Simulation results show a grid connected system with wind and solar installed to be the best option for a small system considering cost and emissions, offering an 11% saving on NPC and 61% saving on CO₂ emissions. For larger systems, wind energy becomes dominant, with a grid connected wind turbine system being the overall favourable setup, offering a 22% saving on NPC and a 34% saving on CO₂ emissions for a one hectare system, and offering a 32% saving on NPC and 39% saving on CO₂ emissions for a two hectare system. Lastly, biomass CHP systems are simulated with consideration of heating and cooling alongside lighting.

In summary this thesis has shown that there is considerable opportunity to optimise the efficiency of LED systems for horticulture, not just by changing spectral light output quality but also by optimising the **the** power system.

Contents

1	Introduction	1
1.1	Literature Review & Background	2
1.1.1	Lighting and LEDs	2
1.1.2	Plant Physiology	12
1.2	Research Aims	18
1.3	Hypothesis	19
2	Growing Little Gem Lettuce Under Different LED Light Spectra	21
2.1	Introduction	21
2.2	Setup & Methodology	21
2.2.1	LED Product Selection	21
2.2.2	Board Designing, Building and Heat Testing	22
2.2.3	Experimental Setup	24
2.2.4	Methodology and Measurement	26
2.3	Results & Discussion	27
2.3.1	Light Data Analysis	27
2.3.2	Lettuce Growth	36
2.3.3	Possible Experimental Improvements	44
2.4	Section Summary	46
3	Neural Network Analysis on LED Lighting for Lettuce	47
3.1	Introduction	47
3.2	Methodology	48
3.2.1	Neural Networks	48
3.2.2	Lettuce Data Collection	51
3.2.3	Normalising and Randomising the Data	54
3.3	Results & Discussion	57
3.4	Section Summary	59
4	A Holistic Approach to Power Saving in LED CEA Systems	60
4.1	Introduction	60

4.2	Case Study Methodology	60
4.3	Savings from Choice of Efficient LED Devices	62
4.4	Running LEDs at Lower Current	65
4.5	Energy Tariff Considerations	68
4.5.1	Systems with Solely Artificial Lighting	68
4.6	Dimming Artificial Lights with Sunlight	71
4.7	Section Summary	76
5	Power Distribution to Lighting Setup - DC vs. AC	78
5.1	Introduction	78
5.2	DC Grids Review	78
5.3	Using DC Supply for LED Lighting Setup in CEA	81
5.4	Conversion Losses and Cabling Losses	83
5.5	Design of Buck Converter and Rectifier	87
5.5.1	Calculation of Power Losses	89
5.6	Section Summary	92
6	Modelling Renewable Technology Integration into LED lit CEA Systems	93
6.1	Introduction	93
6.1.1	HOMER Software	93
6.1.2	Biofuel & CHP	94
6.2	Methodology	95
6.2.1	HOMER Software	95
6.2.2	System Setup	99
6.3	Results & Discussion	101
6.3.1	University of Reading System Model	101
6.3.2	One Hectare System	105
6.3.3	Two Hectare System	111
6.3.4	Biomass CHP Incorporation	113
6.4	Section Summary	119
7	Concluding Remarks & Future Work	121
7.1	Summary	121

7.2	Future Work	124
8	References	126
A	Appendix	139
A.1	Neural Networks	139
A.2	Power Distribution to Lighting Setup - DC vs. AC	140
A.3	Modelling Renewable Technology Integration into LED lit CEA systems	145

List of Abbreviations

LED - Light Emitting Diode

PAR - Photosynthetically Active Radiation

HPS - High Pressure Sodium

CCT - Colour Correlated Temperature

EMI - Electromagnetic Interference

PPF - Photosynthetic Photon Flux

CEA - Controlled Environment Agriculture

SMD - Surface Mounted Device

PCB - Printed Circuit Board

PPFD - Photosynthetic Photon Flux Density

SMPS - Switched Mode Power Supply

ETR - Electron Transport Rate

PFC - Power Factor Correction

NREL - National Renewable Energy Laboratory

HOMER - Hybrid Optimisation for Multiple Energy Resources

MOSFET - Metal-Oxide Semiconductor Field-Effect Transistor

NPC - Net Present Cost

LCOE - Levelised Cost of Electricity

CHP - Combined Heat and Power

1 Introduction

Protected cultivation has developed rapidly worldwide to meet the increasing demand for fresh vegetable and horticulture crops. Greenhouses with supplementary lighting and plant factories are the most recent phases of modern protected horticulture. Artificial lighting systems can be used to improve the quality and quantity of horticultural products. The trend towards protected horticulture has several reasons. Globally, these are because of a growing world population, increasing food demand while arable lands are declining due to climate change, this leads to the need for efficient farming in smaller fields with bigger yields. Urbanisation causes problems by creating overpopulated cities requiring vast amounts of food to be transported from outside farm land. There are also likely to be forthcoming world food security issues due to increasingly volatile weather. Other concerns include increased pesticide and chemical usage in agriculture, water scarcity and fluctuating yield over the year due to the seasons, meanwhile the markets demand all year round production [1,2]. In the UK, climate does not permit year round cultivation of the crops matching the market's demand; controlled environment agriculture can offer a solution to this problem. Optimisation of LED lighting systems has great significance for modern horticulture, as supplementary lighting in greenhouses or sole light source in plant factories.

Light is the sole energy source for photosynthesis and the main factor that shapes plant growth and development. For each plant and each developmental stage, light requirements vary as is discussed in more detail later in the report. This fact gives emphasis on research for light recipes to manipulate the growth of desired species and manipulation of any stage of growth to reach the target yield and quality. Development of solid state light sources gave great opportunity to experiment and optimise the light spectrum for plant growth, from effectively an infinite spectrum of possibilities which LEDs have enabled. Among the broad related literature, red, blue and compound white light are accepted as highly beneficial meanwhile green, purple, yellow and orange are secondarily contributing. Ultraviolet and far-red lights can be beneficial even though they are outside of the photosynthetic active radiation (PAR) region which is from 400 nm to 700 nm in wavelength. Light is acting on chlorophyll for photosynthesis, also it acts on cryptochrome, phototropin and the other photoreceptors after being absorbed by photosynthetic tissue [3,4]. Plant growth and development are regulated by light quality [5], light intensity [6] and photoperiod [7].

LEDs are solid-state, narrow bandwidth lighting devices that give a unique opportunity to realise precise light quality management options to obtain optimal plant responses; such as morphology, yield and nutritional quality. Determination of plant light recipes and optimisation of light sources will save energy by removing the unnecessary light spectra from horticulture lighting while increasing yield and product quality.

1.1 Literature Review & Background

This project focuses on experiments and modelling, so it's important to understand the context of LEDs in plant growth, as well as to understand what is and is not currently known about how different plants respond to different types of light.

The field has many gaps of knowledge due to the vast number of possible setups to investigate, but there still exists a significant amount of research providing a foundation of knowledge to build on.

1.1.1 Lighting and LEDs

Light is a form of electromagnetic energy, conveniently thought of as a wave. Visible light represents only a small part of the electromagnetic spectrum between 380 and 740 nanometers. A photon's energy carriage capacity is inversely proportional to its wavelengths, so shorter wavelength light has higher energy. The strength of the photoelectric effect depends on the wavelength of light; short wavelengths are much more effective than long ones in producing the photoelectric effect. The highest energy photons, at the short-wavelength end of the electromagnetic spectrum are gamma rays, with wavelengths of less than 1 nanometer. The lowest energy photons, with wavelengths of up to thousands of meters, are radio waves. Within the visible portion of the spectrum, violet light has the shortest wavelength and the most energetic photons, and red light has the longest wavelength and the least energetic photons. The electromagnetic spectrum is illustrated in Figure 1.

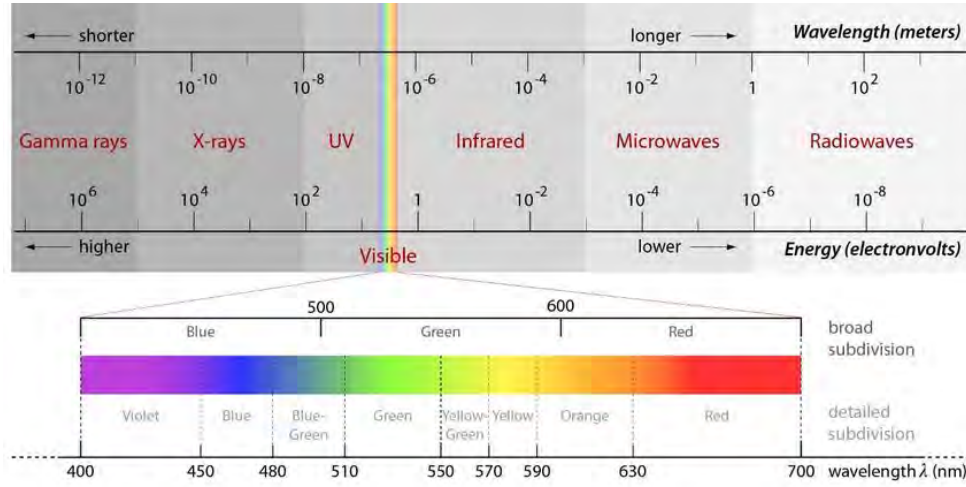


Figure 1: The electromagnetic spectrum [8].

Light is required throughout the entire life-span of a plant. Plant performance is determined primarily by three important light parameters, these are quantity, quality and duration, all of which effect plants in different ways [9].

- **Light Quantity (Intensity)** - This parameter mainly affects the photosynthesis rate of plants. The energy from the light is used to induce a photochemical reaction converting carbon dioxide into carbohydrate in the chloroplasts [6].
- **Light Quality (Spectral Distribution)** - This refers to the spectral distribution of radiation in terms of wavelength composition of a light. Plants respond best to red and blue light with regards to photosynthesis [10]. Spectral distribution affects more than just overall growth of plants, it influences shape and development, as well as playing an important role in the flowering process [5, 11].
- **Light Duration (Photoperiod)** - The photoperiod refers to the duration of time the light works per day. This influences the rate of growth of the plant as well as the development and flowering [7].

The radiation received from the sun contains a continuous spectrum of light, including all visible frequencies. However, plants only absorb discrete wavelengths according to their photochemical reaction mechanisms. The most photo-synthetically active region lies between 400 and 700 nm, which

is approximately the visible spectrum [12].

Due to the flexibility of LEDs in all three of the parameters described above, particularly in their wavelength specificity, they are an extremely useful tool to study the ideal lighting for any species of plant. LEDs emit in discrete wavelengths, whereas other conventional sources of lighting for plant growth emit broad spectra. This means that LEDs have the potential to be extremely efficient and perfectly tuned to fit their purpose, but the design process is challenging. It involves choosing a discrete combination of wavelengths which match the optimum biological response of the specific plant of interest. This is an endeavour which involves vast amounts of data, and as worldwide research accumulates, a database of light recipes can be built by which particular light combinations resonate best with particular plants.

The specific and customisable nature of LEDs also means that plants can be grown in different ways, to produce different morphologies and biochemical compositions within a species, this is interesting since aesthetics and taste can potentially be changed by LED wavelength choice [13]. Currently, much research exists detailing LED spectral compositions which give better responses from plants than others, in terms of mass growth and other commonly measured parameters, typically depending on the plant species [14, 15]. The fact that horticulture includes a huge number of different crops makes research complex, also each crop adopts different shapes and properties throughout its lifetime, so different light environments may be optimum at different stages of a plant's life [16, 17]. This coupled with the huge number of combinations of wavelength, intensity and photoperiod etc. make the field of LED plant response research extremely complex.

LEDs are also advantageous in other ways: they are compact, energy efficient, relatively durable and do not emit much heat, allowing them to be close to the plants while remaining cool, thus reducing watering and ventilation maintenance. Many of these factors add to their overall efficiency, allowing the total energy consumption to be reduced by up to 70% relative to traditional light sources, such as fluorescent lamps, incandescent lamps, high pressure sodium (HPS) lamps and metal halide lamps, which have low electrical efficiency in comparison since they emit many frequencies which are not useful for plants and produce waste heat [18]. A comparison of qualities for the different artificial lighting types for plant growth are shown in Table 1.

Comparison	Incandescent	HID	Fluorescent	LED
Power efficiency	5%	30%	40%	60%
Utilization of radiation	low	low	low	high
Lifetime	low	medium	medium	high
Heat productivity	high	high	low	low
Spectrum Adjustment	no	no	no	yes
Price	low	medium	medium	high

Table 1: Comparison of different lamps in protected horticulture [19]

A study reported that an HPS lamp with 150 W power had a similar effect on the flowering pattern of bedding plants to a 14 W LED [19]. Singh *et al.* [20] estimated savings in operating cost for a system of this kind based on an average greenhouse lighting time (in winter) of 16 hours per day. They then considered the general electricity price and then the buying cost & lifetime, of both HPS and LEDs. Despite an HPS bulb’s lifetime being 20,000 hours and an LED’s being 50,000, the total price of an LED throughout its lifetime (total cost \$95) is far less than for the HPS (total cost \$310), see Figure 2. When comparing the cost of either light for a fixed time, LEDs are estimated to be more than eight times cheaper than HPS.

This considerable difference in power output and efficiency shows how beneficial the adoption of an LED system can be on an economical level for greenhouse growers due to lower energy costs [21]. In terms of installation and initial investment costs, LED systems are comparable to HPS systems, despite HPS being more established [22].

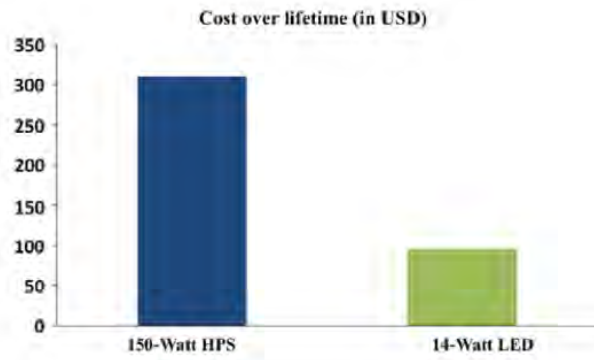


Figure 2: Total lifetime cost comparison of a 150 W HPS lamp and a 14 W LED bulb [20].

LED systems are appropriate for indoor applications. Greenhouses are an important area of application for this field, thus stating the common issues arising in greenhouse growth and their relation to LEDs is useful. Greenhouses are often environments with vertically or otherwise closely packed plants, this means that insufficient light intensity and time under direct light are common problems. Due to greenhouses often relying on natural light, seasons and weather are also factors which can cause issues with plant growth or even crop failure [23]. Implementation of LEDs is desirable in many ways: LED systems are easy to power, can run using a DC supply, and they are energy efficient and economical. They are also sufficiently cool, such that lights can be placed closely and compactly near the plants.

LEDs are semiconductor diodes which permit current to flow in one direction only. The diode is formed by using two slightly different materials to form a PN junction. In a PN junction, the N side contains electrons, and the P side contains electron holes. When a forward voltage is applied to the PN junction, electrons move from the N side towards the P side and holes move from the P side towards the N side and combine in the depletion zone between these the PN junction. Some of these combination events radiate energy in the form of photons [24] (Figure 3).

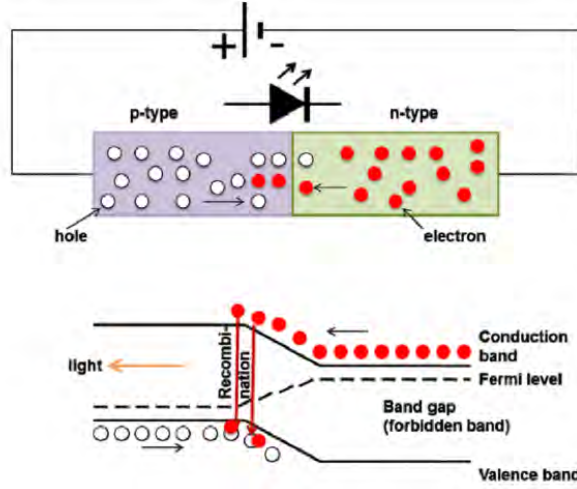


Figure 3: Schematics of light emission mechanism inside an LED chip [25].

The photon energy is approximately equal to the band gap energy (E_g), the energy difference between an electron in the conduction band and the valence band. The conservation of energy from electrical to optical requires a forward voltage (V) through the LED which is equal to the band gap energy. The following equation is derived from energy conservation;

$$V = \frac{h\nu}{e} \approx \frac{E_g}{e} \quad (1)$$

There are mechanisms that cause the forward voltage to differ from the above value. For example, the diode could have series resistance causing voltage loss or energy loss due to holes. These mechanisms change the forward voltage equation of a LED. On the contrary, forward voltage has temperature dependence. The below equation shows the I-V characteristic of an ideal LED.

$$I = I_s \left(e^{\frac{eV - E_g}{kT}} - 1 \right) \quad (2)$$

Where I is forward current for the LED, I_s is saturation current for the LED, V is forward voltage drop of the LED, k is Boltzmann constant, T is temperature, e is electron charge. Diode forward voltage is temperature dependent even when the drive current of the LED is constant. Voltage drop across the diode will change. Solving the equation brings the forward voltage as a function of temperature [24].

In the equation below, the right side is the change of energy level with respect to temperature. As temperature increases, the energy gap of semiconductors decreases. The reason of the LED voltage change is; the recombination process becomes easier and voltage drop decreases by 2 mV for each degree as the temperature rises [25].

$$V_T = \frac{kT}{e} \ln\left(\frac{I}{I_s}\right) + \frac{E_g T}{e} \quad (3)$$

Figure 4 shows the band-gap energies and corresponding wavelengths for two major semiconductor materials used for LEDs today. InGaN (indium gallium nitride) is used for violet, blue, and green LEDs. Whereas InGaAlP (indium gallium aluminum phosphide) is used for green, yellow orange and red LEDs [25].

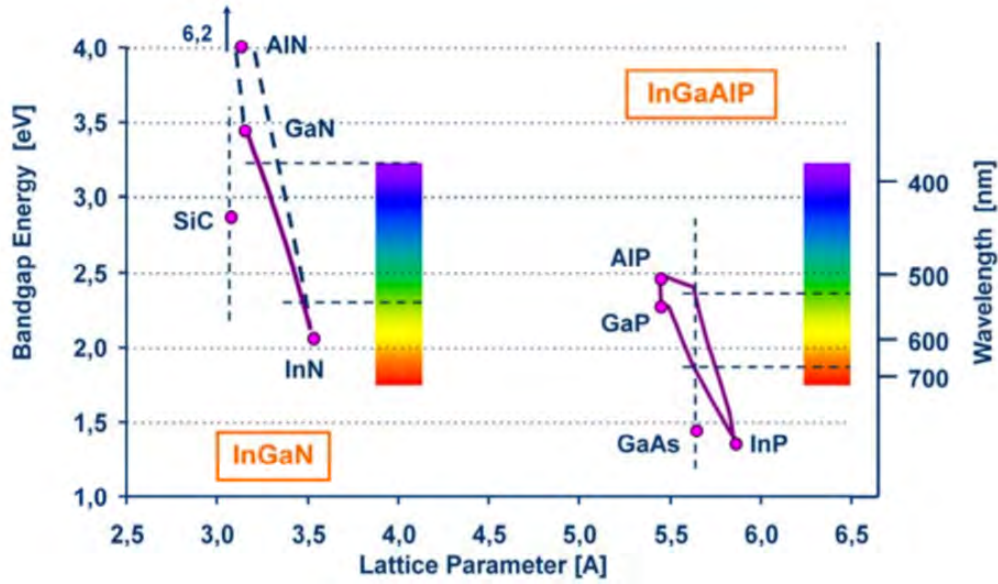


Figure 4: Band gap energies & wavelengths [26].

The wavelength of light is determined by its energy. The energy of a photon emitted by an LED is equivalent to the band gap of the semiconductor material used, which is an intrinsic feature of the semiconductor material itself. Manufacturing an LED with a designated wavelength is all about

engineering the semiconductor materials and their band-gaps.

A single color, or monochromatic LED emits light in a narrow spectral band. The spectral power distribution represents the radiant power emitted by a light source, as a function of its wavelength. InGaN (indium gallium nitride) and InGaAlP (indium gallium aluminum phosphide) are the two primary semiconductor materials and slight change in the composition of these alloys changes the colour of the emitted light [25].

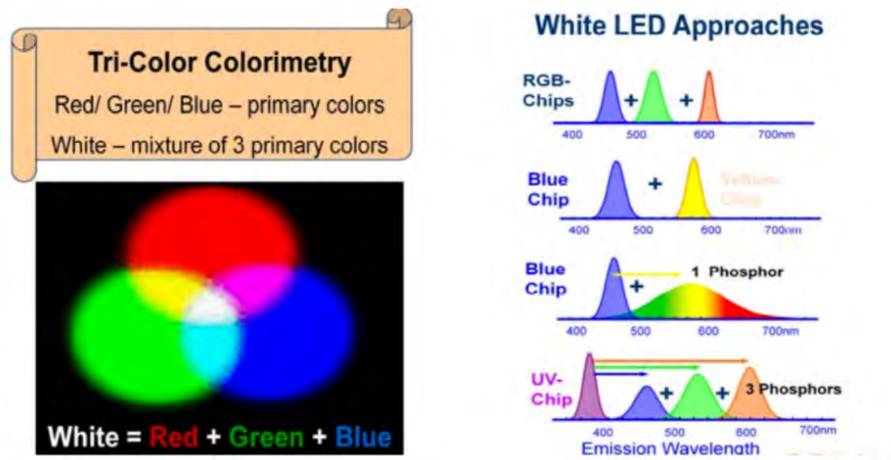


Figure 5: White LED production strategies [26].

Aside from monochromatic LEDs, white LEDs are also used in a number of applications. One approach to generating white light utilises the combination of RGB colours: red, green, and blue LEDs. Another approach is to use blue and yellow LED chips together in a certain ratio to produce white light. A third approach is to use a blue chip and a yellow phosphor to generate white light. Finally, using a UV LED to excite red, green, and blue phosphors is also another approach. These approaches are illustrated in Figure 5. The most widely adopted approach to produce a white LED is to use a blue LED chip combined with a phosphor. This method is preferred due to its low cost and ease of application. The phosphor layer absorbs some of the blue light and emits light at longer wavelengths; the phosphor concentration defines how much of the blue light is converted.

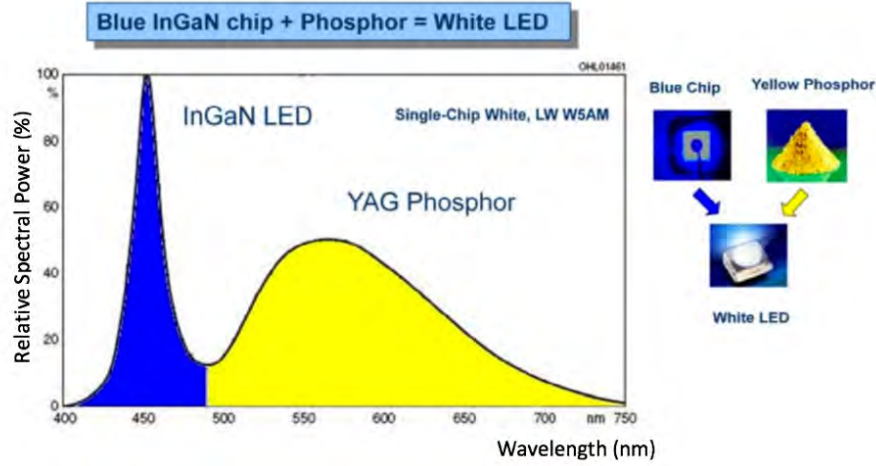


Figure 6: Spectral composition of a blue LED with yellow phosphor coating [26].

Changing the phosphor content enables different colour temperatures of white light. The colour correlated temperature (CCT) for a light source gives a good indication of the lamp's general appearance, but does not give information on its spectral power distribution. In other words, two lamps may appear to be the same white colour, but their spectral composition could be different such that a plant could respond differently.

As previously described in this section's equations, thermal properties and variations on an LED have significant consequences for its lumen output, electrical characteristics and also lifetime. Thus, for LEDs to function optimally, heat generated by them must be managed, being easily transferable away from the LED area, particularly the PN junctions of the LEDs must have their temperature regulated. This is done through careful consideration of the LED's assembly and operation [27].

Thermal resistance is a material's ability to resist heat flow through it, high thermal resistance means a slow transfer of heat. Thermal resistance has units of kelvin per watt. Thermal capacity is the second important parameter and is the ability of the material to store thermal energy. The temperature drop on a material can be calculated with respect to these two variables. Thermal calculations are performed with the thermal model of the circuit element and used for various electronic components which dissipate heat [26]. For heat transfer, the thermal model is used to calculate the temperature value at the junction point of the LED or the expected thermal resistance value for the heat-sink. The temperature difference between two points from ambient to LED junction is found

by calculating the total thermal resistance between two points. LEDs dissipate some of their power as heat and some as light.

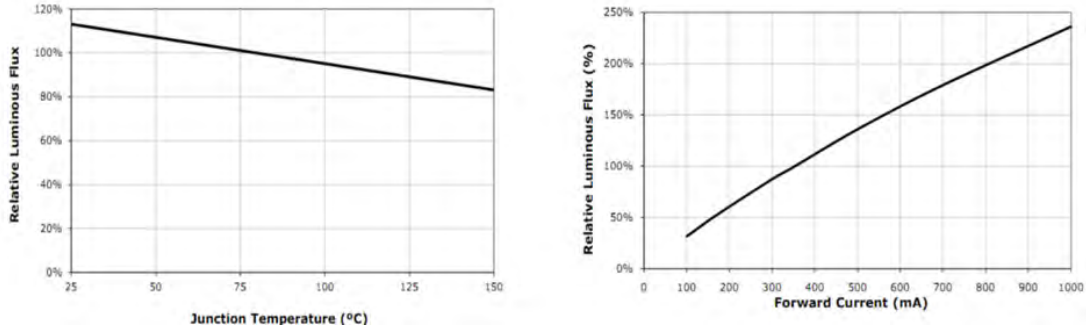


Figure 7: Junction temperature effect on luminous flux and luminous flux vs forward current [26].

An LED's lumen output is highly dependent on the current through the LEDs. As shown in Figure 7, the change of 500 mA creates around 100% luminous flux output difference [27].

The basic drive circuit for LEDs includes linear DC drivers which involve a voltage regulator such as LM317 or an op-amp and active switch. These devices are used as current-sink or current-source circuits in order to comply with constant current output for LEDs. These drivers are preferred on the basis of ease of application and no EMI radiation. However, these devices have some limitations; LED voltage has to be smaller than the supply voltage and voltage differences between supply and LEDs has to be low. This voltage will drop on the active device, and this device dissipates this as excess power. Linear drivers are inefficient solutions because of their operation principle. Another concern is that power dissipation radiates with heat and this can be transferred with a bulk heat-sink. If the supply voltage and LED-voltage have a significant difference, the circuit cannot be applied because of heat and device size conditions. Linear power supplies have been declining in popularity for years, being replaced by Switch Mode Power Supplies (SMPS), which is superior in size and efficiency.

A DC-DC converter, also known as a switching regulator is a power converter that converts a DC energy source from one voltage level to another. Average output voltage is controlled by varying the conduction time of the switch. The DC-DC converters can be designed with regulated output

voltage. For the LED drivers especially, the converters have regulated output currents.

DC-DC converters are a necessity for LEDs to have regulated output and high power efficiency. Typically, first generation converters are used because of ease of application and low cost. The fundamental converters are Buck (Step-Down), Boost (Step-Up) and Buck-Boost (Step-Up and Step-Down). Transformer type and developed converters have a wide range of the output voltage and power like; Flyback, Forward, Push-Pull, Half-Bridge, Bridge and Zeta Converter. These converters have transformers and isolate the input and output circuit. Transformers add an extra property of changeable voltage gain with the ratio of transformer windings and isolation. Additionally there are more developed converters like; P/O (positive output) Luo-converter, N/O (negative output) Luo-converter, Double output Luo converter, Cuk converter, Single-ended primary inductance converter (SEPIC). These converters have more components, having less output voltage ripple than the previous converters.

1.1.2 Plant Physiology

Plants require light for photosynthesis, photomorphogenesis and phototropism. These are impacted by light intensity, light quality and photoperiod [28]. When a photon interacts with a molecule, its energy is either lost as heat or absorbed by the electrons of the molecule, boosting those electrons into higher energy levels. Whether or not the photon's energy is absorbed depends on how much energy it carries (defined by its wavelength) and on the chemical nature of the molecule it hits. To boost an electron into a different energy level requires just the right amount of photon energy (via the photoelectric effect). A specific atom can absorb only certain photons that correspond to the atom's available electron energy levels. As a result, each molecule has a characteristic absorption spectrum, the range and efficiency of photons it is capable of absorbing.

Molecules that are good absorbers of light in the visible range are called pigments. Organisms have evolved a variety of different pigments, but there are only two general types used in green plant photosynthesis: carotenoids and chlorophylls. Chlorophylls absorb photons within narrow energy ranges [28]. There are two kinds of chlorophyll in plants, chlorophyll (a) which has absorbance peaks at violet and orange and chlorophyll (b) which has absorbance peaks at blue and yellow light. Neither of these pigments absorb photons with wavelengths between around 500 and 600 nanometers, and light of these wavelengths is therefore reflected by plants and so they appear

green. Chlorophyll (a) is the main photosynthetic pigment and is the only pigment that can act directly to convert light energy to chemical energy and chlorophyll (b), acting as an accessory or secondary light absorbing pigment, complements and adds to the light absorption of chlorophyll (a). Chlorophyll (b) has an absorption spectrum shifted toward the green wavelengths. Therefore, chlorophyll (b) can absorb photons chlorophyll (a) cannot. Chlorophyll (b) therefore greatly increases the proportion of the photons in sunlight that plants can harvest. An important group of accessory pigments, the carotenoids, take an action in photosynthesis at the wavelengths that are not efficiently absorbed by either chlorophyll [28]. Carotenoids absorb mostly blue and green light and reflect orange and yellow light. Light absorbance information is displayed for both chlorophyll (a) and (b) as well as carotenoids in Figure 8. In summary, photons of light are absorbed differently by different pigments for photosynthesis, but generally absorb green less.

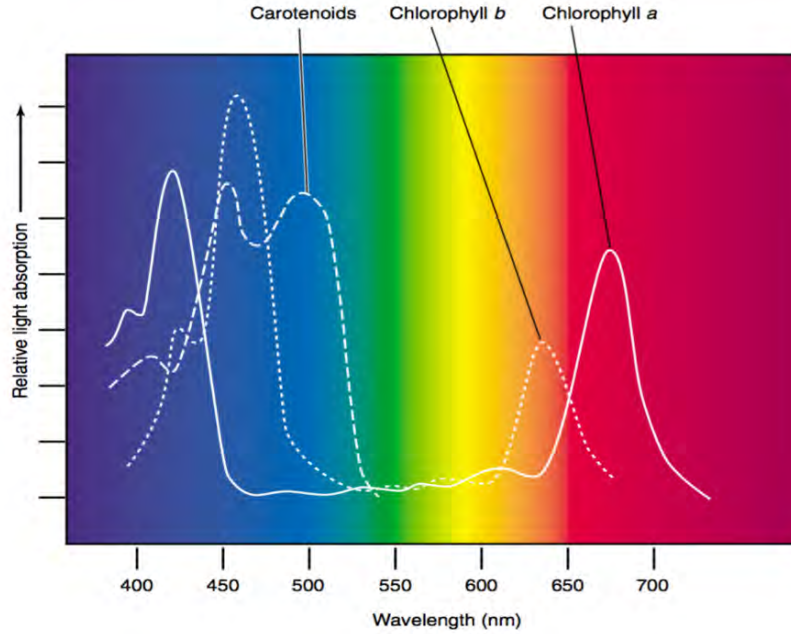


Figure 8: The absorption spectrum of chlorophyll (a) & (b) and carotenoids [28].

LEDs as a source of plant lighting have been investigated for more than 20 years in research [18], with a large number of reports having successfully grown crops under sole or supplemental LED illumination. Different spectral combinations have been used to study the effect of light on plant growth and development and it has been confirmed that plants show a high degree of physiolog-

ical and morphological plasticity to changes in spectral quality. For example, research since the 1990s has looked at photosynthetically active radiation and the biological and physiological effects of blue and red light wavelengths (individually and also mixtures of different ratios) on multiple crop species. These include experiments on strawberry [29], pepper [30], wheat [31], rice [32] and lettuce [33]. Despite there being a great amount of data, much is still unknown about how plants respond to different wavelengths, especially since the plant responses to wavelengths are species specific, although there are general trends of the affects of some wavelengths on plants [34]. These general effects are summarised in Table 2.

Table 2: Summary of the effect of light wavelength on plant growth [13,35]

Optical wavelength (nm)	Influence on the plant growth
280–315	Minimal positive impact on morphological and physiological process, with possible damaging effects at high exposure
315–400	Absorption by chlorophyll is low, but can enhance pigmentation and increase leaf thickening
400–520	Chlorophyll and carotenoid absorption proportion is the largest, the biggest influence on photosynthesis
520–610	The pigment absorption rate is not high, but can have some beneficial effects when used alongside red and blue
610–720	Chlorophyll absorption rate is high, having significant effects on photosynthesis and light cycle effect
720–1000	Absorption rate is low, stimulate cell extended, affecting flowering and seed germination
>1000	Converted into heat

Red light (610-720 nm) is required for the development of the photosynthetic apparatus and has the highest quantum efficiency for photosynthesis [10], while also having many photomorphogenic effects on plant development mediated by the photoreversible pigment phytochrome, such as: enhancing leaf expansion, biomass accumulation, stem elongation and seed germination [36]. However, different wavelengths of red (660, 670, 680 and 690 nm) light can have differing effects on plants dependent on plant species. Far-red infrared LED light (700-725 nm) which is beyond the PAR has been shown to support plant growth and photosynthesis [20,37–39]. Biomass yield of lettuce

increased when the wavelength of red LED emitted light increased from 660 to 690 nm [39]. A comparative study on the physiology of red leaf lettuce showed that application of far-red (730 nm) with red (640 nm) light from LEDs caused an increase in total biomass and leaf length while anthocyanin and antioxidant potential was suppressed [40]. While in a study where red LED (640 nm) was the sole source of light, increased anthocyanin content was observed in red leaf cabbage [41]. Addition of far-red (735 nm) to the red (660 nm) LED light on sweet pepper resulted in taller plants with higher stem biomass than red LEDs alone [30].

After development of the blue LED [42], blue light started to be added to red light for plant growth and has been shown to enhance yield [43]. Blue (400-500 nm) light is important for many aspects of plant physiological development, specifically chloroplast development, chlorophyll synthesis and content, stomatal opening, leaf thickness and photomorphogenesis [20, 44–47]. Experiments with radish, lettuce and potato have shown that blue light (400-500 nm) increased biomass and leaf area [38, 43, 48]. Also, as with red, different wavelengths of blue (430, 440, 460 and 475 nm) light can have differing effects on plants depending on plant species [20, 37–39]. Another study using blue (400-500 nm) LED light in combination with red LED light on green vegetable growth and nutritional showed that LEDs (440 and 476 nm) used in combination with red LEDs caused higher chlorophyll ratio in Chinese cabbage plants and improved overall plant yield and seed production than when grown under sole red light [41, 49]. Blue light has also been shown to increase carotenoid [50], vitamin C [49] and polyphenol levels [51] in green vegetables. A report [52] reviewed studies made previously with blue LEDs and reported that yield of lettuce, spinach and radish crops grown under only red LEDs is less than for the ones which had additional blue LEDs, acted upon by the same total photosynthetic photon flux (PPF). For peppers, studies which looked at different LED colour combinations and their effect on leaf thickness and leaf chlorophyll content, indicated that the blue LEDs combined with red LEDs induce more chloroplast in leaf cells than red and far-red combinations [30, 53], again lamps had fixed PPF values. Research indicated that plants under red & blue, and red & blue & green LEDs were considerably stronger and shorter, whereas plants treated with green, yellow and red light were weaker and higher.

Green light (500-600 nm) is often disregarded for photosynthesis because absorption of green light in chlorophyll is broadly very low. Chlorophyll has major absorption peaks only in the red and blue regions, so researchers initially selected first red, then later blue LEDs for lighting arrays to

support plant growth [19]. However, despite low absorption overall of broad green light, leaves do absorb some green light, with certain wavelengths of green being more efficient for photosynthesis than some wavelengths of blue light. When leaf canopies close, red and blue light are absorbed strongly by upper or outer leaf layers, but green light penetrates beyond the interior leaf layers, where it drives photosynthesis of the inner canopy. Positive contribution of green light for plant growth has been shown in several experiments. Green LEDs with high photosynthetic photon flux have been effective in enhancing growth in a crop of lettuce [51]. Green (505 and 530 nm) LED light in combination with HPS lamps has also contributed to better growth of cucumber, where blue LED (470 nm) slowed growth comparatively [54]. The effect of green (525 nm) LED light on the growth of *Arabidopsis* seedlings was investigated and results showed that seedlings grown under green, red and blue LED light are longer than those grown under red (630 nm) and blue (470 nm) alone [55]. Supplementation of green light enhanced lettuce growth under red and blue LED illumination [56]. Green light alone is not enough to support the growth of plants, but as demonstrated in these studies, green light does influence some important physiological effects. Additionally regarding practicality, if green light is included alongside red and blue, so that all three wavebands (RGB) are present simultaneously in a plant growth lamp, one can visually evaluate the colour status of crops and leaves to help identify incidences of physiological disorders. Whereas an only red and blue combination is delusive for the human eye’s observation of plant colour during experiment [19].

Unlike the narrow waveband LED colours discussed so far, white LEDs (blue LED plus phosphor coating) have a wide spectrum (see Figure 6) and are the choice of many growers because of this quality, but they mainly lack the red spectrum. Energy losses associated with the secondary broad-band photon emissions of the excited phosphor also make white LEDs significantly less electrically efficient than emissions from pure monochromatic blue LEDs. Additionally, the proportions of red, green, and blue wavebands in white LED obtained with phosphor coating varies widely among cool white, neutral white, and warm white LED types and none of them are such a close match for the RGB distribution of midday solar light. Therefore, producing white light from a combination of monochromatic RGB LEDs instead of white (phosphor coated) ones gives a higher electrical efficiency and precision potential for artificial plant lighting [19].

Regarding the non-visible spectrum, far-red (700-800 nm) and ultraviolet, both UVA (320-400 nm)

and UVB (280-320 nm) wavelengths also affect plant growth and are important spectral components for vegetable production [2]. Using LEDs for indoor agriculture scenarios allow incorporation of these wavelengths giving further customisation potential for quality and appearance of plants that respond to far-red and UV light. Far-red light can enhance plant growth alongside red light, and contributes to increased leaf size and stem length [37–39]. There is a reluctance to introduce UVB into indoor commercial growth environments for safety reasons and because it can be damaging to plants [57], but it may be possible to use UVA if certain worker precautions are taken [58]. Studies have investigated the potential of using supplemental selected UV irradiation [59, 60]. Generally, plant height, leaf area, leaf length have been showed to decrease, whereas leaf thickness was increased in response to UVB radiation [61].

Aside from all the LED colours mentioned, other frequencies are being considered for use; wavelengths like yellow, orange, purple and cyan can have potential for horticultural crops to some extent under certain circumstances [62, 63].

Photomorphogenic effects are mainly influenced by Phytochromes. Phytochromes Pr (red) and Pfr (far-red) mainly influence the germination, plant growth, leaf building and flowering. The photomorphogenic effects are controlled by applying a spectrum with a certain mix of 660 nm and 730 nm in order to stimulate the Pr and Pfr phytochromes. One influence of far-red light on a plant is the active shade escape reaction, as illustrated in Figure 9. If the plant is predominantly illuminated with red (660 nm) it senses that illumination is from direct sun and growth is normal, but if instead the plant is illuminated with predominantly far-red (730 nm) it senses that it is in shadow of another plant that shades the direct sun light. In this case, the plant reacts with increased length growth in attempt to escape the shadow, which leads to taller plants without necessarily impacting the cumulated biomass. Pr and Pfr convert back and forth from each other; Pr is converted into Pfr under red light illumination and Pfr into Pr with far-red light. The active form which triggers flowering is Pfr [64]. Pr is produced naturally in the plant. The ratio of Pr to Pfr is in equilibrium when the plant receives light (day) because Pr is converted into Pfr by red light and Pfr is converted back to Pr by far-red light. Back conversion of Pfr is however also possible in a dark reaction, so it is the night (dark) period which mainly affects the ratio of Pr to Pfr and controls the flowering time in plants. Ornamental plants are of high economic importance, therefore manipulating this mechanism with LEDs would contribute positively to this sector.

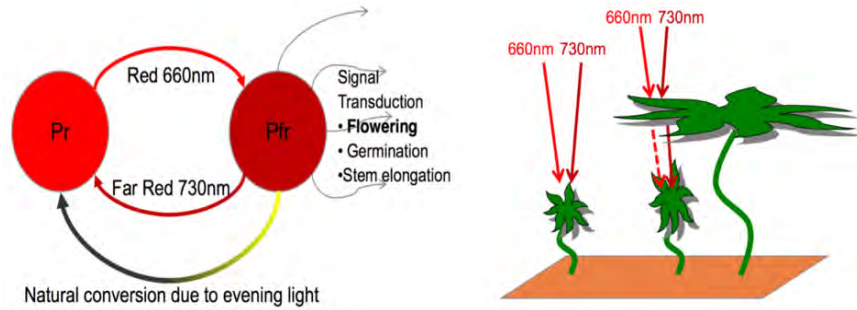


Figure 9: Pr-Pfr cycle and shade avoidance [64].

Overall, LEDs are optimal tools for studies on spectral plant responses as well as having great market potential for the same reason; tailored plant recipes with less consumption of electricity than traditional sources. From the 1990s there has been significant research on spectral responses of plants to LED light, especially NASA’s Kennedy Space Center and Purdue University, who have made great contributions to LED lighting technology [14, 65]. Rapid development of LED technology from the 2000s has improved LED spectral possibilities allowing an increasing number of wavelengths. Through these developments, information on responses to light spectral quality by plant biology and physiology is beginning to be more deeply investigated.

1.2 Research Aims

The overall aim of this research is to maximise energy efficiency of plant growth using LEDs for application in CEA, while also considering carbon footprint and cost. This involves firstly understanding how plants respond to different light and secondly, it involves developing understanding of LED devices and whole artificial lighting system energy consumption. These are researched by both experimental and software modelling based methods.

For understanding plant response to light experimentally, data obtained on plant growth under different light can give important information about which conditions give the most desirable plant growth results, regarding not only size and speed of growth simply, but other aspects such as aesthetic appeal (for ornamental plants) or taste quality (for crops). From a modelling perspective, software along with mathematical models can be used to simulate lighting arrangements and help

elucidate the setups which best favour plant growth. For example, this can involve testing reflector systems to maximise light utilisation on the plant. The modelling approach can also include using machine learning tools and/or mathematical modelling to find patterns in plant growth behaviour under different lighting conditions in order to predict optimal light recipes.

For understanding energy consumption in LED lit plant growth systems, there are many different aspects and solutions to explore and optimise: Consideration of LED device market options and respective device efficiencies, LED board circuit setup and chosen operating forward current to maximise efficiency, power supply to whole system (AC vs DC), dynamic dimming of LED boards synchronised with sunlight to save energy, and finally, augmentation of system energy supply with renewables based on local geographical potential, to reduce carbon footprint and energy costs.

The aims of this project in summary are therefore:

- Develop greater understanding of how plants respond to different wavelength combinations of light, both using experimental and modelling techniques.
- Investigate alternative electrical setups and running options for an optimal (in crop yield) LED lit CEA system and realise implications for energy consumption, cost and carbon footprint.
- Investigate renewable energy setups in the UK for different sized LED lit CEA systems to assess carbon footprint and cost impact in comparison to sole grid energy supplied.

1.3 Hypothesis

The main hypothesis of the project is that because LED CEA systems are relatively new and involve numerous stages of designing and planning based on incomplete research, there are many areas in which large power savings can be made, crop yield can be enhanced and carbon footprint and financial cost of such systems can be reduced.

Optimal setup conditions for an LED CEA system, from the main power supply options to the particular LED wavelength combination choices are sensitive to multiple factors, including system size, site geographical area and particular plant variety being grown. Thus following generic uni-

versal guidance on optimal CEA setups could result in missed opportunities for optimising energy efficiency and crop yield. This project's more specific sub-hypotheses are therefore identified:

- There will be significant differences in crop yield for plants exposed to different light qualities (LED wavelength combinations) under controlled experimental conditions.
- Plant yield can remain optimised under alternative electrical setups and running conditions which increase energy efficiency and reduce carbon footprint and cost.
- Renewable energy production technologies can be integrated into LED CEA systems, small and large, to reduce cost and carbon footprint compared to sole grid powered systems.

2 Growing Little Gem Lettuce Under Different LED Light Spectra

2.1 Introduction

Firstly, an experiment for growing Little Gem lettuce with LEDs was prepared. Little Gem lettuce was chosen due to it being one of the easier, faster and more reliable plants to grow under artificial lighting. Also, of the lettuce varieties, there is a lack of literature about the effect of different light wavelengths on Little Gem.

This section's experiment involved six prepared boards of LEDs comprising of: red (660 nm), blue (440 nm), green (525 nm), green & red, blue & red and warm white (2600-3200 K). Red and blue were used in recipes because they are the most important for photosynthesis. White light was chosen because its the most widely used, particularly in other types of non LED artificial light and of course is most similar to sunlight. Green light, although less absorbed by plants and less important for photosynthesis has been shown to enhance plant growth in some cases (including for lettuce) as discussed in the introduction.

2.2 Setup & Methodology

2.2.1 LED Product Selection

The initial idea was to purchase high brightness Osram SMD LEDs for high W/m^2 values and fewer components (shown on the right of Figure 10). However, using these more compact units would mean having to get the boards assembled externally meaning high expense and any future repairs or adjustments would not have be possible without sending the boards back to the manufacturer or a specialist. Whereas, LED boards comprised of LEDs with a physically bigger unit size, such as the Bridgelux LEDs (see the left of Figure 10) are cheaper and easier to assemble and more practical and manageable if a problem occurs, since circuit repairs can be done by hand if necessary. The larger LEDs in the selected wavelengths from the company Bridgelux were therefore chosen for preliminary tests.

The LED modules built for the lettuce growing experiment include boards with 24 chips, since

it allowed ample variation potential of ratios of selected wavelengths. For the circuit design, 1W chips were selected. The LEDs have a uniform distribution of light with a 120° viewing angle and each LED has a forward current of 350 mA (except red LEDs which have 400 mA). Maximum LED junction temperature is 115°C . Heat tests for junction temperature were conducted and circuits supplied with minimum necessary voltage values.



Figure 10: Bridgelux LEDs chosen for preliminary tests (left) and Osram's more compact LED design (right).

2.2.2 Board Designing, Building and Heat Testing

LED boards with different geometries and colour combinations were designed using the Altium Designer, which is a PCB and electronic design automation software package for printed circuit boards. These designs can be seen in Figure 12. Due to the test plant trays being rectangular, rectangular boards were used for circuit printing. The circuit boards were planned to be both simple and robust, all 24 LED chips on a constant current circuit were designed to be on the same board with different branches for ease of connection. Each board used for the experiment consists of a series connection of six LEDs per branch and four branches per board, with a constant current circuit, as in Figure 11, with LM317t linear regulator chosen as it is an appropriate choice for such low current values rather than sensor control.

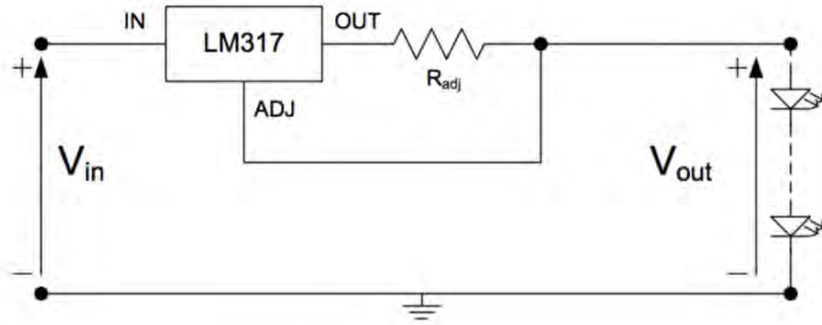


Figure 11: The constant current circuit which was implemented on the four channels per board.

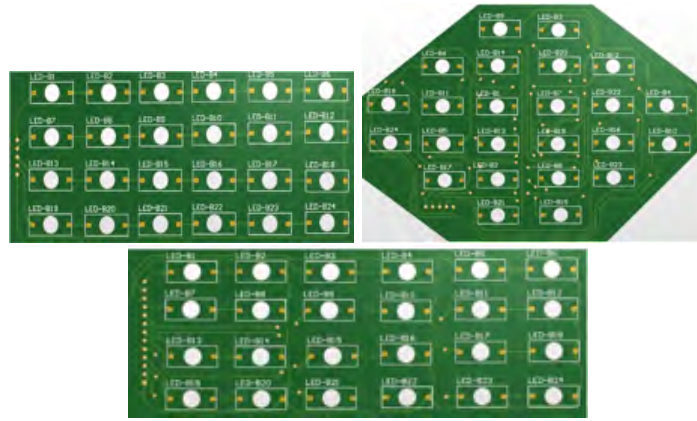


Figure 12: LED board circuit designs. The top left side shows the design used for the experiment. The top right shows alternative geometry, more suitable for a single plant or axisymmetric trays for example. The bottom side shows a design with more channels, increasing capability to customise colour combinations (up to 12).

The boards were then printed and all components including the LEDs were hand soldered. Once all boards were fully assembled, the circuits were tested without plants in a closed tent environment and the temperature measured to make sure overheating would not be a problem for either the components or for the plants. Working examples of the LED boards can be seen in Figure 13. The LEDs have a 115°C maximum junction temperature threshold and the threshold is 125°C for LM317t. The maximum growing temperature for the selected plant (Little Gem lettuce) was defined as 25°C and multiple heat tests were made to reassure the safety of grow tents while the experiment is running. As a result of these tests, use of a cooling fan was found necessary, even

if the supply voltages for circuits were just at minimum necessary values. For cooling, 3600rpm 12V 0.41A brush-less DC (produced by Delta Electronics) fans were found to be sufficient for the cooling of 1 tent. The tents already had two holes for ventilation, so a fan was placed over the bottom hole and the setup was arranged such that airflow was not blocked by the central barrier between the two tent compartments. It was important that the central barriers did not obstruct airflow, while blocking light interference between chambers. The middle tent barriers therefore had air gaps at the edges, but barriers were sufficiently large so as not to allow light interference between tent compartments, see Figure 14. The barrier was also covered with light reflective material to maximise internal light reflection on to the plants.

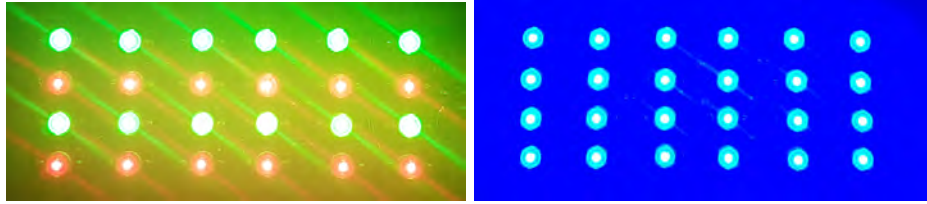


Figure 13: Two of the working LED boards: red & green (left), and blue (right).

2.2.3 Experimental Setup

After LED boards with aforementioned wavelengths were designed, built and implemented with a suitable cooling solution found, the experimental setup allowing six LED boards to run simultaneously was set up. Each tent divided to two compartments by reflective surfaces, the inside of the tents are also reflective and outside is opaque, thus for each compartment, interference is minimised while internal reflection is maximised. For the electrical power, three Voltcraft PS-1302 D power supplies with rating 30V/10A were used to feed all branches at 350 mA. The fourth branch for red lights required 400 mA of forward current and were supplied by another power supply separately.

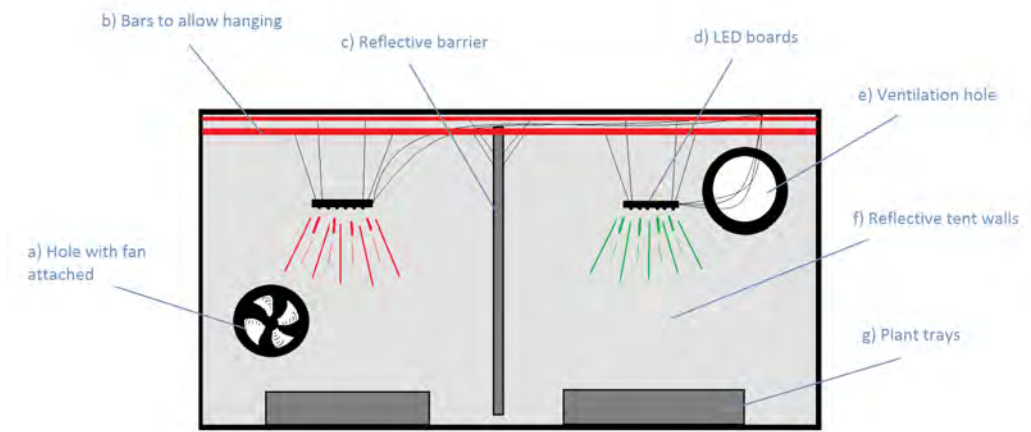


Figure 14: Experimental setup: the top figure shows a photograph of the functioning grow tent & the bottom shows a labelled schematic of the setup. The dimensions of the tent are 70 cm x 70 cm x 140 cm.

Temperature in the tents was regularly measured during the experiment by DFROBOT FIT0507 thermometers, observed maximum temperature was 24°C and average was 22°C . The power supplies were connected to the mains via a timer which remained on for 16 hours and off for 8 hours. For optimal plant lighting, lights were on 16 hours per day to emulate summer daylight hours, from 6 am until 10 pm along the 21 day experiment.

In each of the 40 cm x 30 cm x 10 cm plastic grow trays (from the Riseholme campus greenhouse facility), 12 lettuce seeds were evenly sowed (equally spaced 4 x 3), to ensure the lights' effect on multiple plants and also to account for the fact that each batch of seeds has some variation of

quality and some of them statistically will not germinate. Eight trays of Little Gem lettuce seeds (*Lactuca sativa*) were sowed and left in the heated greenhouse (at around 15°C) until germination time. After germination, which took approximately seven days in the heated greenhouse, seven of the trays were collected to be experimented under prepared light test rigs and one left in dark, but with the same temperature and water as the trays under lights. This was to observe how long the plants could sustain without any light. Finally, one of the trays was left in the heated greenhouse as reference to the LED experiment to compare the results.

Once the equipment was all in place and the plant trays germinated and ready to be treated under the experimental lighting conditions, each rectangular tray was placed below an LED board parallel to its orientation. The full experimental setup with LED boards shown lighting the plant trays in the controlled environment grow tents is shown with a photograph and labelled schematic diagram in Figure 14.

2.2.4 Methodology and Measurement

The light treatments which consisted of LED boards of 24 W power with various wavelength recipes, ran from 6 am to 10 pm (16 hour photo-period) to emulate summer daylight on Little Gem lettuces. The temperature inside the tent was controlled, between 20°C- 24°C while outside the tent is set at 20°C. Watering the lettuces was a process which was learned by observation, the volume and periodicity of watering was perfected after around three days of trial and error. This was mainly due to the tent conditions being much dryer than greenhouse, as soil is dried much faster by the fans and the intense light for 16 hours per day, compared with the soil under only winter sunlight. After three days, 150 ml per day was given and the watering process done after 10 pm when lights had closed, this watering process was then continually conducted until the end of the experiment.

At the end of the 21 day grow, the following properties of each tray were measured; fresh weight (g), dry weight (g), leaf area (cm²), leaf number, leaf height and width (cm) and apex length (cm). These measurements were both practical to take without the need for specific measuring equipment and also the most commonly measured quantities in the literature for plant growth of crops lit under LEDs (such as in the list of lettuce growth literature used later in the neural network chapter). Other measured quantities in the literature such as chlorophyll content, plant color measurement, stomatal conductance and other chemical and physiological measurements were not taken in this

experiment due to equipment limitations and as this project is more about the lighting and electrical engineering aspect than the plant biology side.

In terms of light data obtained, the lux of each LED board at the position of the plant canopy was measured before the plant growth experiment. An Ocean FX spectrometer, once available after the experiment, was also used to determine the irradiance of the LED boards. These were taken in order to fully understand the nature of how the intensity and spectral distribution that the plants were subject to varied between the different boards which were setup in the same way and supplied the same electrical power.

2.3 Results & Discussion

2.3.1 Light Data Analysis

Once the experiment was setup, a YF-170 lux meter by Tenmars was used to determine lux (SI unit of illuminance and measure of light intensity according to human eye perception). Table 3 shows the lux values for the different LED boards, measured at the position of the centre of the trays at plant canopy level. All values give over 2500 lux which suggests that none of the trays were too far from the lights to be considerably disadvantaged by dimness.

Table 3: Lux values for LED boards at the separation distance of the trays, describing apparent light intensity.

Board Colour	Lux Value (lx)
Red	2520
Green	2670
Blue	7930
Red & Blue	4480
Red & Green	2820
White	4860

Spectrometer measurements were initially not possible at the beginning of the experiment due to unavailability of a spectrometer, but one was available after the experiment had finished. Absolute irradiance data was therefore taken, from middle of the trays (on top of canopy levels), and also at each of the four corners of the tray to observe the intensity deviation from the center of tray.

The graphs in Figures 15-20 were created from the Ocean FX spectrometer data taken. From these irradiance plots, mixed behaviour was observed regarding deviation in the corners; for some boards there were clear differences between peaks in the centre and at the corners and different boards had different levels of decreased irradiance at the corners. For the green board (Figure 15) there was a drop of around 40% from the centre to the corners, with there being variation also between corners. For the white board (Figure 20) there is also a drop in irradiance from the centre to the corners, of around 20%, with the shorter wavelength peak dropping proportionally more. However, for the red (Figure 16) and blue (Figure 17) boards, there is no observed drop in irradiance between the centre and corners. For the recipes with more than one colour: red & blue (Figure 19) shows differences in irradiance from the centre to the corners, but only in the red peak. Finally, for the green & red board (Figure 18) there is a drop in irradiance for both peaks (but proportionally more for green). Some of these results are somewhat expected as intensity should be higher at the centre (closer to the LED boards) than the corners.

From these results there is no clear consistent pattern across all boards. Possibly the most likely reason is the orientation of the spectrometer when measurements were taken, which was held by hand to point toward the LED boards at the level of the plant trays. If however, the spectrometer was pointed even slightly away from the LED board, the peaks irradiance could have been read less than if perfectly pointing toward the board. The same applies to each measurement at each corner. Cases where there was difference between corners could be either because this, and/or the angle at which the LED board is hanging, for if a board were to deviate from perfectly horizontal, then one side of the plant tray would receive more light than the other. Otherwise, causes could involve general imperfections in setup, or possible issues with the software which interprets the spectrometer data and renders the irradiance graphs.

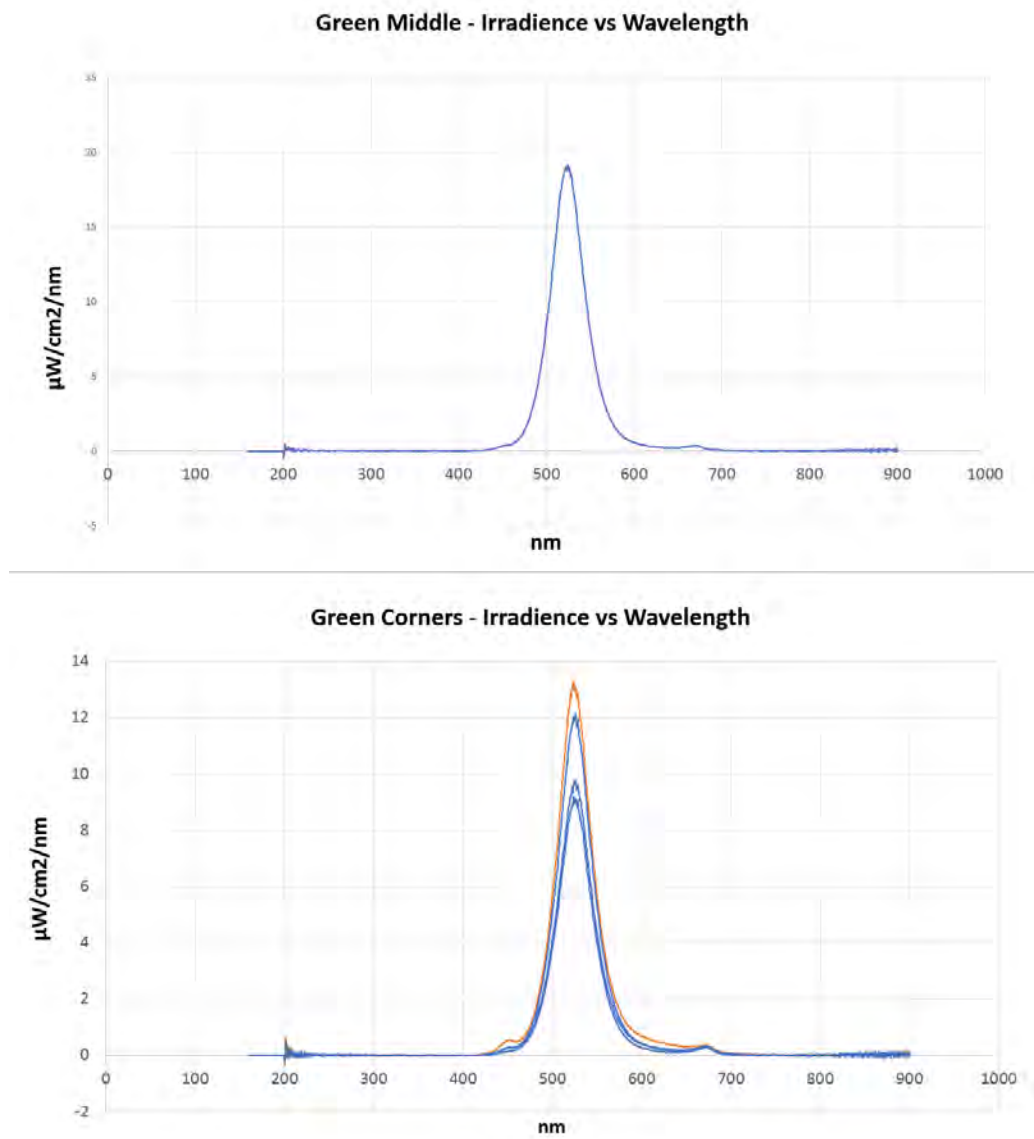


Figure 15: Green board irradiance, with the upper graph showing the irradiance at the centre of the tray and the lower figure showing the four superimposed graphs of irradiance at each corner of the tray.

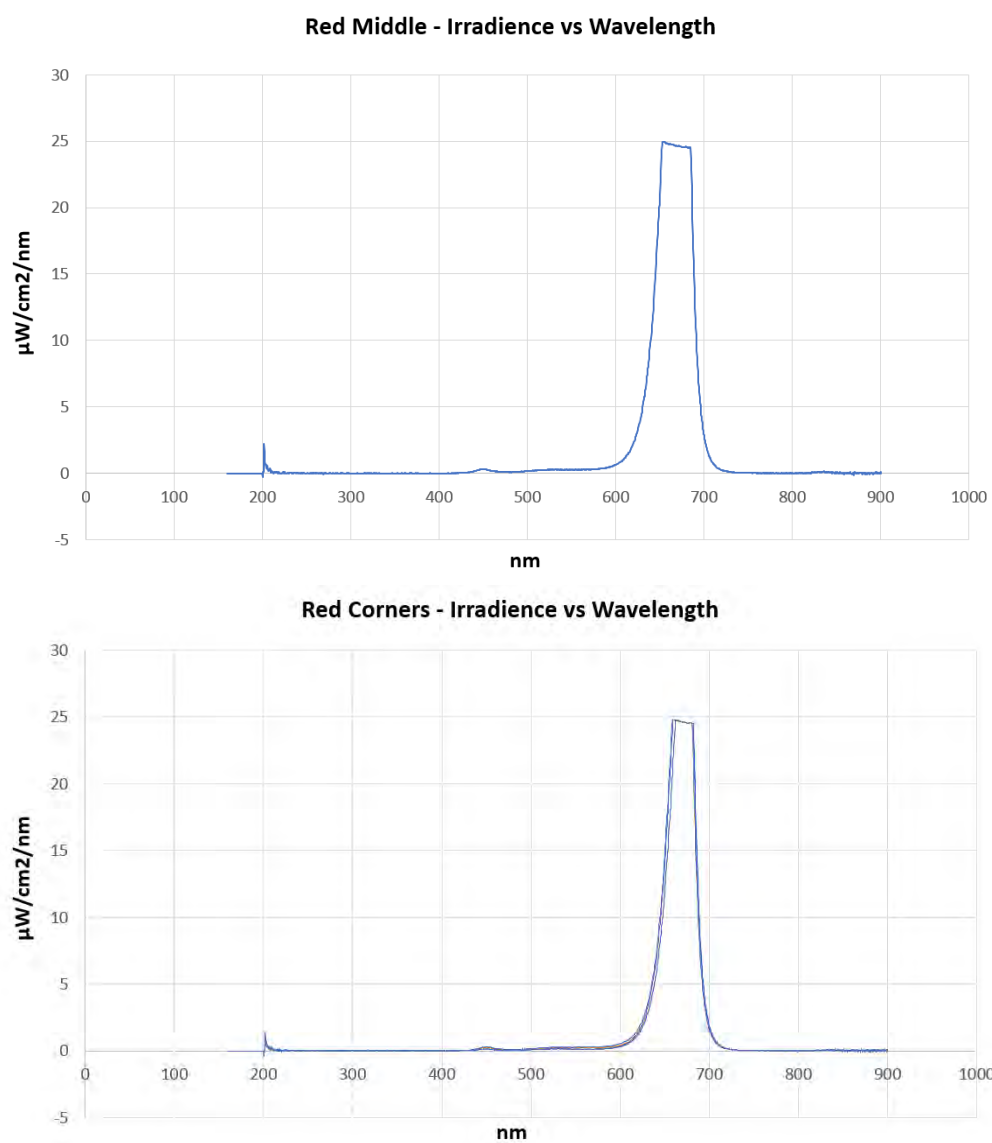


Figure 16: Red board irradiance, with the upper graph showing the irradiance at the centre of the tray and the lower figure showing the four superimposed graphs of irradiance at each corner of the tray.

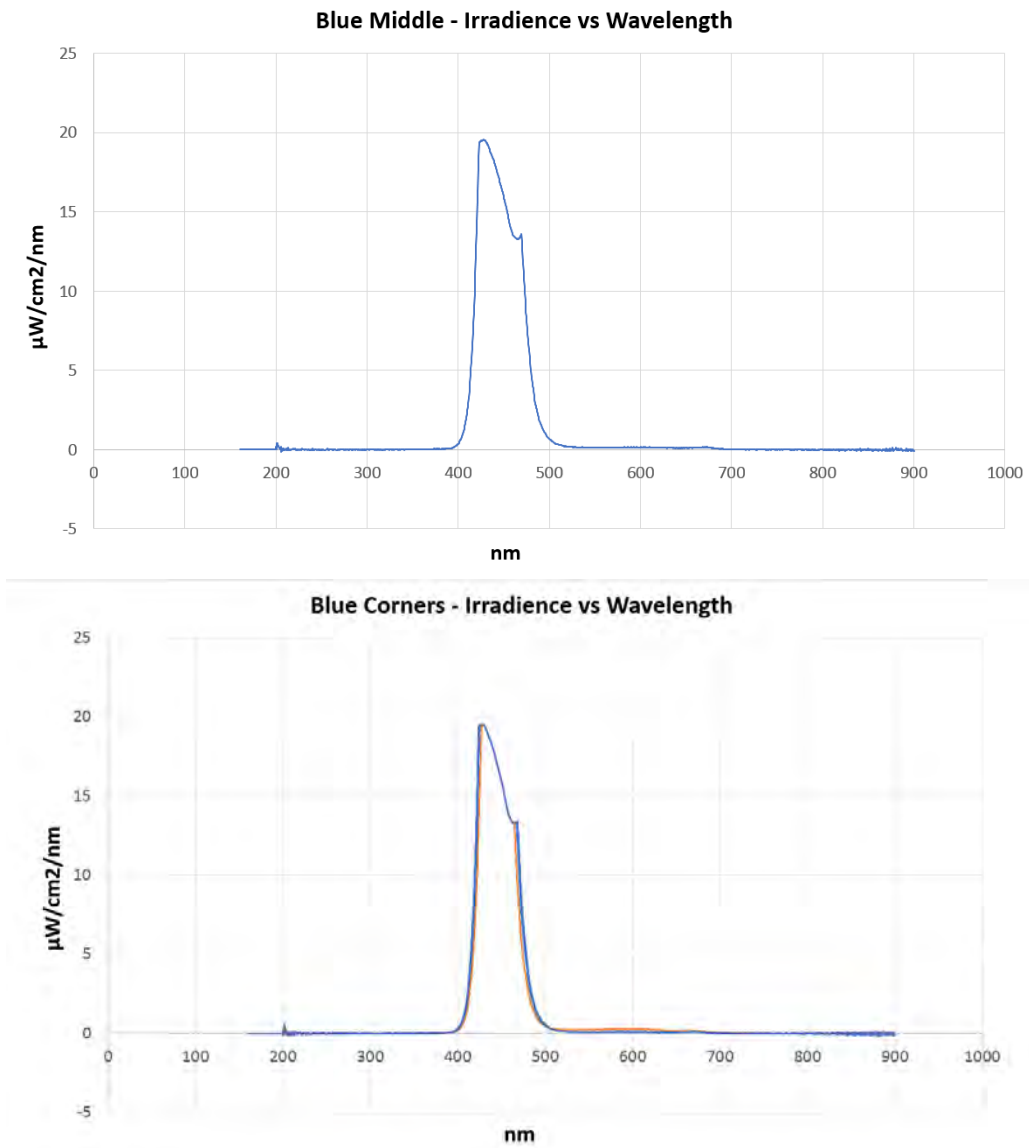


Figure 17: Blue board irradiance, with the upper graph showing the irradiance at the centre of the tray and the lower figure showing the four superimposed graphs of irradiance at each corner of the tray.

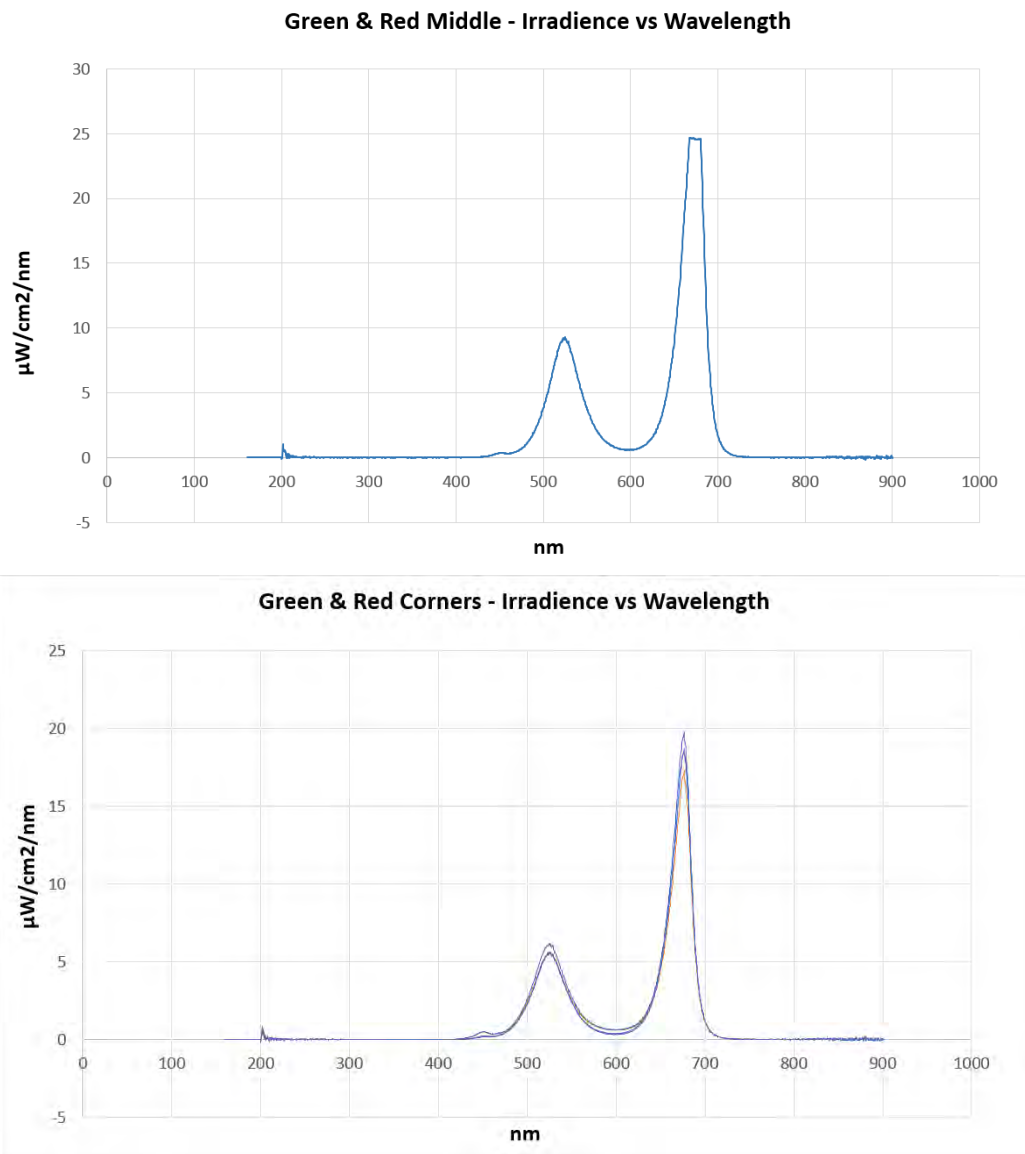


Figure 18: Green & red board irradiance, with the upper graph showing the irradiance at the centre of the tray and the lower figure showing the four superimposed graphs of irradiance at each corner of the tray.

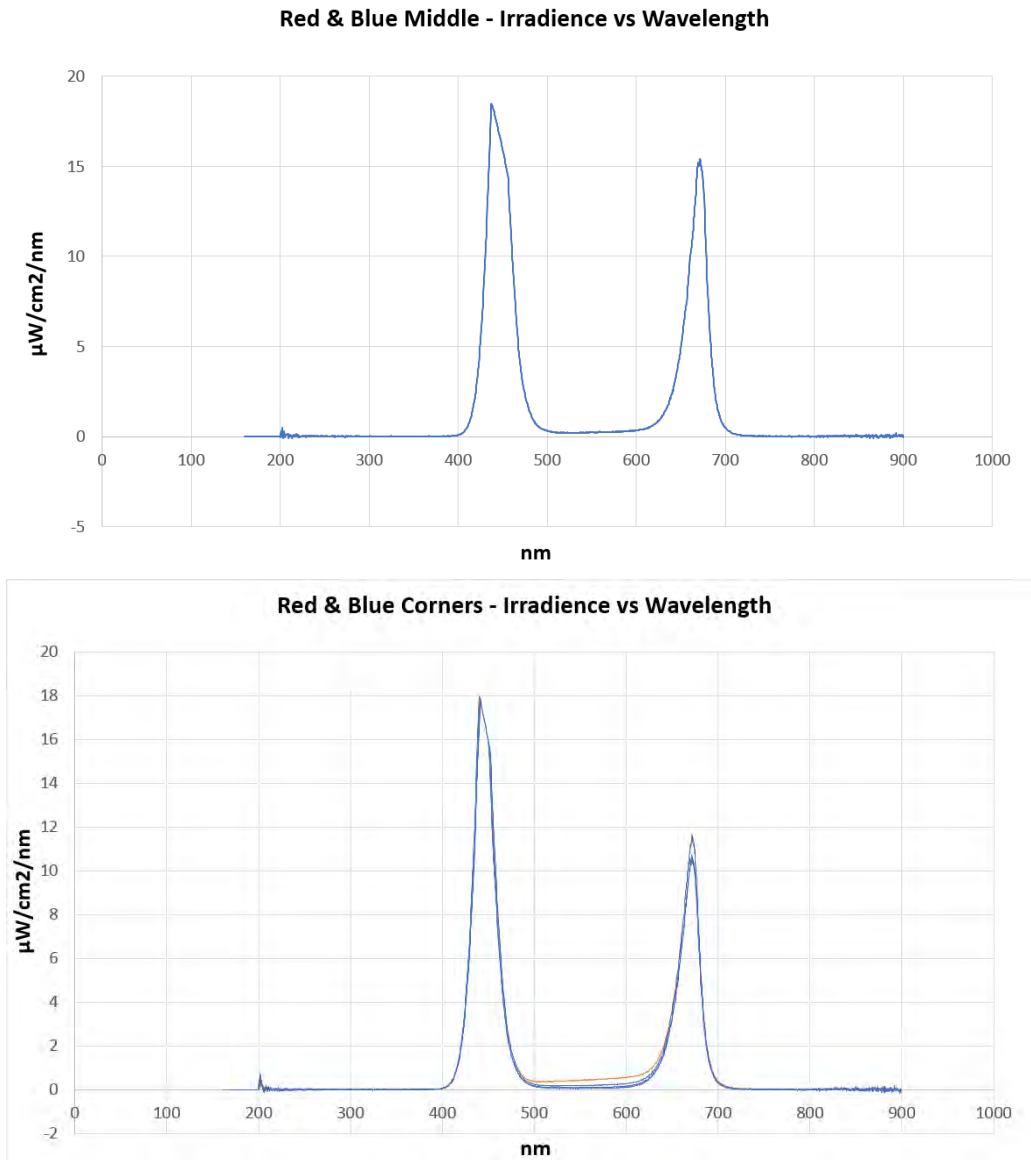


Figure 19: Red & blue board irradiance, with the upper graph showing the irradiance at the centre of the tray and the lower figure showing the four superimposed graphs of irradiance at each corner of the tray.

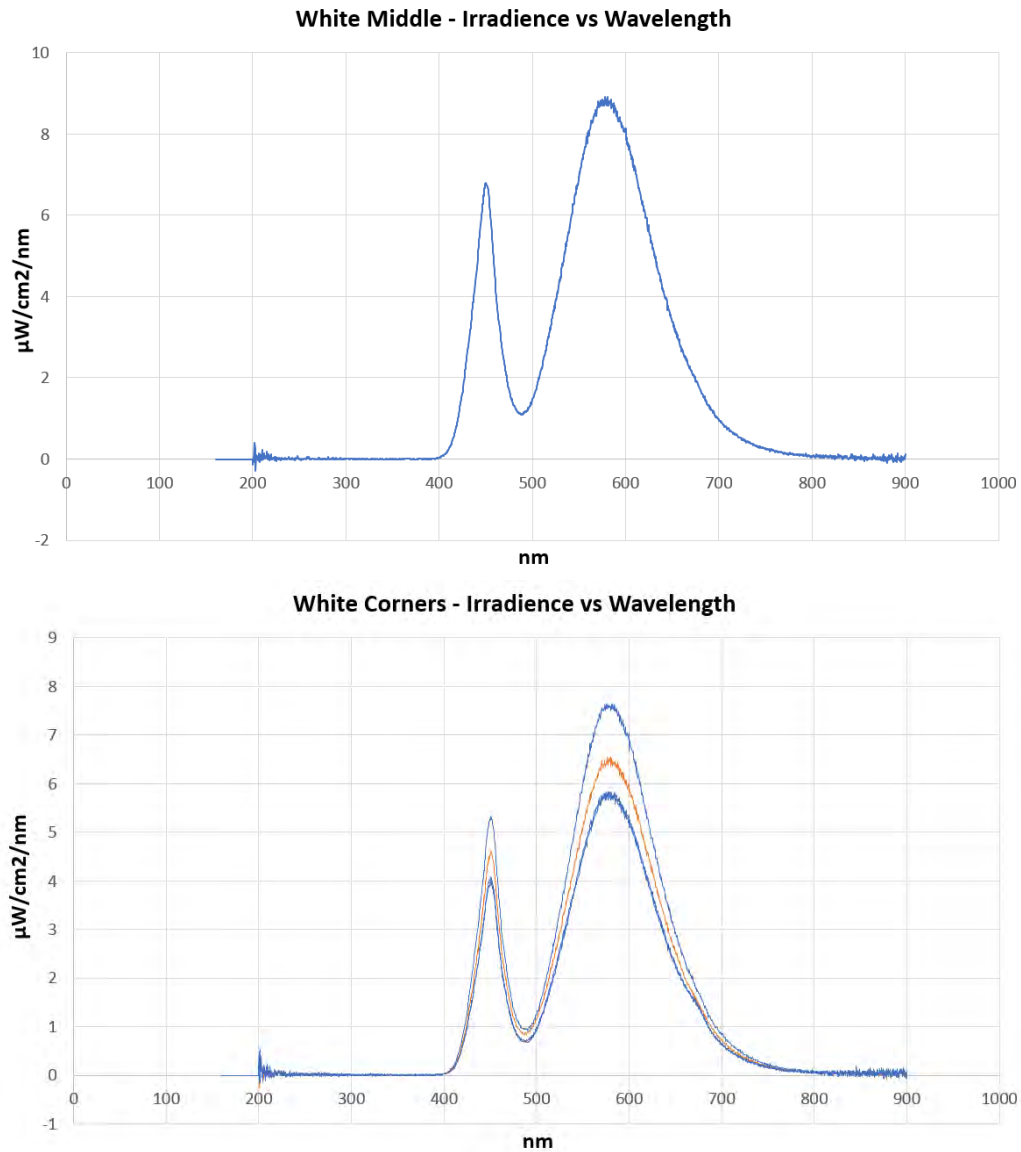


Figure 20: Green & red board irradiance, with the upper graph showing the irradiance at the centre of the tray and the lower figure showing the four superimposed graphs of irradiance at each corner of the tray.

In the scientific literature of plant growth using artificial light, PPFD is the most common and useful measure of light, but due to a PPFD measuring device not being available, light intensity data obtained was only measured from lux meter data. However, light data in the literature for plant growth considers PPFD as the most important quantity. Although a PPFD measuring device

was unavailable, a spectrometer became available after the experiment had taken place in order to gather irradiance data for the LED boards. The PPFD values could then be predicted by numerically finding the area under the curves in Figures 15-20. Spectral data was split into three graphic regions: Blue (400-500 nm), Green (500-600 nm) and Red (600-700 nm). Then for each spectrometer irradiance plot, the area under the curve in each colour region was geometrically approximated to find the PPFD contribution of each colour.

Note, by integrating Figures 15-20, one can obtain $\mu W/cm^2$ values in each of the three colour regions. This can be converted to $\mu mol/m^2/s$ by firstly noting the following equation for light energy:

$$E = N_{\lambda} \frac{hc}{\lambda} \quad (4)$$

where N_{λ} is number of photons at wavelength λ and h and c are the planck constant and speed of light respectively. Appropriately converting units and writing energy as function of irradiance, one can then find the following relation for PPFD value in $\mu mol/m^2/s$:

$$PPFD = 8.3488 \times 10^{-3} \int I d\lambda \quad (5)$$

where the integral is the area under the curve in Figures 15-20. Values of PPFD for all boards in the experiment are given in Table 4.

Table 4: PPFD contributions from blue, green and red light for all boards used in the Little Gem lettuce growth experiment as calculated by Equation 5 with the integral calculated from the area under the curve in spectrometer data displayed in Figures 15-20.

Board	Blue	$\mu\text{mol}/\text{m}^2/\text{s}$ Green	Red	Total
Green	0	50.3	0	50.3
Red	0	0	70.2	70.2
Blue	43.1	0	0	43.1
RG	0	22.9	48.6	71.5
RB	24.4	0	24.3	48.7
White	9.8	28.3	20.5	58.6

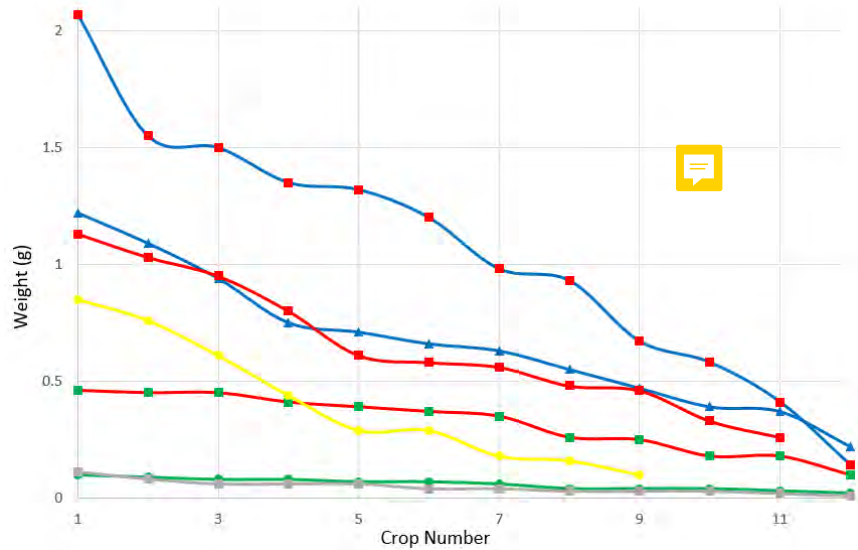
2.3.2 Lettuce Growth

At the end of 21st day, the experiment time finished. From the lettuces that were initially planted, the tray under no light died within one week, while all of the trays under light show growth with different characteristics, as can be seen from the photographs in Figure 22. The lettuce tray left in the heated glasshouse (approx 15°C) as a reference showed very slow development by the end of 21 days, this shows the effect of the winter short daylight hours as well as temperature sensitivity of Little Gem lettuces.

Table 5: Lettuce crop weights after 21 days, with green and red describing a relatively high and low weight compared to the mean of the total crops respectively. Also included are the total combined weight, the average weight, the standard deviation and the variance for each crop tray. Numbers in bold are above or below one standard deviation from their tray's average.

	Lettuce Crops After 21 Days						
	<i>Weight of Crop (g)</i>						
	Blue & Red	Blue	Red	Red & Green	White	Green	Greenhouse
	2.07	1.22	1.13	0.46	0.85	0.1	0.11
	1.55	1.09	1.03	0.45	0.76	0.09	0.08
	1.5	0.94	0.95	0.45	0.61	0.08	0.06
	1.35	0.75	0.8	0.41	0.44	0.08	0.06
	1.32	0.71	0.61	0.39	0.29	0.07	0.06
	1.2	0.66	0.58	0.37	0.29	0.07	0.04
	0.98	0.63	0.56	0.35	0.18	0.06	0.04
	0.93	0.55	0.48	0.26	0.16	0.04	0.03
	0.67	0.47	0.46	0.25	0.1	0.04	0.03
	0.58	0.39	0.33	0.18	N/A	0.04	0.03
	0.41	0.37	0.26	0.18	N/A	0.03	0.02
	0.14	0.22	N/A	0.1	N/A	0.02	0.01
Total	12.7	8	7.19	3.85	3.68	0.72	0.57
Average	1.06	0.67	0.65	0.32	0.41	0.06	0.05
Std Dev	0.55	0.3	0.29	0.12	0.27	0.03	0.03
Variance	0.3	0.09	0.08	0.02	0.07	0.001	0.001
CV	0.52	0.45	0.45	0.38	0.67	0.5	0.6

Figure 21: Weights of each of the 12 planted lettuce crops in each tray after 21 days, with each colour graph corresponding to the respective LED colour treatment, and the grey line corresponding to the natural light outdoor greenhouse tray.



In Table 5 and Figure 21, the weights of all the crops are displayed, these represent the weights of the plant cut from the root immediately after being cut. It is interesting to note the variety of weights both within one tray and across the experiment. For example, the lettuce with the highest weight within the red & green tray (0.46 g) is considerably higher than the lowest weight within the red & blue tray (0.14 g) despite the red & blue board giving a much higher average weight (1.06 g) than the red & green board's average crop weight (0.32 g). This high variation in weight within trays under the same light exposes a difficulty in controlling the experimental parameters, namely that plant growth is sensitive to the individual nature of each seed and its behaviour, as seeds in effectively identical conditions can vary considerable in growth behaviour. This makes it difficult to deduce clear general patterns about plant growth response to light, particularly based on relatively small sets of data. Statistically, from Table 5 averages, standard deviations and variances are given. From looking at the standard deviations and the averages it can be seen that within each tray there is significant variation in crop weight for each tray, with the standard deviation equal to approximately half of the average.

From Table 6, results are shown measuring the weight of the crops both immediately after cut-

ting from trays and then after 12 hours of drying at 80°C. Most of the trays under LED lighting boards show a fractional weight loss of 0.92 - 0.94, apart from green which had a fractional loss of only 0.81. This could be possibly due to the fact that, as discussed in the introduction, red and blue frequencies of light are crucial for photosynthesis and the green board is the only one without any element of either red or blue light. Also, the fractional weight loss of the greenhouse tray was very low, but as this was the only plant tray outside of the controlled environment LED growing lab and instead out in a greenhouse, the winter conditions were very much colder and light intake levels much lower, thus the level of photosynthesis possible must have also been greatly inhibited.

Table 6: Weight of crops before and after drying, to show water retention.

Board Colour	Weight (g)	Dry Weight (g)	Fractional Loss
Red	7.19	0.4	0.94
Green	0.72	0.14	0.81
Blue	8.00	0.6	0.93
Red & Blue	12.70	0.8	0.94
Red & Green	3.85	0.26	0.93
White	3.68	0.28	0.92
Greenhouse	0.57	0.18	0.68

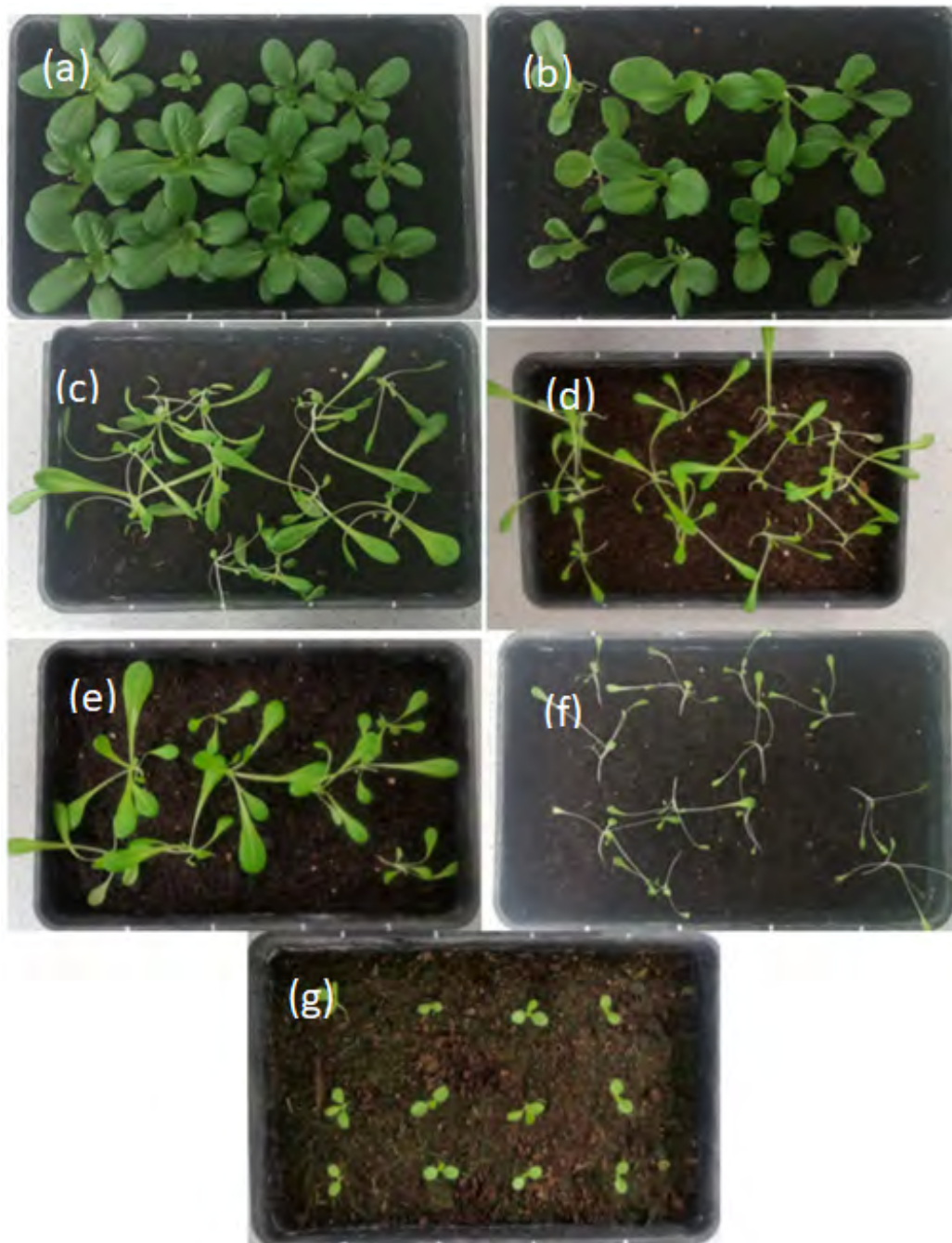


Figure 22: Lettuce trays after 21 days of growing. Test treatments as follows: red & blue (a), blue (b), red (c), red & green (d), white (e), green (f) and the reference greenhouse (g).

Treatments	White	Red	Blue	Green	Red Green	& Red Blue	& Greenhou
Average Leaf Number	7.1	7.4	7.0	5.5	6.6	8.3	2.8
Maximum shoot (apex) length (cm)	1.7	1.2	1.5	2.5	1.5	1.0	1.5
Minimum shoot (apex) length (cm)	1.0	1.0	0.9	1.0	1.0	0.4	0.9
Average shoot (apex) length (cm)	1.3	1.2	1.2	1.8	1.3	0.6	1.1
Maximum leaf area (cm²)	6.8	7.5	12.3	0.8	2.5	10.6	1.1
Minimum leaf area (cm²)	1.5	4.1	6.8	0.1	1.9	3.4	0.9
Average leaf area (cm²)	4.4	5.7	8.9	0.6	2.3	8.2	1.1
Maximum leaf height and width (cm)	H = 5.7 W = 2.2	H = 5.8 W = 2.2	H = 5.7 W = 3.7	H = 1.8 W = 0.7	H = 3.8 W = 1.9	H = 5.0 W = 4.5	H = 1.6 W = 1.6
Minimum leaf height and width (cm)	H = 3.0 W = 1.0	H = 4.5 W = 1.6	H = 3.3 W = 1.9	H = 0.5 W = 0.3	H = 3.0 W = 1.0	H = 3.0 W = 2.0	H = 1.4 W = 1.1
Average leaf height and width (cm)	H = 4.2 W = 1.6	H = 5.3 W = 1.8	H = 4.9 W = 3.0	H = 1.3 W = 0.6	H = 3.5 W = 1.4	H = 4.2 W = 3.0	H = 1.5 W = 1.2

Table 7: Lettuce parameter measurements, including shoot lengths, leaf areas, and leaf geometries taken from multiple leaves in each tray.

As Figure 22 shows and Tables 6 and 7 quantify, the lettuces' growth varied greatly between trays after 21 days.

Firstly, the lettuces fed with red & blue (50%-50%) light mix gave the most healthy and compact result with big dark green leaves that have close length and width values, plants have a small apex length but strong and show no bending (meaning mechanical drooping of the stem and plant due to weak plant relative to the stem length) unlike all other lettuces. This tray gave the biggest

yield. The second best growth results came from 100% blue light. The plants seem compact and have large and dark green leaves, apex length is small but not as strong as for the red & blue and has small bending. Leaves have close length and width and so appear compact.

On the contrary, the lettuces grown under red light (100%) have the opposite growth pattern, with excess elongation at branches and very stretched leaves with poor length/width ratio. This means the leaves grew mostly horizontally without the ability to hold their own weight and therefore tangled with each other. However, if measuring only yield (in weight and leaf area), this tray was the third largest.

The tray under green & red (50%-50%) LED treatment gave excessive stem elongation and leaves with low width to length ratio, similar to both the 100% red and 100% green LED lit trays. Plants under green (100%) light treatment gave the weakest results by having the smallest leaf area and long apex length with a weak body. White LEDs gave a moderate result more similar to the green & red mixture, but with slightly bigger leaves and better leaf length to width ratio. The plants which grew in the greenhouse appear to be in a much earlier phase of growth, equivalent to the end of the first week for LED experiment lettuces. This probably due to short day length and a 7-10 °C temperature variation even though the glasshouse is heated.

Overall, it is clear from both the photos and measurements of weight, water retention and leaf & shoot size that the boards which produced the best lettuces were the blue, and blue & red lights, the latter being the best of all. Both the green and the greenhouse reference tray produced the weakest growth. Red & blue and blue LED boards gave the best result in colour, compact growth and total weight. Sole green light is observed to produce the weakest crops among all other LED boards in the trial. Red light gave excessive elongation while exhibiting a reasonably high amount of leaf area and dry weight. Statistical analysis of all properties measured and the variation between data under different light recipes is shown in Table 8. If we use the coefficient of variation (CV) of a measure of how much the data varies under different light recipes, because it is a proportional representation of how much the data varies about the average, it is clear that some properties varied more than others. For example the CV for fresh weight is 0.83 and for leaf area it is 0.74, but for leaf number and shoot length the CV is 0.28 and 0.29 respectively. This means that leaf area and fresh weight, as expected, are very sensitive to different light quality, but shoot length and leaf number

are not as sensitive.

	Blue & Red	Blue	Red	Red & Green	Green	White	Greenhouse	Average	Stdev	Variance	CV
Weight (g)	12.7	8	7.19	3.85	0.72	3.68	0.57	5.24	4.35	18.9	0.83
Dry Weight (g)	0.8	0.6	0.4	0.26	0.14	0.28	0.18	0.38	0.24	0.06	0.63
Leaf number	8.3	7	7.4	6.6	5.5	7.1	2.8	6.39	1.79	3.21	0.28
Shoot Length (cm)	0.6	1.2	1.2	1.3	1.8	1.3	1.1	1.21	0.35	0.12	0.29
Leaf Area (cm ²)	8.2	8.9	5.7	2.3	0.6	4.4	1.1	4.46	3.32	11	0.74
Leaf Height (cm)	4.2	4.9	5.3	3.5	1.3	4.2	1.5	3.56	1.58	2.5	0.44
Leaf Width (cm)	3	3	1.8	1.4	0.6	1.6	1.2	1.8	0.9	0.81	0.5

Table 8: Averaged values for measured parameters in each tray combined, with mean, standard deviation, variance and coefficient of variation (CV) calculated for each parameter.

2.3.3 Possible Experimental Improvements

This experiment was both short term and limited by the fact that the experiment was designed and built from scratch with no pre-existing experimental conditions or equipment already built or implemented. If the designing and building of the experiment were somewhat outsourced appropriately, both time and technical limitations would be less and there would be areas which could be easily improved on, for more extensive future tests.

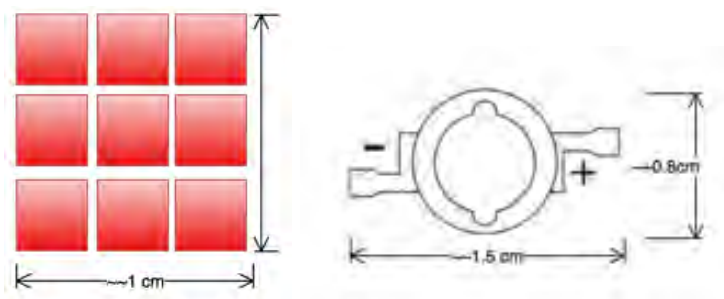


Figure 23: Nine Osram LED units could fit into 1 cm^2 of space shown on the left, this is comparable to one Bridgelux light as seen on the right.

Regarding the size of the experiment, more light recipes could be tested, with all boards including some level of red and blue light, as it is clear from both literature and this experiment's results that red and blue are necessary elements of any optimal plant light recipe for crop growth. Additionally, given the variable results measured within each tray, a higher number of seeds per light recipe could increase the validity of results.

This experiment kept the electrical energy supplied to each LED board constant as well as the experimental setup and conditions, but the light data from the spectrometer which was measured and analysed after the experiment shows quite significant differences in PPFD between different LED boards and therefore PPFD becomes a second variable of consideration for a plant's growth (alongside LED spectral recipe). Therefore, if a PPF detector or spectrometer is available before future tests were to begin, PPFD could be known for each board and then either the current through the LEDs or the distance to the crops adjusted until all the boards are giving constant PPFD to trays. This would ensure that the experiment's only independent variable (from the perspective of the plants) would be light spectral recipe and not intensity, so later modelling of plant response

to different wavelengths of light would be more effective. However, this project's primary focus, unlike most of the related experimental literature, is energy efficiency and not solely plant science, so varying the current between LED boards or moving them closer or further from the plant canopy would compromise the constant energy consumption and setup, thus taking the experiment's focus away from energy efficiency.

With regards to the boards and LEDs chosen, a potential improvement could be to instead choose the Osram LEDs instead of the Bridgelux. During the preliminary tests, some of the solder joints became loose and temporarily affected the performance of the board, requiring to be re-soldered. This issue could be eradicated by using the Osram lights and having the lights professionally fixed to a circuit. Also, as visible in Figure 23, the Osram lights are considerably more spatially compact, meaning a higher efficacy. The Osram lights are also more energy efficient and therefore higher PPFD values are possible with less energy consumption. Also, an Arduino based temperature trip could be designed to make the tests safer and easier to manage. An SMPS power supply design could implement different duty cycles on the lighting rig.

Other environmental conditions could also be improved by running experiments in an existing CEA facility where equipment is available to regulate humidity and CO₂ concentration at an optimum level and at a sufficient scale to investigate a large number of different light recipes. This project's experiment had controlled environmental conditions such as CO₂ concentration and humidity constant, but these were not optimum, so although growth differences from spectral recipe could be seen without interference of variable environmental conditions, overall magnitude of plant growth could have been inhibited by the other controlled conditions. It is therefore not possible to comment objectively on maximum yield potential of crops under particular light recipes.

Regarding additional quantities which could be measured at the end of the experiment, the use of a colorimeter could be useful to determine precisely and quantitatively the colours of the plants. Measurements of chlorophyll should also be considered to gain full information about the health of the plants. Other data such as stomatal conductance could also been taken, as the more available output data there is, the better the potential for modelling, particularly with sophisticated non-linear fitting models like deep neural networks. The field of horticulture is one where the number of possible output variables is very high, as demonstrated for example in the literature, where data

from 70 different traits from molecules to whole plant performance was used to meta-analyse plant responses to light intensity [6].

2.4 Section Summary

Lactuca Sativa "Little Gem" lettuce was grown using six different light spectral recipes containing red, blue, green and white LED bulbs, each in identical growth tents under controlled heating and ventilation environments. Although there is existing research on light recipe optimisation for Lettuce, none looked specifically at Little Gem and instead looked at other varieties. This is despite increasing interest in Little Gem lettuce for its ease of growth and commercial potential. However as one may expect, the recipe which was most favourable for Little Gem growth was the blue and red combination, which is also generally seen for other lettuce varieties in the literature.

3 Neural Network Analysis on LED Lighting for Lettuce

3.1 Introduction

Although some trends can be observed from experimental data about the response of plants to various spectral distributions of light, whole spectral modelling of plant spectral response can be difficult using traditional modelling techniques such as linear regression. This is because there are a large number of input conditions, including light intensity and spectral distribution, but also CO₂ concentration, photo period, temperature, humidity, choice of nutrients etc. Additionally, there are a vast number of measurable output parameters, all of which are related to each other in a complex way [6], which make choosing optimal light recipes based on simpler modelling techniques such as linear regression difficult.

Neural networks are commonly used for image recognition and function fitting and prediction. They are useful for modelling systems with large amounts of available data and can be useful for systems with a high number of input and output variables. Neural networks also have good generalisation to regions where data is not available, making them predictive. But due to the multilevel complexity of these networks, the function relating inputs to outputs, although analytic, is effectively impossible to understand.

In a recent review paper, 72 studies on neural networks for CEA were highlighted, suggesting the application of neural networks in CEA is growing in popularity [66]. For example, a study which used neural networks for predicting plant growth and yield in greenhouse environments compared a neural network approach to other fitting methods such as non-linear regression and found it to be superior [67]. It is for these reasons that this work tests neural networks for optimal light quality prediction, this is using the neural network fitting app in MATLAB on LED recipes for growing lettuce. The MATLAB neural network fitting app is a simplified neural network tool, it does not allow complete fundamental customisation of neural network structure and working, but it is practical and sufficient as this project is interested in assessing the applicability of neural networks as a method without spending too much time in doing so.

3.2 Methodology

3.2.1 Neural Networks

A method suitable for modelling systems with nonlinear behaviour and many input and output parameters is neural network machine learning [68]. Artificial neural networks in computing are based on the neural network structures in the brain, with a complex network of nodes (neurons) and connections.

Complex neural networks can have multiple neurons within multiple layers and multiple output values, Figure 24 shows the key features and structure of a complex neural network.

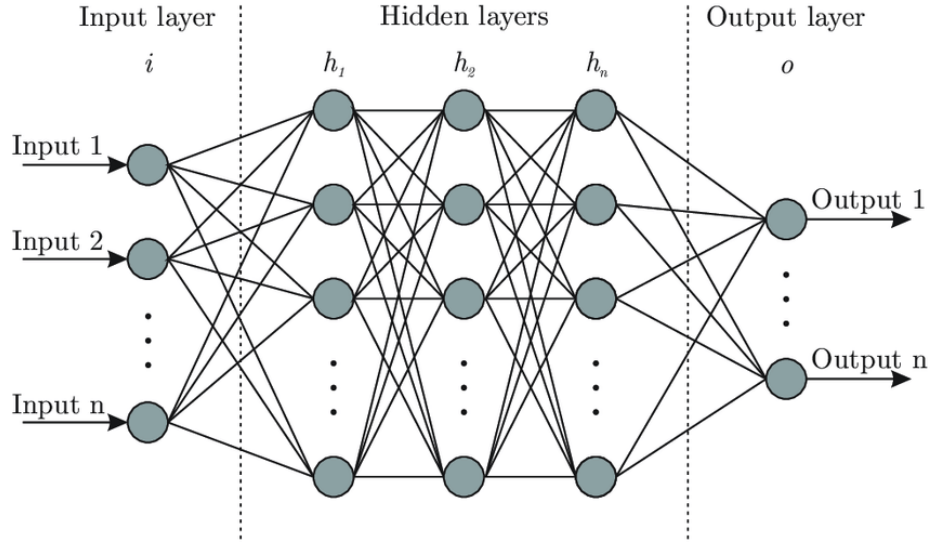


Figure 24: Explanatory diagram of the architecture of a neural network [69].

However, for introducing the basic mathematics of how neural networks are modelled, it is best to start with the most simple case: a neural network consisting of n inputs, one neuron and one output, this is called a perceptron [70] and the schematics of this are shown in Figure 25.

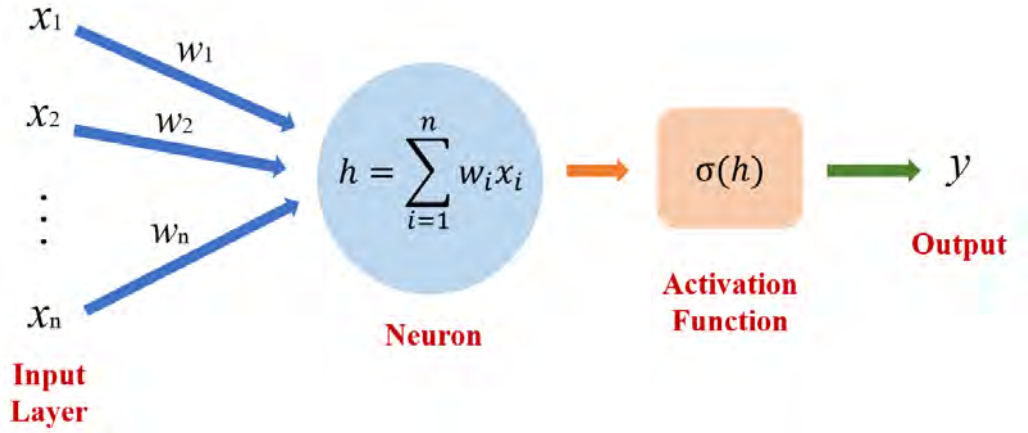


Figure 25: Schematic diagram of a perceptron: a neural network with only one neuron and one output value.

As data passes through a neural network from the input stage to the output stage this is called forward propagation. For a perceptron, this occurs in three stages:

1. Each input value, x_i is multiplied by a respective synaptic weight w_i to decide how strongly x_i will influence the following neuron in the network. This is summed over all input values and weights:

$$\Sigma = (x_1 \times w_1) + (x_2 \times w_2) + \dots + (x_n \times w_n) = \vec{x} \cdot \vec{w}$$

2. A value, b , known as the bias (or offset) is added to the sum from the previous point. This is necessary to move the entire activation function to the left or right to generate the required output values. Now we have:

$$h = \vec{x} \cdot \vec{w} + b$$

3. Finally, enter the value h into a non-linear *activation function*. These are important and used to introduce non-linearity to the output of the neurons, they decide whether the signal is strong enough for the neuron to fire. A simple example of an activation function for a perceptron is a step function, which determines whether the neuron will fire or not, dependent on the value of some threshold value θ [71]:

$$\hat{y} = \sigma(h) \begin{cases} 0, & \text{if } h \leq \theta \\ 1, & \text{if } h > \theta \end{cases}$$

So far, this explains only how a neural network takes inputs and reaches an output, but the main advantage and reason for the application of artificial neural networks is their ability to learn from a set of data in order to be able to predict accurate outputs from new input data. For this, back propagation and optimisation are needed.

Backpropagation (backward propagation of errors) refers to the algorithm for computing the gradient of the loss function with respect to the weights. The backpropagation carried out in a perceptron is explained in the following steps. The first involves a *loss function*, which is a measure of how far the outputs from the neural network are from the desired output. This is often quantified by the *mean squared error* when computing regression problems. The mean squared errors between actual and predicted output data are used to determine a *cost function*, such that:

$$MSE_i = (y_i - \hat{y}_i)^2$$

$$C = \frac{1}{n} \sum_{i=1}^n (y_i - \hat{y}_i)^2$$

The cost function will therefore give information about the extent to which the current weights and biases in the neuron(s) are wrong. In order to use this information to redetermine better values and reduce the error, understanding of how the cost function changes in relation to weights and bias by calculating gradients is required. The gradients of the cost function are found with respect to the weights and bias ($\frac{\partial C}{\partial w_i}$ and $\frac{\partial C}{\partial b}$) and this information is used by an optimisation algorithm, for example the *gradient descent* algorithm. This changes the weights and bias, proportional to the negative of the corresponding gradient of the cost function. With the new weights and bias, the cost function is recalculated and backpropagation repeated, until the error between neural network produced outputs and desired outputs is sufficiently small.

In order to train a neural network on a data set, the input and output data is split into three sets:

1. **Training Set:** This is the set of data that the neural network analyses and learns from using backpropagation and optimisation; both inputs and correct outputs are needed.

2. **Validation Set:** Used to validate the model and its hyperparameters, e.g., number of hidden layers and the learning rate; both inputs and correct outputs are needed.
3. **Test Set:** The sample of data used to provide an unbiased evaluation of a final model fit on the training dataset; only inputs needed.

In the practical application of artificial neural networks, the parameters chosen by the user (hyperparameters) will firstly be the number of hidden layers & neurons in these layers, which control the complexity of the functions that will produce the output predictions and secondly, the learning rate which determines how much variation there will be in the weights and bias in each iteration of backpropagation.

There are a number of empirically derived rules of thumb for choosing hidden layers and neurons, one of the most common is for the number of hidden neurons to be between the size of the input and output layers. Increasing the number of hidden neurons and/or layers by too much can lead to over-fitting because it will make it easier for the neural network to memorize the training set, that is to learn a function that perfectly separates the training set but that does not generalise to unseen data. Regarding the learning rate, default choices are typically between 0 and 1, i.e. in each iteration of the optimisation algorithm, the weights and bias are changed by a factor of this number multiplied by the estimated error, to form new values for weights and bias which go back through the neural network.

3.2.2 Lettuce Data Collection

To begin with, the experimental data from the section 2.3 of this report was used for fitting. However, due to the small amount of data in this experiment (six LED spectral recipes), neural network training expectantly gave no meaningful fit. This is to be expected for a neural network fed with only six inputs and outputs. However, with an extensive literature search of LED light recipe tests for lettuce variants, data gathered from these sources was combined with experimental results from this project and then fitted to. This is no simple task however due to the differences in data between each different experiment in the literature.

Firstly, the $\mu\text{mol m}^{-2} \text{s}^{-1}$ values were established, both total and individual contributions from blue (400-500 nm), green (500-600 nm) and red (600-700 nm) LEDs for all experiments in the literature,

the same as was done in this project's lettuce experiment data analysis (displayed in Table 4). Output data was also gathered, with three output variables chosen to be plant weight, stem length and leaf area, as these were most commonly taken quantities in the literature and were also measured in section 2's experiment.

A large amount of data was gathered from the following experimental literature:

1. 'Light emitting diodes as a radiation source for plants' - R. J. Bula, R. C. Morrow, T. Tibbitts, D. Barta, R. Ignatius, and T. Martin, *HortScience*, vol. 26, no. 2, pp. 203-205, **1991** [15]
2. 'Stomatal conductance of lettuce grown under or exposed to different light qualities' - H.-H. Kim, G. D. Goins, R. M. Wheeler, and J. C. Sager, *Annals of Botany*, vol. 94, no. 5, pp. 691-697 **2004** [72]
3. 'Leaf Shape Index, Growth, and Phytochemicals in Two Leaf Lettuce Cultivars Grown under Monochromatic Light-emitting Diodes' - K. Son, J. Park, D. Kim, M. Oh, et al., *Korean Journal of Horticultural Science & Technology*, vol. 30, no. 6, pp. 664-672, **2012** [73]
4. 'Effect of green light wavelength and intensity on photomorphogenesis and photosynthesis in *Lactuca sativa*' - M. Johkan, K. Shoji, F. Goto, S.-n. Hahida, and T. Yoshihara, *Environmental and Experimental Botany*, vol. 75, pp. 128-133, **2012** [51]
5. 'Leaf Shape, Growth, and Antioxidant Phenolic Compounds of Two Lettuce Cultivars Grown under Various Combinations of Blue and Red Light-emitting Diodes' - K.-H. Son and M.-M. Oh, *HortScience*, vol. 48, no. 8, pp. 988-995, **2013** [74]
6. 'Light intensity and photoperiod influence the growth and development of hydroponically grown leaf lettuce in a closed-type plant factory system' - J. H. Kang, S. KrishnaKumar, S. L. S. Atulba, B. R. Jeong, and S. J. Hwang, *Horticulture, Environment, and Biotechnology*, vol. 54, no. 6, pp. 501-509, **2013** [75]
7. 'The effects of red, blue, and white light-emitting diodes on the growth, development, and edible quality of hydroponically grown lettuce (*Lactuca sativa* L. var. capitata)' - K.-H. Lin, M.-Y. Huang, W.-D. Huang, M.-H. Hsu, Z.-W. Yang, and C.-M. Yang, *Scientia Horticulturae*, vol. 150, pp. 86-91, **2013** [76]

8. 'Influence of Green, Red and Blue Light Emitting Diodes on Multiprotein Complex Proteins and Photosynthetic Activity under Different Light Intensities in Lettuce Leaves (*Lactuca sativa* L.)' - S. Muneer, E. J. Kim, J. S. Park, and J. H. Lee, *International journal of molecular sciences*, vol. 15, no. 3, pp. 4657-4670, **2014** [77]
9. 'Photobiological Interactions of Blue Light and Photosynthetic Photon Flux: Effects of Monochromatic and Broad-Spectrum Light Sources' - K. R. Cope, M. C. Snowden, and B. Bugbee, *Photochemistry and photobiology*, vol. 90, no. 3, pp. 574-584, **2014** [78]
10. 'Growth, Photosynthetic and Antioxidant Parameters of Two Lettuce Cultivars as Affected by Red, Green, and Blue Light-emitting Diodes' - K.-H. Son and M.-M. Oh, *Horticulture, Environment, and Biotechnology*, vol. 56, no. 5, pp. 639-653, **2015** [79]
11. 'Effect of the Spectral Quality and Intensity of Light-emitting Diodes on Several Horticultural Crops' - M. Urrestarazu, C. Najera, and M. del Mar Gea, *HortScience*, vol. 51, no. 3, pp. 268-271, **2016** [80]
12. 'Growth and nutritional properties of lettuce affected by mixed irradiation of white and supplemental light provided by light-emitting diode' - X.-l. Chen, X.-z. Xue, W.-z. Guo, L.-c. Wang, and X.-j. Qiao, *Scientia horticulturae*, vol. 200, pp. 111-118 **2016** [81]
13. 'Leaf Photosynthetic Rate, Growth, and Morphology of Lettuce under Different Fractions of Red, Blue, and Green Light from Light-Emitting Diodes (LEDs)' - W. H. Kang, J. S. Park, K. S. Park, and J. E. Son, *Horticulture, Environment, and Biotechnology*, vol. 57, no. 6, pp. 573-579, **2016** [82]
14. 'Green light enhances growth, photosynthetic pigments and CO₂ assimilation efficiency of lettuce as revealed by 'knock out' of the 480–560 nm spectral waveband' - H. Liu, Y. Fu, and M. Wang, *Photosynthetica*, vol. 55, no. 1, pp. 144-152, **2017** [83]
15. 'Improving "color rendering" of LED lighting for the growth of lettuce' - T. Han, V. Vaganov, S. Cao, Q. Li, L. Ling, X. Cheng, L. Peng, C. Zhang, A. N. Yakovlev, Y. Zhong, et al., *Scientific Reports*, vol. 7, p. 45944, **2017** [84]
16. 'Growth differences among eight leaf lettuces cultivated under led light and comparison of two leaf lettuces grown in 2016 and in 2018' - M. OZAWA, Y. SANO, Y. NAKANO, and M.

AKUTSU, *ICIC express letters. Part B, Applications: an international journal of research and surveys*, vol. 10, no. 11, pp. 985-993, **2019** [85]

The problem with inputting large amounts of data from multiple different experiments is that although the data on lighting intensity and spectrum is well documented, the other experimental conditions such as treatment in seedling phase, photoperiod, temperature and carbon dioxide concentration are not usually identical. It is therefore difficult to find direct relations between lighting and output data across all the experiments without results being obscured by other important factors outside light.

Additionally, as noted by Ozawa *et al.* [85], the two sets of data for lettuce grown in separate 2016 and 2018 experiments saw large differences in output results, even with the same light recipes and intensities. Their results show that plants grown in 2016 had significantly lower fresh weight, leaf weight, and dry weight: one-sixth to one-eighth of those in 2018. This lead them to conclude that: "When growing plants in a commercial plant factory, it might be necessary to use an automatic system for all of them. Furthermore, when conducting experiments even in a growth cabinet and chamber, one must grow plants during the same period and with the same people conducting experiments. The same experiments should be repeated even after changing the personnel conducting the experiments."

Some of the experimental data in the literature did not give information about PPFD contributions in micromoles, but like for this project's Little Gem lettuce growing experiment, gave spectral distributions, by which PPFD is deducible similarly to in section 2.3 of this thesis. Also, regarding output data, from the 137 light recipes throughout all 16 papers, only 24 recipes had information about fresh weight, leaf area and stem length. Because of that limitation, for the neural network fitting, only fresh weight and leaf area were considered. This increased the number of data points from 24 to 77. So although some output information is lost, two key output parameters are still available to fit to with an increased 77 data points for each of the two outputs.

3.2.3 Normalising and Randomising the Data

Importantly, both input and output data gathered from the literature was normalised such that in each experiment the highest total $\mu\text{mol}/\text{m}^2/\text{s}$ value was set to 1, as were all of the highest output


values. All of the other values were then proportionally reduced relative to their own experiment's maximum values. This is shown for section 2's experiment in Table 9. Normalisation here aims to increase compatibility between the different experiments, as the different experiments in the literature were conducted for different lengths of time, and the germination duration and conditions were also different. Also importantly, most of the experiments looked at different types of lettuce, thus normalising their output values is particularly important.

Given Ozawa *et al.*'s findings, it further highlights how sensitive output data is to slight variations in experimental conditions excluding light intensity and recipe. It is for this reason too that the data inputted to the neural network fitting program is normalised, whereby each experiment's data was normalised with respect to its own maximum values. This is so that no input or output value could be above one and that all other data points scale proportionally with the raw data. An example of this normalising method is shown for section 2's experimental data in Table 9. Note, the full table of normalised data from all studies used in the neural network can be seen in the appendix (Table 19).

This normalisation is important in ensuring that experimental differences (excluding lighting) such as setup environmental conditions, germination time, photoperiod etc. are levelled out between different studies. The normalisation also aims to level differences between varieties of lettuce, as each variant has naturally different weight and size and dimensions, so by normalising the data the general trends of light effectiveness (both spectral contribution and light intensity) may be seen across multiple different experiments. With regards to testing a model's accuracy and precision, normalised data is also much easier to analyse, with statistical errors for example.

The data also needs to be in a random order before feeding into the neural network. As discussed previously, the training set is the data set the neural network builds the model on, it then validates it on the validation set until performance is optimised, the finalised neural network is then tested on previously unseen test data to measure its predictive effectiveness. Randomisation is important to ensure experimental data from each of the independent experiments is randomly distributed throughout the three data sets. Otherwise data from the first experiments may be predominantly in the training set and latter data in the test data set and so forth.

Raw Data							
Board	PPFD (mmol/m2/s)				Output Data		
	Blue	Green	Red	Total	Weight (g)	Shoot Length (cm)	Leaf Area (cm2)
Green	0	50.27	0	50.27	7.19	1.16	5.725
Red	0	0	70.2	70.2	0.72	1.8	0.583
Blue	43.125	0	0	43.125	8	1.18	8.875
RG	0	22.85	48.6	71.45	12.7	0.55	8.1875
RB	24.375	0	24.3	48.675	3.85	1.32	2.275
White	9.75	28.334	20.52	58.604	3.68	1.34	4.375



Normalised Data							
Board	PPFD				Output Data		
	Blue	Green	Red	Total	Weight	Shoot Length	Leaf Area
Green	0	0.70357	0	0.70357	0.05669291	1	0.065690141
Red	0	0	0.98251	0.98251	0.56614173	0.644444444	0.645070423
Blue	0.60357	0	0	0.60357	0.62992126	0.655555556	1
RG	0	0.3198	0.6802	1	0.30314961	0.733333333	0.256338028
RB	0.34115	0	0.3401	0.68125	1	0.305555556	0.922535211
White	0.13646	0.39656	0.28719	0.82021	0.28976378	0.744444444	0.492957746

Table 9: The normalisation of data from section 2's Little Gem lettuce growing experiment.

3.3 Results & Discussion

Multiple ratios of training/validation/test data were tested for neural networks of varying hidden neuron number during neural network testing. Figure 26 shows the best performing preliminary fitting results for a neural network with five hidden neurons and 70%/15%/15% training, validation and test data respectively. All plots show an R value of around 0.8 which shows reasonable fit to data generally, however the variance is high, meaning that the probability is low that any one data point is within a small error margin of the true value. An error histogram for this data is shown in Figure 27, where for all data sets, there are high errors.

Overall, this neural network generally fits well to the data and predicts output data with some accuracy. This seems to be enough to believe that both a trend exists between input and output data, and that the neural network can somewhat understand the trend. However, significant errors and large variations between accuracy in data points suggest that either the model needs improvement, or the data does not contain consistent enough behaviour to see a solid trend between inputs and outputs, to a great enough extent to allow prediction of optimal light recipes.

It is likely that the error in this model stems, at least in part, from the incoherence in data from different experiments. As discussed in the literature, even the same research group repeating the same experiment two years apart have observed large differences in output data for the same lighting recipe and intensity [85], suggesting that subtle differences in the setup have large consequences. For a more accurate model to be developed therefore, either the data set must be much larger and contain additional input and output variables to account for variations in setup conditions between different experiments, or data must be gathered from the same research group at the same time with identical conditions and environments, with only light recipe and intensity varied. In these circumstances, one might expect trends to become clear and fitting to be accurate via neural network modelling.

Additionally, neural networks could be useful to determine which output variables correlate most with light recipe and intensity. For example, leaf area and fresh weight may be less correlated with light recipe and intensity than stomatal conductance and dry weight. This would be easy to investigate due to the speed and ease of neural network fitting. But only experiments with large data

sets investigating the same plant variant in the same environmental conditions can help elucidate trends via neural network fitting.

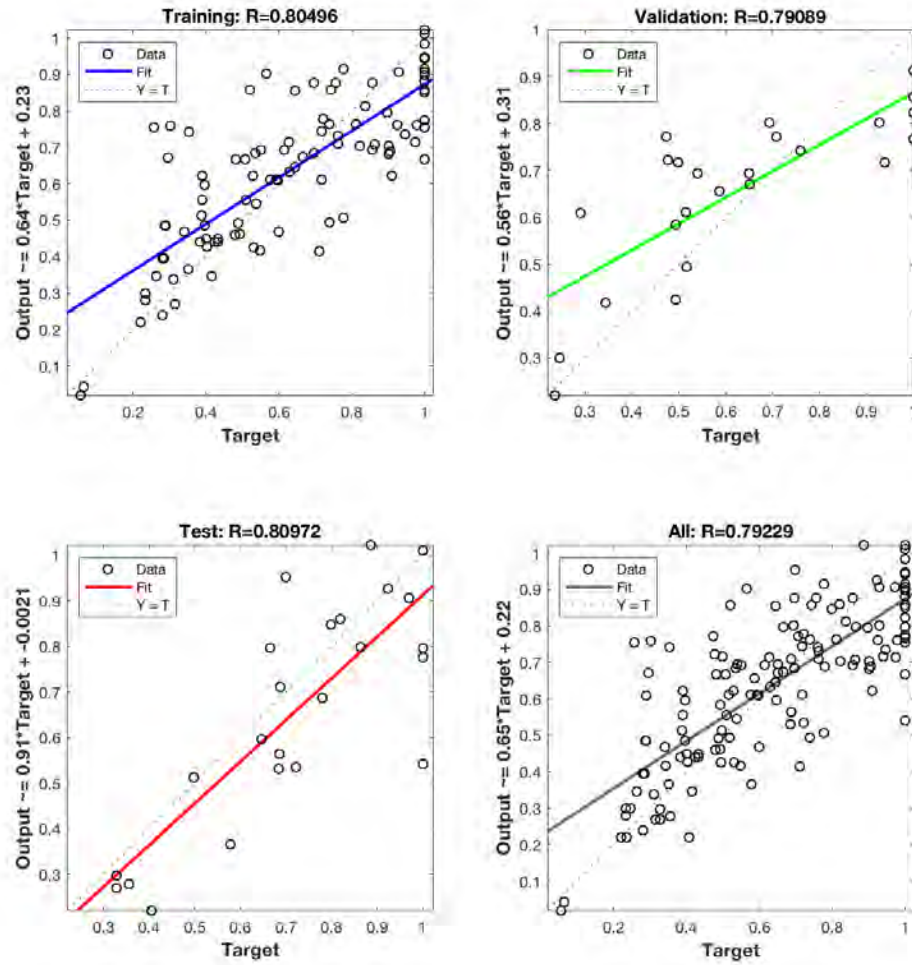


Figure 26: Output values from neural network vs the normalised target output data from experiment, for training, validation, test and all data.

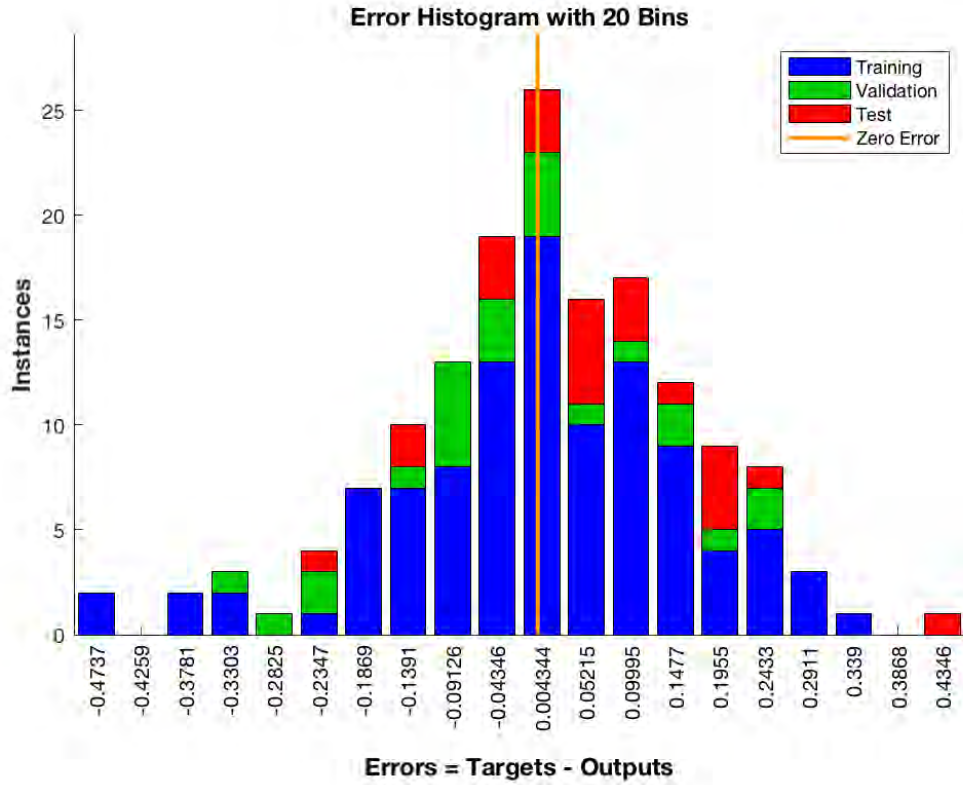


Figure 27: Error histogram of differences between neural network predicted output and target data from experiment.

3.4 Section Summary

This section aimed to collect and organise LED grown lettuce data from the literature, then combine this data with the Little Gem experimental results from section 2 of this thesis, to form a large enough data set to apply deep neural network methodology in order to test whether a deep neural network could aid in predicting an optimal light recipe for lettuce growth. Again, no such research currently exists in the literature testing neural networks for use in predicting optimal light spectral recipes for lettuce growth. A neural network which generally fit the data was found, but not with sufficient accuracy to be able to predict optimal spectral recipes.

4 A Holistic Approach to Power Saving in LED CEA Systems

4.1 Introduction

The previous experiment (from section 2) and following feasibility study of neural networks for modelling and predicting optimal spectral recipes (from section 3) suggested that in order to build an accurate predictive model, a much larger amount of highly coherent data is needed. As this is beyond the scope of possibility for this project, a new area in which to investigate potential efficiency increases for LED lit greenhouses is required to move forward.

This chapter therefore details a holistic approach to power saving in LED CEA systems, where multiple factors, from the power setup to the LED light recipe are considered in order to develop an idea of which areas are worth investigating in more detail to find novel efficiency gaining strategies.

4.2 Case Study Methodology

To study the likely impact of various approaches to reduce energy consumption, it is best to model our study on a working experimental system, so that any conclusions drawn about energy saving are practically relevant. The CEA facility growing strawberries at the University of Reading was chosen to base following calculations on.

In order to analyse power input vs useful power output, key parameters and the product details of the LEDs used were identified. The system uses Sulis series rectangular 56 W LED modules, each comprised of 56 x 1 W white bulbs. These modules are arranged in a configuration shown in Figure 28.

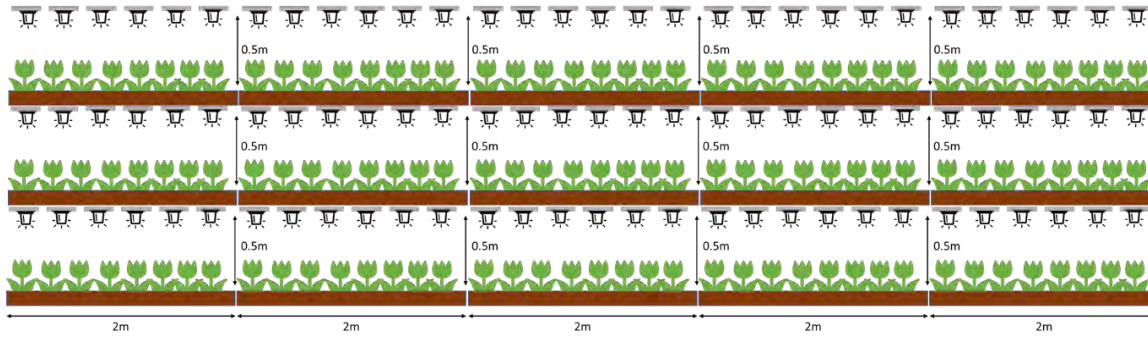


Figure 28: Schematic visualisation of the setup of the strawberry indoor growing facility at the University of Reading, with each 2-metre-long strawberry tray containing six Sulis series rectangular modules of 56 x 1 W white LED bulbs. This is repeated five times along the row and three times vertically. The whole system shown was repeated four times in parallel aisles, making a total of $[(6 \times 3) \times 5] \times 4 = 360$ modules.

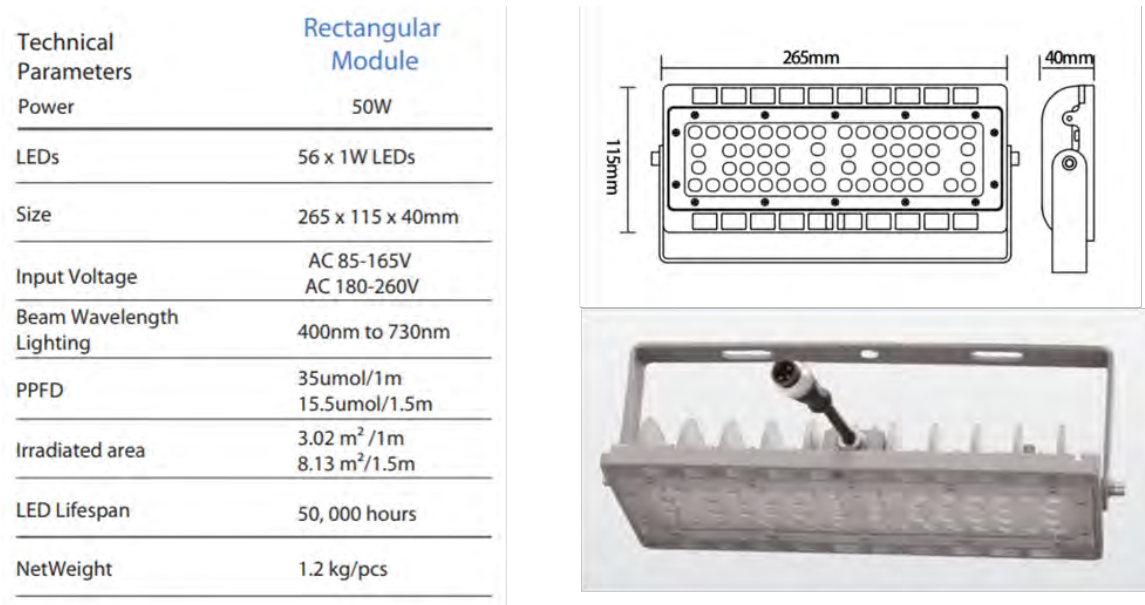


Figure 29: Technical parameters of the Sulis LED boards used at the University of Reading strawberry growing facility. Schematic and photographic images are shown on the right.

The assumption was made that the ideal amount of light was being received by the plants in the existing setup, this is because in order to do a comparison of the initial system to systems with energy saving measures, the amount of photosynthetically active radiation received by the plants

should be kept constant so that energy consumption remains the only key variable, without possibly affecting the amount of valuable light the plants would receive.

It is for this reason that the total amount of light required throughout the system was calculated using the parameters from the setup at the University of Reading with the technical data from the LED modules:

Installed Power:

$$P = [(1 \text{ W} \times 56) \times 6] \times 3 \times 5 \times 4$$

$$P = 20.16 \text{ kW}$$

The system is therefore consisting of 20,160 x 1 W bulbs in total. To get from the power input to the useful light output, technical information was gathered about the modules from the resources online, which state that for a 6 x 56 W unit at 0.5 m from the plants, the associated light output is 670 $\mu\text{mol/s}$, from which it follows that a single 1W bulb has a light output of $670 \mu\text{mol/s} / (6 \times 56) = 1.99 \mu\text{mol/s}$. Therefore, the whole system has a light output value of $20,160 \times 1.99 \mu\text{mol/s} = 40118.4 \mu\text{mol/s}$. The values based around the photosynthetic photon flux PPF ($\mu\text{mol/s}$) quantity are most valuable for LED lighting in plant growth as plant growth is related to the number of photons (in the photosynthetically active spectral region) interacting with the plant, with one molecule of CO_2 requiring 8-10 photons to bind for photosynthesis.

There is limited technical information about the Sulis series rectangular modules, particularly regarding efficacy at lower current, which is one of the aspects this project aims to investigate. Also, the Sulis system uses white light and therefore gives little room for varying recipe. For Osram LEDs however, the available information on the data sheets and in their online resources is more extensive particularly regarding operation at different current and their selection of products is larger and therefore more suitable for investigation.

4.3 Savings from Choice of Efficient LED Devices

Two sets of Osram LED were chosen for this study based on their recommendation in Osram's recent literature for CEA application: high power components (2.0 W) as displayed in Figure 30

and low power components (1.0 W) as displayed in Figure 31.

High Power Components (2.0 W)								
								
OSLON® Square 3.0 mm x 3.00 mm								
GH CSSRM4.24 Hyper Red 660 nm			GD CSSRM2.14 Deep Blue 450 nm			GW CSSRM3.PM White 4000 K, CRI 70		
mW	μmol/s	μmol/J	mW	μmol/s	μmol/J	lm	μmol/s	μmol/J
1025	5.6	4	1512	5.67	2.79	338	4.54	2.32

Figure 30: High power components (2.0 W) Osram LED light, with Hyper Red, Deep Blue and White shown respectively.

High Power Components (1.0 W)								
								
OSCONIQ® P 3030 3.0 mm x 3.00 mm								
GH QSSPA1.24 Hyper Red 660 nm			GD QSSPA1.14 Deep Blue 450 nm			GW QSSPA1.PM White 5000 K, CRI 70		
mW	μmol/s	μmol/J	mW	μmol/s	μmol/J	lm	μmol/s	μmol/J
440	2.39	3.25	716	2.7	2.71	157	2.13	2.14

Figure 31: Low power components (1.0 W) Osram LED light, with Hyper Red, Deep Blue and White shown respectively.

First, a direct comparison of performance for Osram LEDs vs. those in the Sulis modules (with the technical information displayed in Figure 29). The required light power output has been set as $40118.4 \mu\text{mol/s}$, calculated previously to be the light output in the system at the University of Reading working as it is. The number of Osram LEDs needed to match this requirement in the same experimental setup can then be calculated. This is also dependent on the choice of light recipes;

thus three basic light recipes were chosen, and one recipe chosen based on findings in the Literature for most successful light recipes for the growth of strawberries [86]:

1. 100% White.
2. 75% Hyper Red and 25% Deep Blue.
3. 50% White, 37.5% Hyper Red, 12.5% Deep Blue
4. 40% Hyper Red, 30% Deep Blue and 30% White [86].

Firstly, for the higher power components (2.0 W) displayed in Figure 30:

1. For 100% White LEDs requiring a light output of 40118.4 $\mu\text{mol/s}$, the number of LEDs required can be calculated from the $\mu\text{mol/s}$ value in Figure 30 to be: $40118.4/4.54=8837$ LEDs (rounded up to the nearest integer). The data sheet of this LED specifies that each bulb is at 1.96 W, therefore the total installed power for this system is: **P=17.32 kW**.
2. For 75% Hyper Red and 25% Deep Blue LEDs requiring a total light output of 40118.4 $\mu\text{mol/s}$, the number of LEDs required can be calculated from the $\mu\text{mol/s}$ value in Figure 30 to be $40118.4/((0.75 \times 5.65) + (0.25 \times 5.22)) = 7239$ LEDs (rounded up to the nearest integer) (5429 Red and 1810 Blue). The data sheet of these LEDs specify that the power of the Red and Blue bulbs are 1.4 W and 2.03 W respectively, therefore the total installed power for this system is: **P=11.27 kW**.
3. For 50% White, 37.5% Hyper Red and 12.5% Deep Blue, the number of LEDs and power input can be calculated from the previous two recipes to be: 4418 White, 2715 Red and 905 Blue LED bulbs, with a total installed power required of: **P=14.30 kW**.
4. For 40% Hyper Red, 30% Deep Blue and 30% White LEDs requiring a total light output of 40118.4 $\mu\text{mol/s}$, the number of LEDs required can be calculated from the $\mu\text{mol/s}$ value in Figure 30 to be $40118.4/((0.4 \times 5.65) + (0.3 \times 5.22) + (0.3 \times 4.54)) = 7733$ LEDs (rounded up) (3093 Hyper Red, 2320 Deep Blue and 2320 White). Again, from the power information on the data sheets, the installed power required can be calculated as: **P=13.59 kW**.

Secondly, for the lower power components (1.0 W) displayed in Figure 31, the same set of calculations leads to the following results:

1. For 100% White LEDs: 18835 LEDs required and installed power required: **P=17.89 kW**.
2. For 75% Hyper Red and 25% Deep Blue LEDs: 15460 LEDs required (11595 Hyper Red and 3865 Deep Blue) and installed power required: **P=12.22 kW**.
3. For 50% White, 37.5% Hyper Red and 12.5% Deep Blue LEDs: 17148 LEDs required (9418 White, 5798 Hyper Red and 1932 Deep Blue) and installed power required: **P=15.06 kW**.
4. For 40% Hyper Red, 30% Deep Blue and 30% White LEDs: 16289 LEDs required (6515 Hyper Red, 4887 Deep Blue and 4887 White) and installed power required: **P=14.22 kW**.

From these results, three key observations can be made:

- A) For very similar light spectra and output, choice of manufacturer and product can make significant difference, with installed power for the pure white LED systems showing a potential 14% power saving by choosing Osram 2.0 W high power component lights over the Sulis series modules.
- B) The power consumption is very sensitive to light recipe. Despite the system's light requirements being at a fixed output $\mu\text{mol/s}$, there was still large variation in installed power values. More studies should therefore consider the impact of light recipe on both plant response and power consumption together to better optimise CEA systems.
- C) From the two different Osram bulb groups, the higher power 2.0 W bulbs use less energy and would be a better choice for lowering power consumption while maintaining fixed level of light output.

4.4 Running LEDs at Lower Current

Using the same parameters and photosynthetic photon flux requirement as calculated in the methodology section, the impact on power consumption is investigated by reducing the operating current of the LEDs. In this section, the Osram 2.0 W bulb group from Figure 30 were chosen as they gave

the best results for power consumption previously.

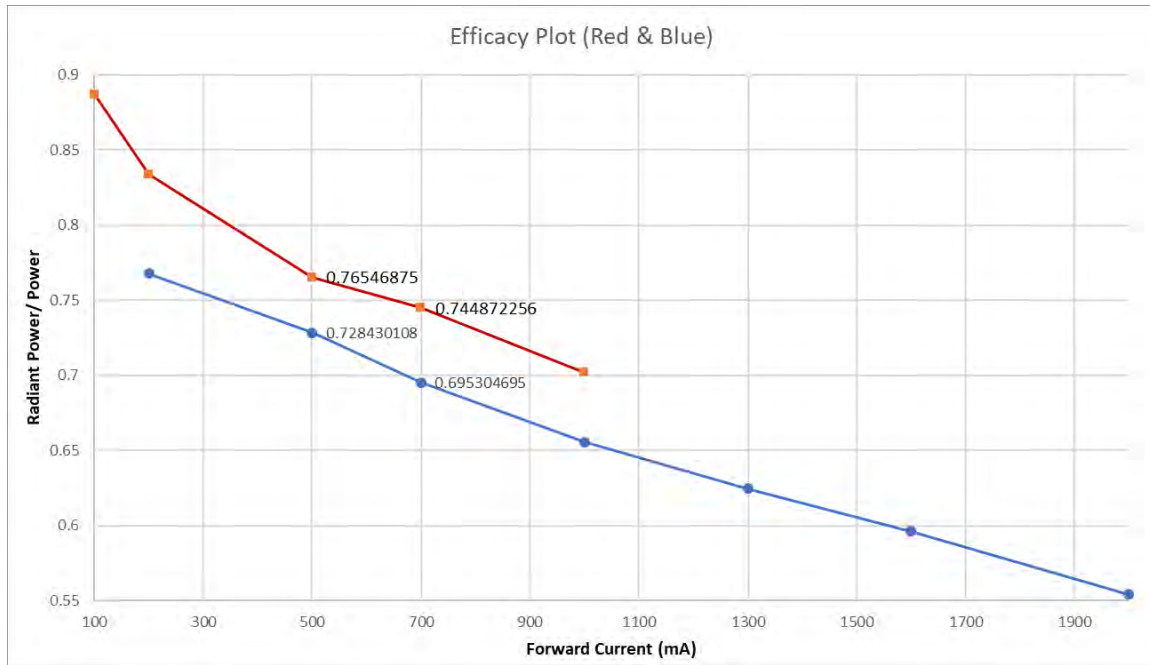


Figure 32: Efficacy vs forward current for both red and blue Osram 2 W LEDs. Efficacy values highlighted for 500 mA and 700 mA.

It is stated in the data sheets that efficacy is increased by reducing the current in both the Hyper Red and Deep Blue LEDs. For the Hyper Red LEDs, efficiency is increased from 73% to 78% at 700 mA and 350 mA respectively. For the Deep Blue LEDs, efficiency increases from 69% to 72% at 700 mA and 350 mA respectively.

More detailed analysis of the relationship between efficacy and forward current was possible for the chosen Osram red and blue LEDs due to the graphs available on their data sheets, the graph in Figure 32 shows increased efficacy at lower forward currents, for LEDs of both red and blue (the same was also true for a white LED).

This section therefore considers how much energy would be saved if the PPFD requirement is again kept constant, but the current is lowered from 700 mA. This therefore means more LEDs are required.

As only the Hyper Red and Deep Blue LEDs have available data on efficiency increase at lower current, only light recipe number two from the previous section is selected for the calculation of a system running at 350 mA. Results for the number of LEDs required and installed power:

- For 75% Hyper Red and 25% Deep Blue LEDs: 13611 LEDs required (10208 Hyper Red and 3403 Deep Blue) and installed power required: **P = 10.60 kW**

The implications of this finding are that when comparing to the previous section's equivalent scenario, where the Osram 2.0 W system is running at 700 mA, there is an overall possible **power saving of around 6%** with the same light output, with the condition that the system has 1.88 times the number of lights. Alternatively, the case can be calculated for running the LEDs at 500 mA, giving an **power saving of 3.3%** and requiring 1.4 times the number of lights. This should also be expected for other Osram lights (i.e. white) and therefore for all light recipes discussed previously.

Additionally, running LEDs at lower currents would reduce the junction temperature, which not only increases efficiency of light output, but would inevitably increase the lifetime of the LED, further contributing to the energy and overall cost saving of the setup. Quantitative analysis of this is currently not possible however, as there is no available data showing how much lifetime is affected by variations in forward current. There is however existing data which shows that the difference in lifetime (L_{70}) between an LED with a forward current of 1 A and 1.5 A is more than double ($\geq 35,000$ extra hours), as shown in Figure 33 [87]. It is difficult to extrapolate the expected lifetime increase for the case of a reduction in current from 700 mA to either 500 mA or 350 mA. However, note that if the lifetime is increased by a factor of 1.88 or more for the 350 mA case, or 1.4 or more for the 500 mA case, the cost of installing extra lights initially is outweighed entirely by the increased lifetime (replacement LEDs require purchasing less often), this is aside from the additional accumulated energy cost saving over the lifetime of the LEDs. For full quantitative analysis of this, data is needed on the relationship between forward current and LED lifetime.

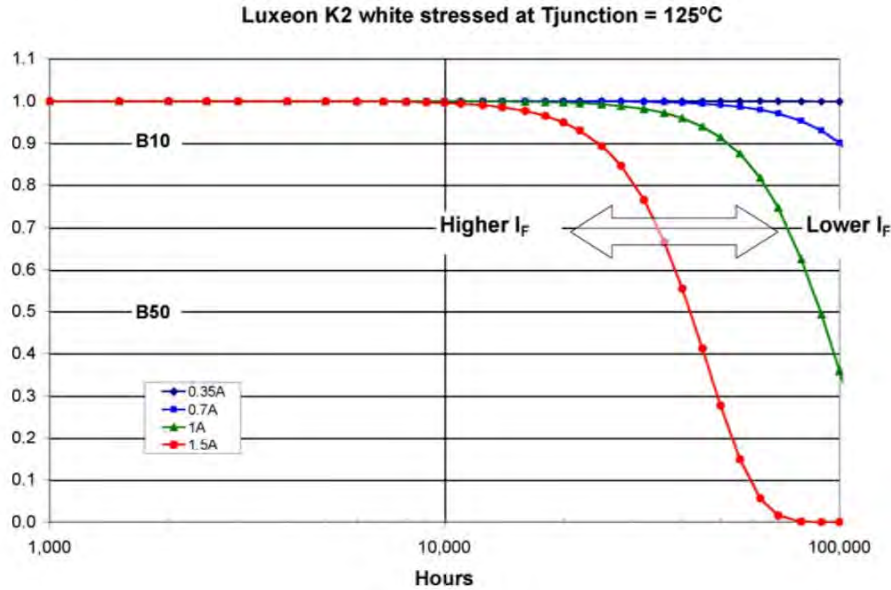


Figure 33: How forward current effects the lifetime of an LED (whose nominal current is 1 W) [87].

4.5 Energy Tariff Considerations

Electricity supply and demand varies during the day, this means firstly that when demand is high, the grid relies more on non-renewable sources to supplement supply than when the demand is lower. Therefore, energy consumed in high demand periods is effectively less environmentally friendly. Secondly, the cost of electricity per kWh increases during peak times and decreases during off-peak times and at night. Overall, this means that considering the hours of the day in choice of photoperiod for artificial lighting could lead to a reduction in both carbon emissions and energy cost. The aim of this section is to consider variation of photo-period for artificial lighting systems in order to minimise CO₂ emission and cost.

4.5.1 Systems with Solely Artificial Lighting

Firstly, the carbon emission variation throughout the hours of the day is considered. Data on carbon intensity (grams of carbon dioxide emitted per kilowatt hour of electricity produced) for the UK grid is available via carbonintensity.org.uk, showing the national gCO₂/kWh values on a half hourly basis, with existing downloadable data going as far back as September 2017; it also offers 48 hour UK forecasts. Average half-hourly carbon intensity values were taken throughout seven day periods in each quadrant of the year: the first week of October 2019, December 2019, March 2020 and June

2020 respectively. This is to give an indication of how the carbon intensity varies throughout the day seasonally, as it is expected that although the data varies on a non-repeating daily basis, trends would be visible seasonally.

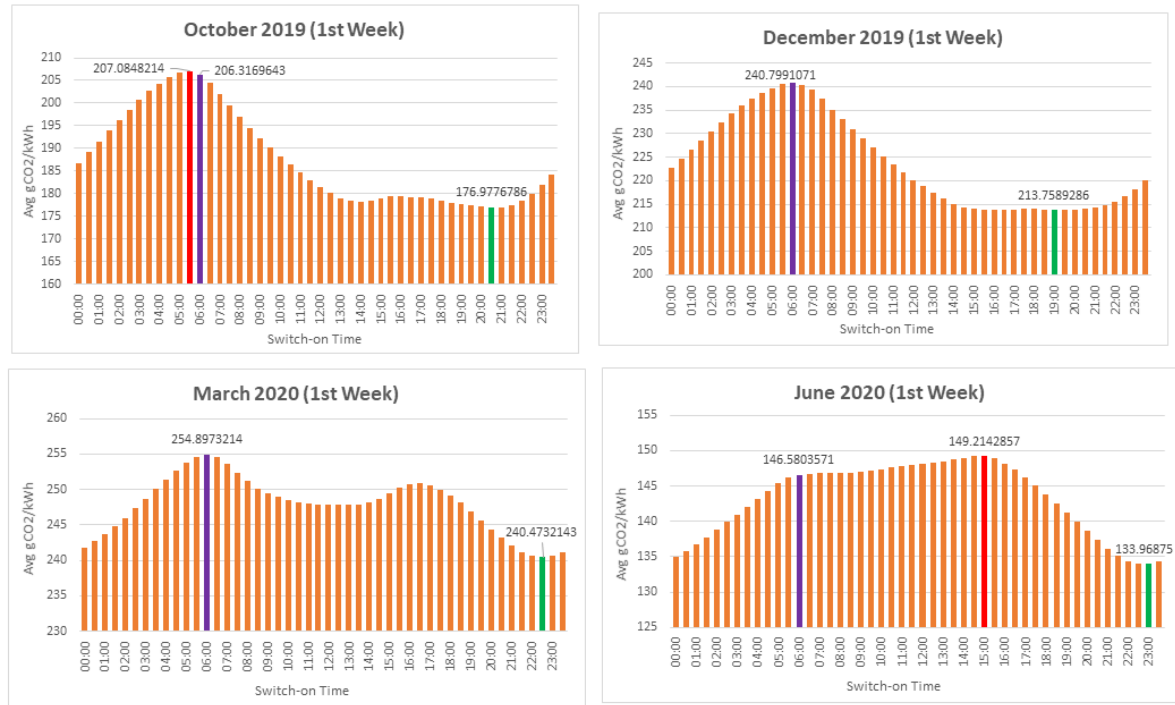


Figure 34: Average carbon emission intensity throughout a 16 hour period dependent on when the LED cycle begins. Data was taken from *carbonintensity.org.uk*. Avg gCO₂/kWh values plotted were calculated from weekly averaged carbon intensity values. Red and green bars show the least and most environmentally friendly times to switch the LEDs on respectively. The purple bar shows the commonly chosen 6 am - 10 pm plant growing photoperiod cycle point.

Once this data was gathered, average carbon intensity values were found for all possible choices of 16 hour photo-period, as shown in Figure 34. This figure shows that for each season, beginning a 16 hour LED photo-period at 6am, which is a commonly chosen time, is the least environmentally friendly due to increasing the demand on the grid during higher carbon intensive energy supply periods. Beginning the 16 hour cycle instead in the evening is therefore the less carbon intensive option, though only feasible for solely artificially lit systems such as plant factories which do not rely on sunlight. For October, switching an LED system on at 20:30 would reduce effective carbon

emissions by 14% compared with a 6:00am switch on time. For December, March and June, the savings are 11%, 5.7% and 8.6% respectively. This implies an average possible saving of around **10% carbon emissions** yearly if choice of switch-on time is based on carbon intensity data.

An alternative method to consider reducing carbon footprint is to choose energy suppliers which offer solely green energy: electricity prices were noted for one such energy supplier in the UK offering electricity from 100% renewable sources. As the prices of electricity vary depending on the time of day, consideration must be given to minimise cost. For this example supplier, the prices for electricity in the East Midlands area are:

- Off-Peak (8 am - 5 pm & 8 pm - 12 am) - 12.18 p/kWh
- Peak (5 pm - 8 pm) - 25.47 p/kWh
- Night (12 am - 8 am) - 8.2 p/kWh

With these prices, the calculated cost saving from choosing the cheapest (12am - 4pm) in place of the standard (6am - 10pm) 16 hour photo-period is **28% cost saved**. It can also be seen that this cheapest photo-period is broadly consistent with the graphs shown in Figure 34 for the carbon intensity on the supply side.

Systems Working in Conjunction with Sunlight

The work in the previous section is only applicable to plant lighting environments which do not work in conjunction with sunlight, such as plant factories or closed vertical farms. In these systems, one has complete freedom over when the artificial lighting is on and off. However, many CEA systems use artificial lighting as supplementary alongside sunlight and so the choice of switch-on time for the 16 hour lighting cycles is limited to those spanning the daylight hours as artificial lighting should be synchronised with sunlight. More careful consideration therefore needs to be given to investigate emission and cost saving for these systems.

Average sunset times for each month of the year were noted and optimum 16 hour photo-periods chosen for each month which minimise price while ensuring the photo-period spans the duration of

the sunlight. Calculations for yearly savings give an approximate **cost saving of 11%**. This is a significantly lower saving than for the above case in systems working with solely artificial lighting because in this case the months in the spring and summer with later sunsets coincide with peak hours. However, 11% is still significant cost reduction, especially considering that yield and energy consumption should remain exactly the same.

4.6 Dimming Artificial Lights with Sunlight

Another energy and cost saving strategy involves dimming the artificial lighting when the sunlight is sufficiently strong to significantly contribute to the PPFD on the plant surface. In reality, optimal dimming solutions employ dynamic light sensors which adjust the artificial lighting's intensity based on real-time sunlight brightness values, but for the sake of this study, dimming is based on average seasonal data for sunlight to gauge an approximate amount of possible energy and cost saving.

To assess the energy and cost saving potential, seasonal daily dimming levels were proposed for the UoR system modelled thus far. These dimming values were estimated based on information from the literature. Firstly, Figure 35 shows the difference in PPFD for a sunny clear day and a cloudy day in the summer in New Zealand [88]. The evidently large difference in the PPFD values dependent on these weather conditions lead to the following choice for dimming calculations: on cloudy days no dimming occurs. Only on clear days is dimming considered. Average data on UK weather gives a clear sunlight to daylight proportion of 0.41, 0.39, 0.31 and 0.25 for summer, spring, autumn and winter respectively, accounting for overcast periods. This means that for calculations, lights were only dimmed 41%, 39%, 31% and 25% of the time in summer, spring, autumn and winter respectively.

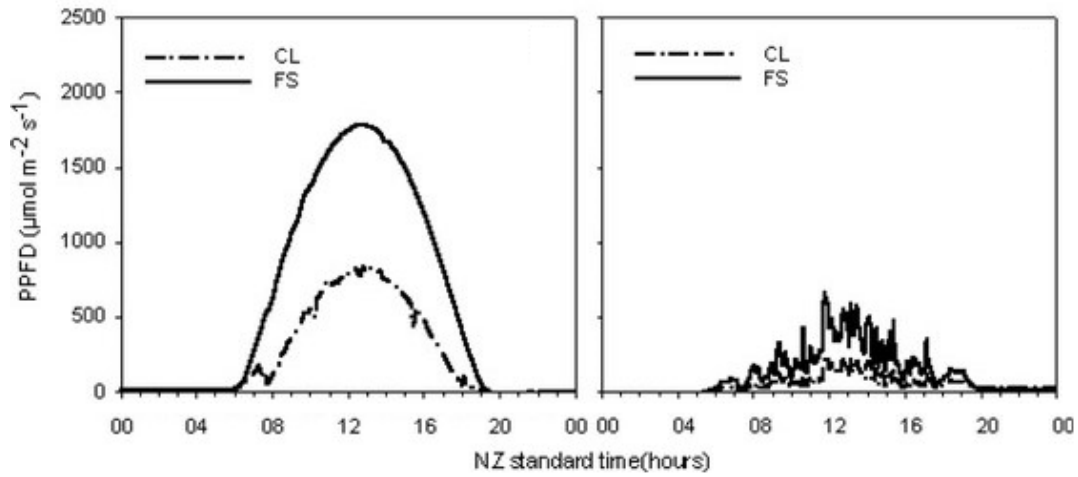


Figure 35: Comparison of PPFD values throughout the day for a clear summer day vs a cloudy overcast summer day in New Zealand is shown on the left and right respectively [88].

Additionally, sunlight intensity distribution throughout the day for each different season needs to be considered. The average seasonal hourly sunlight intensity is shown in Figure 36. On a summer day, the peak shows an intensity of around 500 W/m^2 , and from various sources it is generally accepted that the summer peak sun produces around $2000 \mu\text{mol/m}^2/\text{s}$ PPFD. As W/m^2 is approximately proportional to PPFD, the hourly PPFD on a clear day can be approximated for each season from Figure 36.

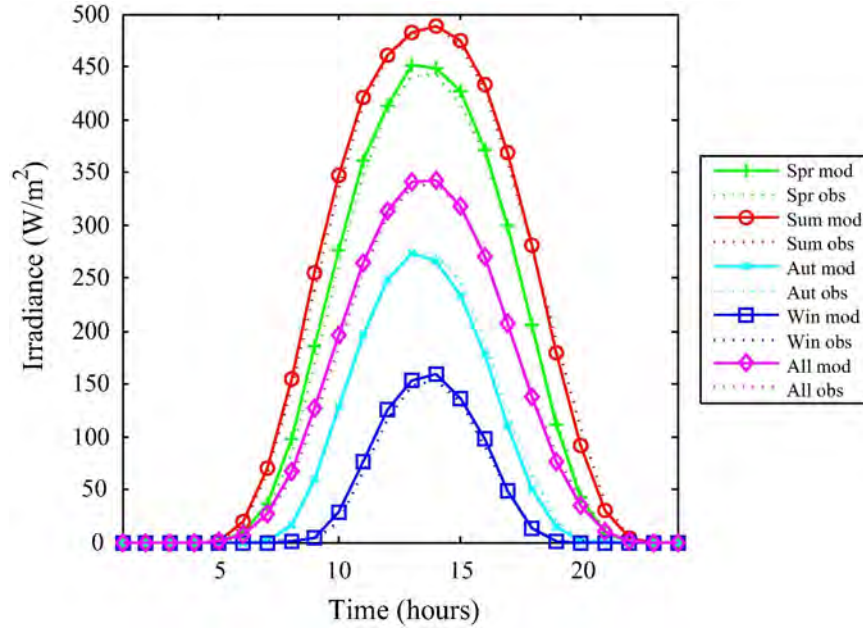


Figure 36: Hourly sun intensity for spring, summer, autumn, winter and year average (for Leeds in the UK). [89]

The amount by which the top lights are dimmed in the three tier vertical system is based on these estimated PPFD seasonal values from Figure 36. The lights are dimmed such that the total PPFD value remains at least $200 \mu\text{mol}/\text{m}^2/\text{s}$ throughout the 16 hour photo-period, as this is a suitable PPFD value for Strawberry [86] (the plant variety in this case study), this is also a suitable PPFD level for many other plant species.

Piecing together information from Figures 35 and 36, approximate PPFD values can be found throughout clear days in each season. With this information, the amount of dimming can be adjusted to keep the PPFD value recieved by plants at least $200 \mu\text{mol}/\text{m}^2/\text{s}$.

Table 10 shows dimming levels and their associated energy and cost saving. Calculations yield a total yearly energy saving of around 8.1%, but this is arguably a very conservative estimate. Firstly because dimming was only assumed to be for the top shelf of a three tier system (the University of Reading case study system), as though only the top shelf sees the sunlight and therefore the bottom two layers are not dimmed. In reality however, particularly with diffuse greenhouse barriers, which spread light while transmitting more than 80% of the PAR (see Figure 37), some fraction of

the sunlight getting through would light at least the middle tier of plants as well. Secondly, it is also assumed that cloudy days give no contribution to the $\mu\text{mol}/m^2/s$ on the plants in the greenhouse. In reality, even on cloudy days particularly in summer, the sun would give some $\mu\text{mol}/m^2/s$ contribution warranting some level of dimming to the LEDs. This 8.1% saving is therefore likely to represent a conservative minimum saving under any dimming strategy which does not compromise crop yield.

Table 10: Approximate total yearly energy and cost savings from dimming artificial lights during daylight hours on clear days. Dimming values are correlated with Figure 36 and dimming percentages represent dimming on clear days.

Season	% Dimming	Sunlight/Daylight	% Energy Saving	% Cost Saving
Summer	6-7am & 8-9pm (16.7%) 7am-8pm (33.3%)	0.41	12.4	13.5
Spring	7-8am & 7-8pm (16.7%) 8am-7pm (33.3%)	0.39	9.8	10.1
Autumn	7-8am & 5-6pm (16.7%) 8am-5pm (33.3%)	0.31	6.5	7.4
Winter	9-10am & 3-4pm (16.7%) 10am-3pm (33.3%)	0.25	3.6	4.1
Yearly		0.34	8.1	8.8

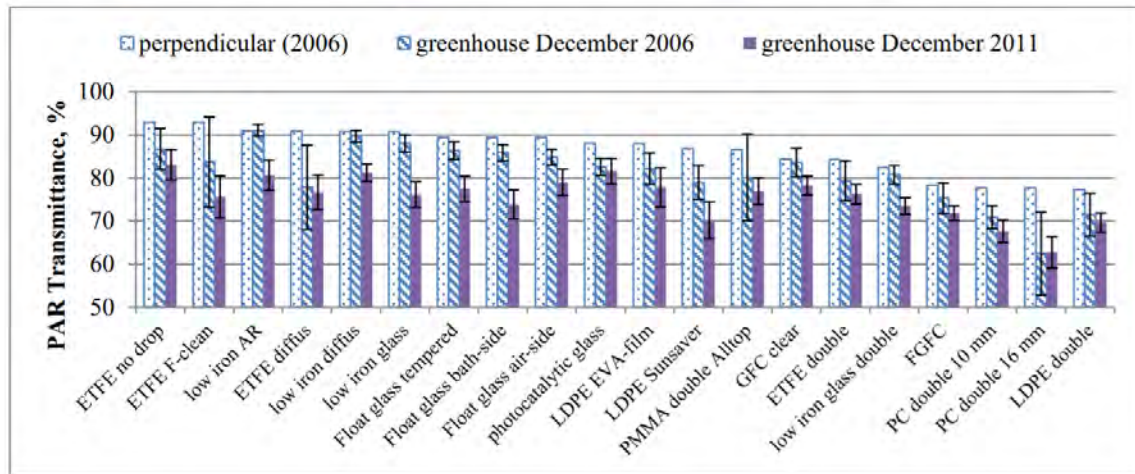


Figure 37: PAR Transmittance of sunlight through 20 different greenhouse cover materials [90].

Another important consideration is that when the sun is supplying more than $200 \mu\text{mol}/\text{m}^2/\text{s}$, the growth rate would be increased. However, the relationship between electron transport rate (ETR) and PPF is nonlinear and as PPF increases, the rate at which ETR increases lowers, this is shown in Figure 38. This could be a contributing factor to further possible dimming in a more detailed study, leading to more energy savings than stated earlier in Table 10.

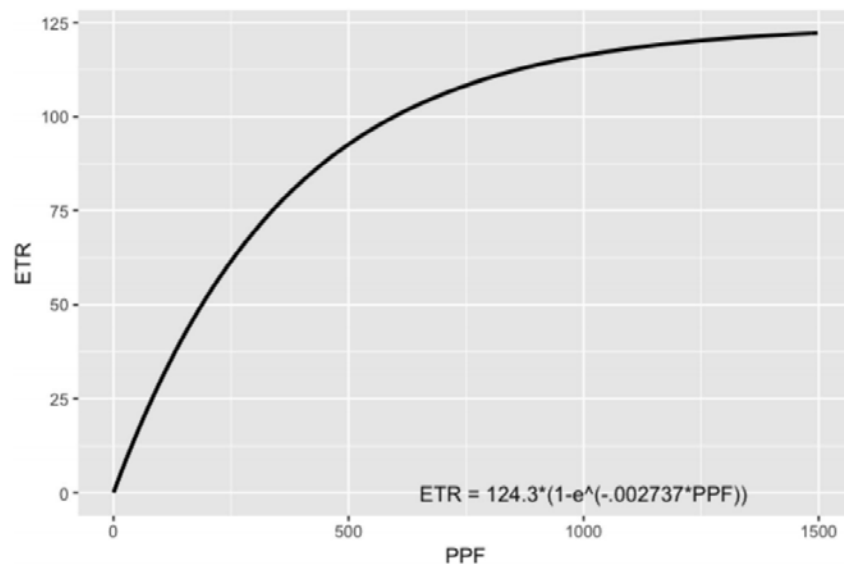


Figure 38: Electron transport rate vs PPF for Lettuce [91].

From a costing perspective, average yearly cost saving was calculated to be **8.8%**, as shown in Table 10. If this is combined with the previously derived **11%**, calculation gives **18% total yearly cost saving for dimming LEDs and working LEDs at cheapest suitable times**. Note, this is a simplified and conservative approximation. If a more in depth simulation study was done for costing under more careful consideration, a higher cost saving would be expected.

Also, at first it seems suspect that cost calculations give a 10% higher saving for solely artificial lit systems compared to dimmed systems working in conjunction with sunlight. However, this just highlights the magnitude of cost difference of electricity at night/off-peak hours compared to peak hours, particularly for the tariff chosen, which sources all electricity from renewable sources.

A more elaborate study of such dimming and associate energy saving exists in the literature [91]. Watson *et al.* ran three simulations with increasing levels of sophistication, based around Athens in Georgia. As they explain: "The first simulation leverages LED adaptive lighting. The second incorporates a daily decision, where the adaptive lights are turned off for the day when the expected daily solar radiation exceeds the ETR that optimises growth. As to the third simulation, it leverages "within day" decision making, where the adaptive lights are turned off when the target solar radiation for the day has been achieved."

At the most sophisticated level of dimming strategy, they predict around a 66% energy and cost saving (they assumed a constant electricity cost per kWh) in comparison to their baseline level. However, this is based on data in a sunnier geographical location and also simulates a single tier greenhouse rather than a vertical stacked plant system.

4.7 Section Summary

By taking a holistic approach to power saving throughout LED lit plant growing systems, many possible strategies have been identified and discussed, both by considering various literature and by performing calculations. It is clear that in many cases, a single aspect of the system can be altered such that large energy savings are possible. If many of these are adopted, the total system power requirement employing these strategies could be radically reduced from that of a conventional setup.

Specifically, this section has estimated energy savings of various strategies, based on a case study three tier vertical strawberry growing facility at the University of Reading, supplemented by LED lights. These strategies include: choosing a more efficient Osram LED device (with an estimated energy saving of 14%), choosing a more efficient spectral recipe based on literature for strawberry growth (with an estimated energy saving of 21%), dimming some of the LEDs during sunlight hours (with an estimated energy saving of 8%), and running LEDs at lower current where efficiency is higher (with an estimated energy saving of 6%). These strategies combine to give a total estimated energy saving of 41%. This demonstrates that a series of simple and independent energy saving strategies can be implemented together and significantly cut energy consumption.

5 Power Distribution to Lighting Setup - DC vs. AC

5.1 Introduction

In section 4, a series of simple strategies were investigated individually and combined to show that an approach to energy saving measures employing multiple small improvements in energy efficiency leads to great energy savings on the whole system level. This section however looks more in depth at a specific energy saving strategy which considers AC grid supply vs DC grid supply.

An increasing amount of DC appliances and a growing number of integrated DC renewable sources has put emphasis on research of DC grids, especially at local scales where loads are mainly DC. Normally, as the grid supplies standard AC 230V, every appliance has to have a double stage conversion within consisting of AC-DC and DC-DC for the desired rating of the device. This added conversion stage, plus power factor correction (PFC), expectantly decreases efficiency and increases the complexity and bulkiness of each module.

5.2 DC Grids Review

DC distribution systems have been proposed and implemented in a variety of different applications. For example in data centers, where electricity savings between 7% and 28% have been estimated for a 380 V DC distribution system compared to an equivalent system operating at 208 V AC [92]. Commercial buildings in the United States, which currently consume 61% of their energy in electricity [93], have seen early adoption use cases for DC distribution systems (primarily in lighting applications) due to the high coincidence of solar generation and commercial loads [94, 95].

A number of studies have addressed the potential electricity savings from DC distribution systems in buildings [92, 96–104]. For the commercial sector, the reported savings differ significantly, from 2% [105] up to 19% [106]. A table of studies assessing DC grids in various systems and their respective energy saving, either through modelling or experiment, is shown in Table 11. Higher savings were reported in systems that were connected to a DC source such as PV and batteries. In general, the reported savings are highly dependent on the converter efficiencies for the AC and DC distribution systems, the DC distributions system topology and voltage levels, and the coincidence of loads with PV generation. US National Renewable Energy Laboratory (NREL) considered various

commercial building types, operating schedules, system configurations, and geographical climates to predict 6%-8% electricity savings by using DC distribution.

Study Type	Scenario	Electricity Savings
Modelling	Building with Battery Storage	2%–3%
	All-DC building (res. and com.) No battery storage	5% residential 8% commercial
	All-DC Residential Building	5% w/o battery 14% w/ battery
	All-DC Residential Building	5.0% conventional building 7.5% smart bldg. (PV-load match)
Experimental	LED DC system (no battery)	6%–8% (modelled)
	All-DC office building (battery, EV)	4.2%
	All-DC Building (battery, EV)	2.7%–5.5% daily energy savings

Table 11: Literature review on energy savings from DC distribution over AC distribution. Top to bottom references: [92–95, 105, 107, 108]

Converters contribute the most to overall building network electricity loss, and the DC building network is designed to reduce the number of conversions. In general, the efficiency of converter products increases with power capacity and operating voltage. Each converter has an efficiency curve (efficiency as a function of power output proportion to maximum) which varies based on different market options for converters [98]. Efficiency data can be obtained as visual curves from data sheets. In order for a converter's efficiency curve to simulated, its rated power capacity must be known.

In summary, DC power distributions over DC networks have many benefits including:

- Higher power system efficiency due to fewer AC/DC or DC/AC conversion losses.
- DC system components tend to be more compact than equivalent AC components because of

higher efficiency and due to not being frequency dependent.

- Lower capital costs due to fewer electronic components used (no inverters).
- Higher survivability (lower power control system complexity) when subjected to external and internal disturbances due to elimination of synchronisation requirements associated with AC systems.
- Most distributed energy sources and storage devices have inherently DC outputs, making DC architectures more natural options for their integration.

The efficiency of AC/DC converters increases with the output power and also changes with loading conditions; at low loads the efficiency can be very low, wasting a large amount of energy that goes through the converter as heat. Research shows that the average efficiency of individual AC/DC converters for individual appliances is 68% while for centralised converters it is 90% [109]. A single centralised conversion stage, as opposed to many dedicated conversion stages, reduce points of losses and thus improves reliability and overall efficiency [110].

AC/DC power supplies with a power rating under 100–150 W are considered as modular power supplies and the AC/DC power supplies rated above 1000–1500 W are considered as main power supplies. For DC/DC converters, where the first conversion stage in AC/DC converters is removed, the overall efficiency is about 2.5% higher, and thus a modular DC/DC power supply is 88.4% efficient while a main DC/DC power supply is 92.3% efficient [110]. When supply is from AC sources, power is first converted to DC, then a DC/DC converter is used to reduce the voltage to the level required by the appliance. All of these conversion stages are points of power losses. For a typical residential household, use of DC-technologies in DC-inherent appliances lead to an average saving of 33% in energy consumption. This includes current-controlled loads and loads with multiple internal voltage rails.

LEDs are a current-controlled load since their luminosity is nearly proportional to their current. DC LED drivers are often 95-98% efficient, whereas AC LED drivers commonly have 86-93% efficiency [98, 104]. In addition, AC LED drivers are more expensive because they have to rectify the AC input, apply power factor correction (PFC), and cancel the 120 Hz AC power ripple with a large electrolytic capacitor.

5.3 Using DC Supply for LED Lighting Setup in CEA

Greenhouses and other CEA implementations are increasingly adopting LEDs because of their many advantages over traditional supplementary and sole lighting, as discussed in previous sections. Consideration of AC supply vs DC supply for these systems is therefore crucial to increasing LED lighting system efficiencies; decreasing the energy consumption and negative environmental impacts of CEA on climate through lowering CO₂ emissions.

As LED use in horticulture is a relatively new area of research, the main sources of review for comparison of AC and DC scenarios discussed in the previous section are in various other applications. Since LEDs are DC devices, there are more advantages for systems consisting of them to be supplied via DC distribution systems, rather than systems with mixed DC and AC loads (which are still indicated as more beneficial over AC distribution systems). The advantages and feasibility of a DC grid for large scale CEA lighting systems consisting of many DC LED loads, in comparison to an AC fed system aim to be examined in this section. Note, consideration of a DC grid is particularly relevant for cases where power supply is aided by locally installed renewable systems, which are often DC based power technologies, this is investigated in more detail later in the report.

Normally for LED lighting systems in agriculture, each LED module has its own local AC/DC rectifier before a DC/DC driver for supplying LEDs, this is shown with each constituent component in Figure 39.

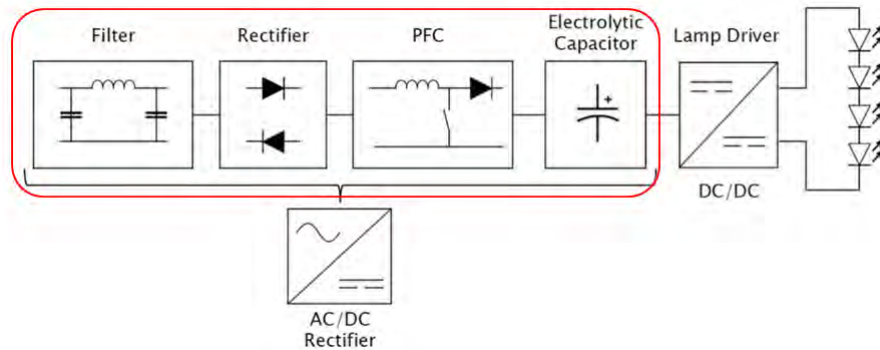
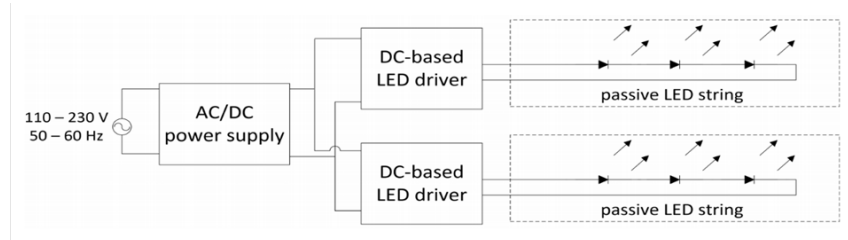
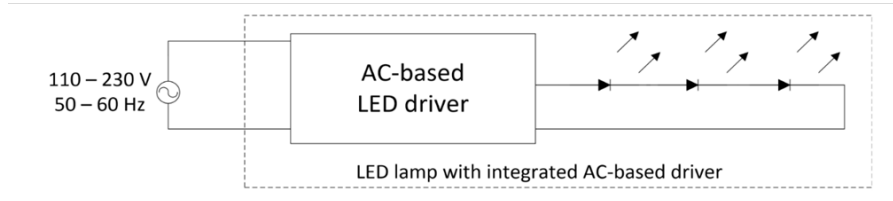


Figure 39: Schematic diagram of a rectifier converting AC supply to DC [111].

These components before the DC/DC driver have an associated loss which combine to give total losses of around 10% more than for the DC/DC LED driver case. The difference in overall setup for an AC LED driver and DC based LED driver (where AC is converted to DC beforehand) is shown schematically in Figure 40. Examples of efficiency comparison for both AC powered and DC powered market LED drivers are shown in Table 12. Additionally, these components take up around 40% or more of the space in each printed circuit board, making the modules less space efficient. A higher number of components also decreases system reliability, and generally for LED modules the power converter side is more susceptible to fail than LEDs themselves. Therefore, removing the AC/DC converter from each module would increase lifetime of the module as well as decreasing the converter losses.



LED lamps with external drivers operating on a DC infrastructure.



LED lamps with integrated driver operating on AC mains.

Figure 40: Schematic comparison of DC LED driver vs AC LED driver [112].

AC-Powered LED Drivers	Current (A)	Power (W)	Efficiency (%)
Osram OT FIT 50/220-240/1A0 CS	1.06	42.7	85.2
Mean Well NPF-40D-42	0.96	37.8	86.6
XP Power DLE45PS48	0.99	39.2	87.1
DC-Powered LED Drivers	Current (A)	Power (W)	Efficiency (%)
XP Power LDU4860S1000	0.90	35.2	95.1
Generic LED driver	1.07	42.8	96.3
Mean Well LDD-1000H	0.97	38.3	96.9

Table 12: Efficiency comparison of three market AC and DC LED drivers [112].

If the AC grid is to supply a DC grid for lighting purposes, a central rectifier is needed. However, this central rectifier can be more efficient than those on individual LED modules due to its larger size. Its losses are estimated at about 2% (generally smaller rectifiers have lower efficiency).

5.4 Conversion Losses and Cabling Losses

DC/DC converters convert DC power from one voltage level to another. They are predominantly used in low power and voltage applications and are found in appliances with electronic circuits. High power DC/DC converters are typically more efficient than lower power models. Figure 41 shows efficiency curves for step down DC/DC converters with power ratings above 1 and below 5 kW.

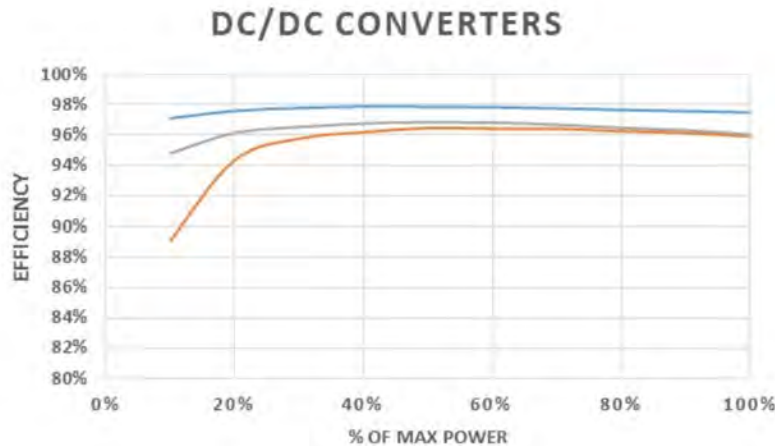


Figure 41: Efficiency curves for different market DC/DC converters ($V_{in} \leq 140 - 400V_{DC}$, $V_{out}=48V_{DC}$, P_{max} : 1-5 kW) [93].

AC LED drivers typically convert AC power to a lower voltage DC. They also regulate voltage and current through the LED circuit. DC LED drivers operate similarly to their AC counterparts, but do not require rectification. Popular manufacturers of LED drivers include Philips, Delta Electronics, Meanwell, and others. Figure 42 shows efficiency curves for AC LED drivers with power ratings less than 500 W and input voltage at 120V.

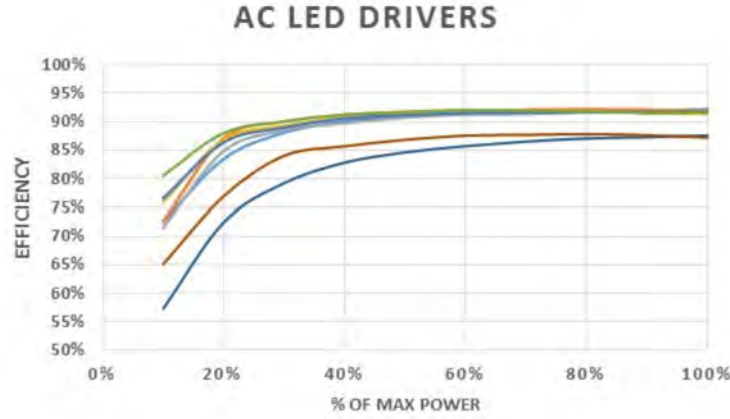


Figure 42: Efficiency curves for different market AC LED drivers ($P_{max} \leq 500W$, $V_{in}=120V_{AC}$, $V_{out}=48V_{DC}$) [93].

Rectifiers are used to convert AC power to DC. In the AC distribution system, rectifiers are used in DC internal appliances. In the DC distribution system, one or more higher power rectifiers can be used to convert AC power from the grid to DC when power from the PV system or the battery is not sufficient for the loads. Popular manufacturers for rectifiers include Eltek, Delta Electronics, Murata, XPPower, Emerson, and others. Figure 43 shows the efficiency curve for market rectifiers rated at 1-12 kW.

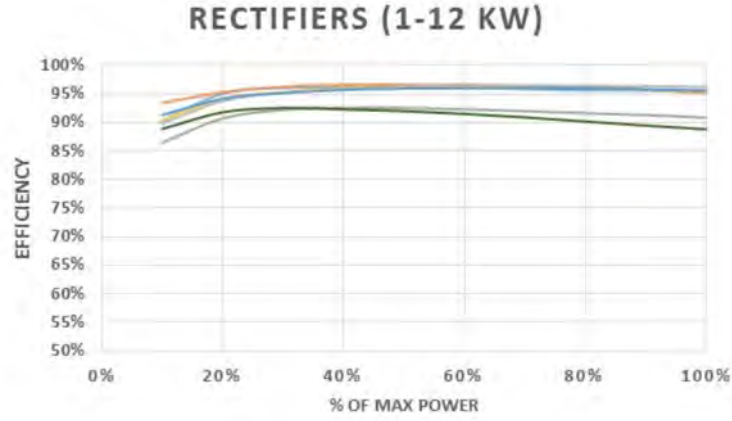


Figure 43: Efficiency curves for different market rectifiers ($V_{in}=120/277/480V_{AC}$, $V_{out}=48V_{DC}$, P_{max} : 1-12 kW) [93].

For cabling losses, length of cable and the load power both linearly effect the fraction of power lost. This is represented as a 3D plot in Figure 44.

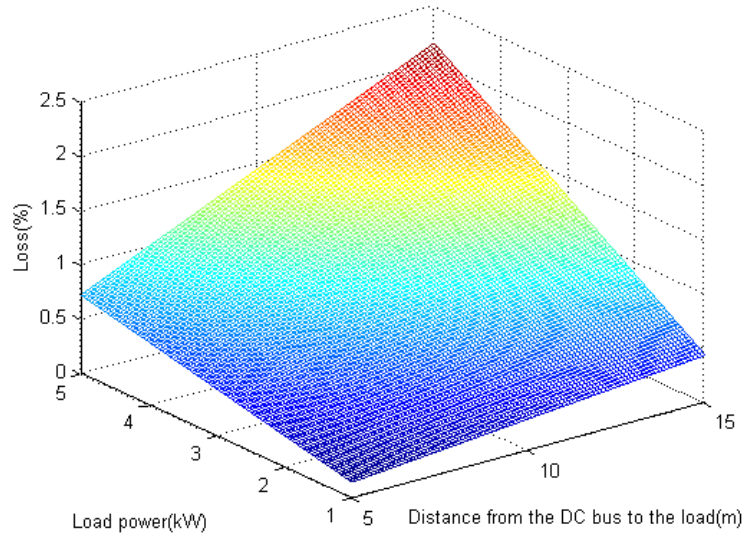


Figure 44: Line power loss in relation to the load power and L_{dis} (the distance between the DC bus and the load) for 120 V DC and AWG 8 copper wire [113].

Voltage drop and power loss are two important indexes for determining wise voltage levels and wire

cross-sections.

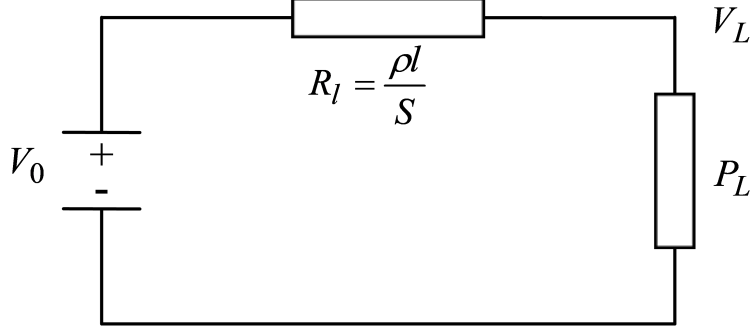


Figure 45: A simple two bus DC circuit.

For simplicity, a two-bus DC circuit shown in Figure 45 is used to derive the formulations for both voltage drop and power loss. R_l denotes the line resistance from the load to the source. V_0 is the source voltage. P_L and V_L are the load power and voltage. Thus, the ratio of the line power loss (P_{loss}) to the load power can be expressed as:

$$\frac{P_{loss}}{P_L} = \frac{2(P_L/V_L)^2 R_L}{P_L} = \frac{2P_L}{V_L^2} R_L \quad (6)$$

Since the line voltage drop (V_{loss}) is required to be significantly less than V_0 , the ratio of V_{loss} to the source voltage can be approximately calculated below:

$$\frac{V_{loss}}{V_0} = \frac{V_0 - V_L}{V_0} \approx \frac{V_0 - V_L}{V_L} = \frac{2P_L}{V_L^2} R_L \quad (7)$$

Thus, we can derive:

$$\frac{V_{loss}}{V_0} \approx \frac{P_{loss}}{P_0} = \frac{2P_L}{V_L^2} \frac{\rho l}{S} \quad (8)$$

where ρ , l and S are resistivity, line length, and cross-section, respectively.

The line voltage drop ratio is approximately equivalent to the line power loss ratio, and it is proportional to P_L and l , and inversely proportional to line voltage squared (V_L^2) and cross section (S). In addition to the voltage drop and power loss, the wire's thermal limit is another important index to be taken into consideration for the design of an indoor microgrid.

5.5 Design of Buck Converter and Rectifier

To accurately calculate efficiency and power losses for a system converting AC grid electricity to DC, the specific components for a system have been modelled in MATLAB Simulink. Firstly, this is a buck DC-DC converter, as shown in Figure 46.

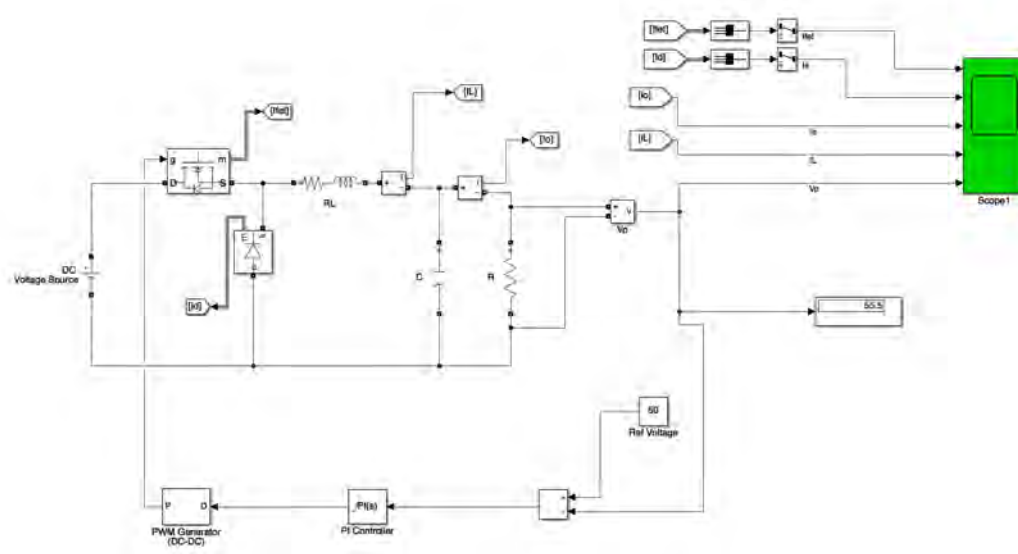


Figure 46: Circuit diagram for a buck DC-DC converter designed on MATLAB Simulink.

Next, a single phase rectifier (basic schematic shown in Figure 47) with a buck converter circuit was designed in Simulink, as shown in Figure 48.

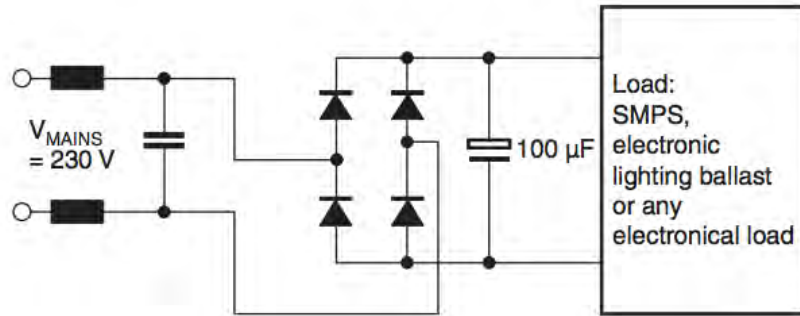


Figure 47: Schematic circuit of a rectifier.

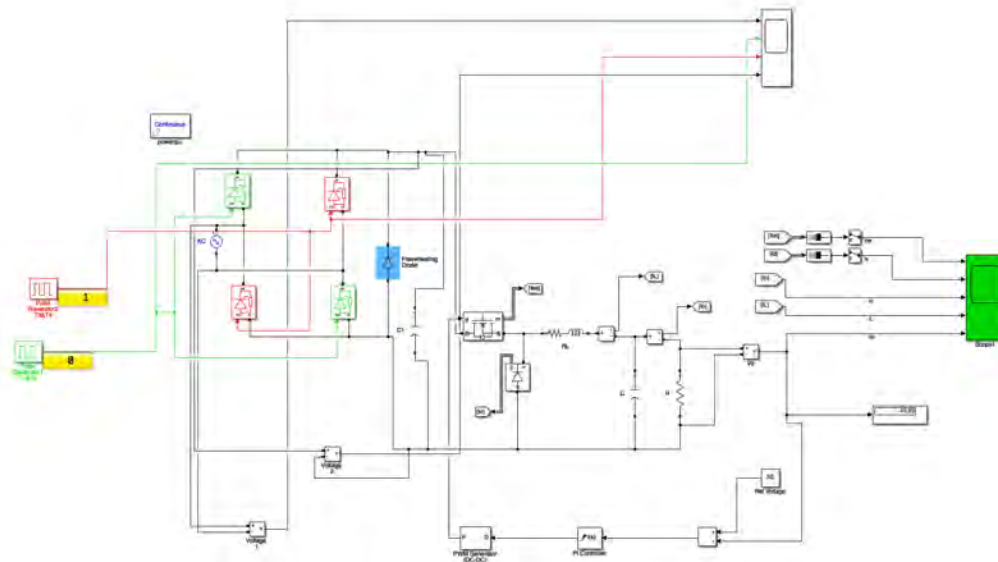


Figure 48: Circuit diagram for a single phase rectifier and buck converter designed on MATLAB Simulink.

Lastly in Figure 49, design of a three phase controlled full wave bridge rectifier using Simulink is shown.

Firstly, the inductor conduction loss is given by:

$$P_L = I_{RMS-L}^2 \times R_{DCR} \quad (9)$$

Where R_{DCR} is the DC-Resistance of the inductor. The RMS inductor current is given by:

$$I_{RMS-L}^2 = I_0^2 + \frac{\Delta I^2}{12} \quad (10)$$

where ΔI = ripple current. Typically ΔI is about 30% of the output current. Therefore, the inductor current can be calculated to be:

$$I_{RMS-L} = 1.00375 \times I_0 \quad (11)$$

Because the ripple current contributes only 0.375% of I_{RMS-L} , it can be neglected. The power dissipated in the inductor now can be calculated as:

$$P_L = I_0^2 \times R_{DCR} \quad (12)$$

Next, for the MOSFET losses, the power dissipated in the **high-side** MOSFET is given by:

$$P_{Q1} = I_{RMS-Q1}^2 \times R_{DSO1} \quad (13)$$

Where R_{DSO1} is the on-time drain-to-source resistance of the high-side MOSFET. Substituting for I_{RMS-Q1} :

$$P_{Q1} = \frac{V_0}{V_{IN}} \times \left(I_0^2 + \frac{\Delta I^2}{12} \right) \times R_{DSO1} \quad (14)$$

The power dissipated in the **low-side** MOSFET is given by:

$$P_{Q2} = I_{RMS-Q2}^2 \times R_{DSO2} \quad (15)$$

Where $R_{DS_{ON2}}$ is the on time drain-to-source resistance of the low-side MOSFET. Substituting for $I_{RMS_{Q2}}$:

$$P_{Q2} = \left(1 - \frac{V_0}{V_{IN}}\right) \times \left(I_0^2 + \frac{\Delta I^2}{12}\right) \times R_{DS_{ON2}} \quad (16)$$

The total power dissipated in both MOSFET's is given by:

$$P_{FET} = P_{Q1} + P_{Q2} \quad (17)$$

Substituting for P_{Q1} and P_{Q2} :

$$P_{FET} = \left(I_0^2 + \frac{\Delta I^2}{12}\right) \left[\frac{V_0}{V_{IN}} \times (R_{DS_{ON1}} - R_{DS_{ON2}}) + R_{DS_{ON2}} \right] \quad (18)$$

where $\Delta I = \frac{(V_{IN}-V_0) \times V_0}{L \times f \times V_{IN}}$

and where L = Inductance (H), f = Frequency (Hz), V_{IN} = Input voltage (V), V_O = Output voltage (V).

For typical buck power supply designs, the inductor's ripple current, ΔI , is less than 30% of the total output current, so the contribution of $\Delta I^2/12$ is negligible and can be dropped to get:

$$P_{FET} = I_0^2 \times \left[\frac{V_0}{V_{IN}} \times (R_{DS_{ON1}} - R_{DS_{ON2}}) + R_{DS_{ON2}} \right] \quad (19)$$

Note that when $R_{DS_{ON1}} = R_{DS_{ON2}}$, the power dissipated in the MOSFETs is independent of the output voltage. From Equation 19, the MOSFET conduction losses at any output voltage can be calculated. The other losses, such as switching losses and inductor conduction losses are independent of output voltage and remain constant with changes in output voltage. Hence, P_D now can be computed as:

$$P_D = P_L + P_{FET} + OtherLosses \quad (20)$$

The other losses include the MOSFET switching losses, quiescent current losses etc. If both the total power supply losses and power supply output power are known, the overall efficiency at any output voltage can be calculated with:

$$\eta = \frac{P_0}{P_0 + P_D} \quad (21)$$

5.6 Section Summary

Firstly DC grids were assessed from the literature, where increasingly they are being seen as more favourable than conventional AC systems, especially for long distance transmission or in small distribution systems where most of the connected devices are DC and requiring conversion from AC to DC feed.

For a greenhouse with vast amount of LEDs it is inevitable to have a substantial amount of losses and in this chapter this situation is explored and a DC distribution for a greenhouse system to feed LEDs is suggested as an improvement for electrical losses. A review and preliminary qualitative feasibility study has been done for this aim, and initial designs on Simulink modelled for necessary components in a system converting AC grid electricity to DC. However, further investigation would be needed to apply the idea for practical purposes and calculate real efficiency differences between AC and DC supplied systems of interest.

6 Modelling Renewable Technology Integration into LED lit CEA Systems

6.1 Introduction

With climate change becoming an increasingly concerning world issue, the agriculture sector, like many other sectors, is having to evolve to become more sustainable and aid in lowering greenhouse gas emissions. Currently, vertical farms and plant factories offer higher space efficiency for crop production than traditional farming methods, as well as consistent year round crop production independent of geographical location. Their main problem is the cost and associated emissions from high energy usage, primarily in lighting and heating/cooling. Previous sections have discussed strategies to lower energy consumption whilst maintaining optimal plant growth. This section focuses on how, given a system of a particular size and therefore power demand, one can incorporate renewable technologies either solely or alongside grid supply in order to lower carbon footprint and energy costs. Of course, systems of different size may benefit from different power setup configurations as the practicality of different energy production technologies can depend on scale. This section herein evaluates different combinations of various grid connected and off-grid renewable generation regimes for different system sizes, with power demand predictions being based on the University of Reading's strawberry growing facility case study system from section 4 (for which setup, system size and power requirement are known). This is in order to assess which power setups can best reduce carbon footprint and energy costs for greenhouses with LED supplemental lighting.

6.1.1 HOMER Software

In order to assess and compare different renewable power setups for greenhouses of different sizes, the HOMER (Hybrid Optimisation for Multiple Energy Resources) software is used to simulate and optimise the various chosen configurations.

The HOMER software by NREL (National Renewable Energy Laboratory) is the global standard for optimising microgrid design in all sectors [114]. It is a useful tool for investigating renewable technology integration for a given load and system preferences, with grid option available. Using this software it is possible to calculate the total project cost, cost of electricity per kWh and importantly the CO₂ emissions for chosen generation options. HOMER can model systems serving both

electric and thermal loads, and can incorporate any combination of the following energy technologies: photovoltaic (PV) modules, wind turbines, small hydro, biomass power, reciprocating engine generators, microturbines, fuel cells, batteries, and hydrogen storage.

Many studies have been done using HOMER, mainly techno-economic feasibility studies for a wide range of applications and sectors to supply power, demonstrating its versatility and popularity. Off-grid examples include a study for agriculture [115], for rural communities without grid access [116, 117], on an island in the UK [118, 119] and for LED street lighting power supply [120]. On-grid examples include for island power supply [121], for a rural area with grid access [122], for a rural area comparing both on and off-grid setups [123].

6.1.2 Biofuel & CHP

Biomass energy is a growing sustainable energy technology which is already a big part of the modern green energy system. Biomass is the most widespread form of renewable energy [124] where it is readily available in most parts of the world [125–128] and comes in many forms, such as dedicated energy crops, agricultural crop residues, forestry residues, algae, wood processing residues, municipal waste, and wet waste; any organic matter can produce biomass energy. There is significant recent growth in the energy crops area, where crops are specifically grown for biomass production.

Although biomass energy is often deemed carbon neutral, this is contended and dependent on the sourcing and processing of the biomass [129]. Biomass is cheaper than fossil fuels and can even make use of landfill waste material, further contributing to a cleaner environment. There are also many different processes to convert biomass into energy. A comparison of the different types and their respective efficiencies can be seen in Figure 50. From the chart, it is clear that the combustion method to produce only electricity is not very efficient and therefore, for a solely electrical load, biomass does not perform best. However, if the system has mixed thermal and electrical load requirements, cogeneration can offer a much higher efficiency.

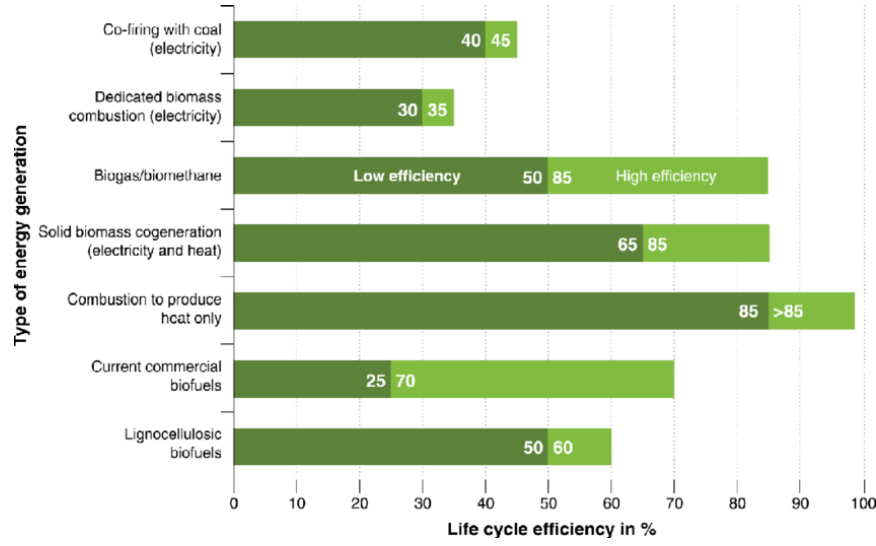


Figure 50: Comparison of efficiencies for different biomass to energy technologies [130].

Cogeneration is a biomass technology which produces both electricity and heat, and offers high efficiency for systems requiring both [131, 132]. Cogeneration is also of interest for application in greenhouses, where typically around 40% of the energy usage is for heating and cooling, so the heat produced by a biomass cogeneration system would be highly suitable.

If biomass is readily available, whether from agricultural waste or otherwise, biomass energy technology is a cost effective, efficient and green way to produce energy to meet the demand of a CEA greenhouse.

6.2 Methodology

6.2.1 HOMER Software

In the simulations throughout this chapter, for both the small UoR case study system from section 4 and larger (one and two hectare) systems, a variety of combinations of grid, wind, solar, battery and biomass CHP technologies are considered and optimised using the HOMER software to see which configurations reduce cost and emissions most effectively. The assessment for the best micro-power systems can be difficult because of the huge number of design option possibilities. An additional factor contributing to this difficulty is that the power output for renewables can be intermittent and uncertain. HOMER was designed to overcome these challenges using sophisticated methods which

are outlined in this methodology.

The HOMER software incorporates the material cost, installation cost, device efficiency and power generation capacity of a wide range of renewable technologies to feed a given energy demand. HOMER also incorporates weather data such as yearly average sunlight and wind speed data in order to give accurate estimations for wind and solar generation potential given a particular geographical area (in this case, the midlands, UK). This is illustrated for the chosen location in Figure 51.

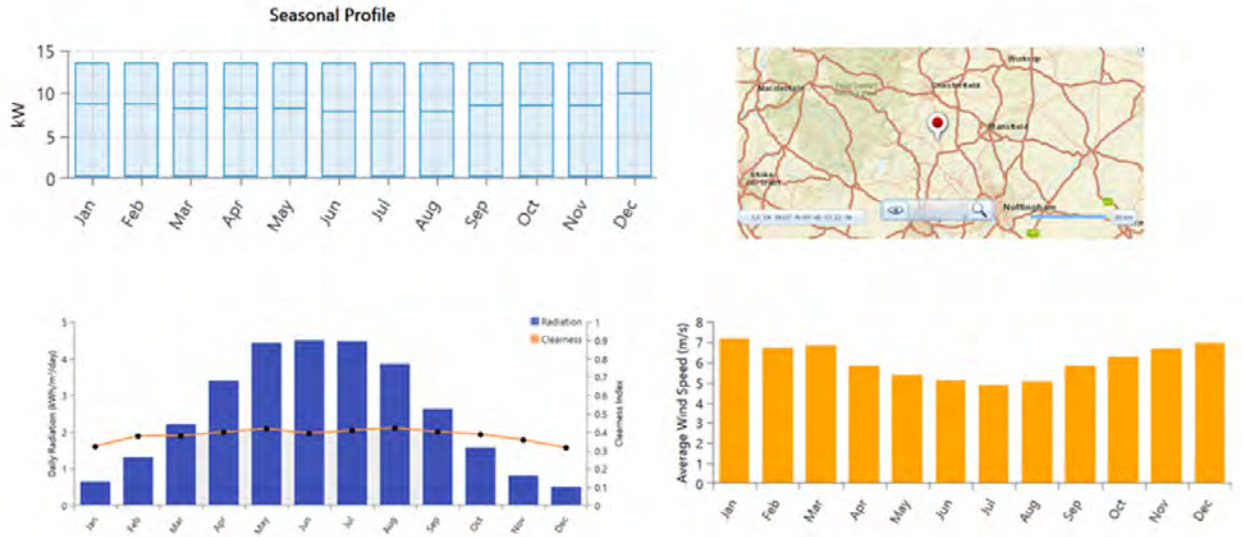


Figure 51: Monthly load profile (for the UoR case study system), chosen geographical location, yearly solar irradiation and wind data respectively.

The HOMER software operates in three principle steps: simulation, optimisation and sensitivity analysis, in order to find the best setup for a given set of power supply technologies. These three steps are illustrated conceptually in Figure 52, where the ovals represent a set and subsets such that each single optimisation includes a set of multiple simulations and each single sensitivity analysis includes a set of multiple optimisations.

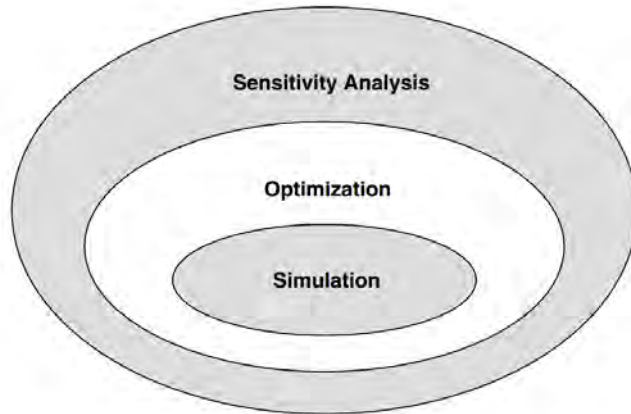


Figure 52: Abstract representation of the simulation, optimisation and sensitivity analysis processes in the HOMER software [114].

Simulation

The first objective of simulation is to determine whether a system is feasible. It is deemed feasible if the load requirements can be satisfied while respecting any other constraints imposed by the user. Once considered feasible, simulation estimates the total cost, or life-cycle cost of the system over its lifetime.

Simulating the long term operation of a micro-power system is the fundamental aspect of the HOMER software. Simulations evaluate how a particular setup configuration, with a fixed combination of system components of specific size, behaves over a whole year using small (one hour) increments. Hourly time-steps are necessarily small because energy production potential fluctuates at small time scales, particularly for systems with renewables. Daily, weekly or monthly averaged information for wind and solar availability would not provide enough insight to accurately model how a real system using these resources would behave, as the variability within a day would impact the operation and behaviour of a power system. While some extra effects cannot be modelled effectively with hourly time steps, smaller time steps such as minutes or seconds would mean extremely slow simulation times. Overall, one hour time steps are deemed the ideal compromise between accuracy and time practicality: small enough to allow the most important statistical aspects of the load and the intermittent renewable resources to be captured, but large enough to avoid slow computation,

where optimisation and sensitivity analysis would become impractical.

For each hourly time step, HOMER calculates available renewable power and compares it to the electric load. Also every hour, HOMER decides what to do with surplus renewable energy when it exceeds load requirement, or how much to purchase from the grid in times of energy deficit. After a whole year of these one hour time step simulations, HOMER assesses whether the user defined constraints and conditions, if any, have been satisfied.

Finally, the total life-cycle cost, or net present cost (NPC) is calculated for this system using all costing information particular to the simulation's energy setup. The NPC is the present value of all the costs, including capitals costs, replacement costs, operation and management costs, fuel costs, emission penalties and costs of buying power from the grid over the project lifetime. Total pollutant emissions are also calculated for the whole project length.

Optimisation

Having described the process behind a single simulation, the next stage is to perform multiple simulations which aim to approach an optimum setup solution, this is done by optimisation. Optimisation of chosen system configurations is performed by minimisation of the objective function with respect to the boundaries and constraints. The objective function is the net present cost (NPC), which includes all costs combined throughout the chosen duration of the project, in this case 15 years. The boundaries and constraints include load requirement, hourly availability of wind and solar power for the chosen geographical site, and charging and discharging capacity of lithium ion batteries, for example.

The finding of the optimal system involves choosing what mix of components it will contain. For this project these are PV panels, wind turbines, lithium ion batteries, biofuel CHP and grid electricity. Optimisation considers the quantity of each component and the overall set of rules governing how the system operates. During optimisation, HOMER simulates multiple systems, presenting the feasible system with the lowest NPC as the optimal system. Infeasible cases which do not meet any user constraints are discarded. Other feasible but more expensive systems than the optimal system are also presented, this allows the user to present an alternative system from the lowest

cost one, which may be desirable if, for example, the cost is only slightly higher while emissions are significantly lower.

Sensitivity Analysis

Sensitivity analysis builds on the optimisation process and assesses the sensitivity of optimisation under changes in chosen variables, by performing multiple optimisations under different values of chosen sensitivity variables. This tells the user how sensitive output variables (such as NPC and pollutant emission levels) are to changes in chosen sensitivity inputs (such as grid power price, fuel price and interest rates).

If there is uncertainty in one or more input variables in a user's system, sensitivity analysis can be very beneficial. It may be the case in some systems for example that an optimal system with lowest NPC could be very sensitive to changes in a volatile and unpredictable variable. It could therefore be better to choose a slightly more expensive option than the lowest cost optimisation, but with more stability under possible differences of input values to the predicted ones entered into HOMER. Beyond uncertainty, one could also use sensitivity analysis to determine at what fuel and electricity prices a certain technology (for example fuel cells) competes with alternatives.

6.2.2 System Setup

In this project's simulations, some real tariff prices of the UK grid were introduced to the desired system in HOMER as shown in Figure 53, these were the same prices as the ones used earlier in section 4 of the thesis. Throughout all of the following simulations in all systems, capital costs calculated for lighting are entered as well as the estimated load throughout a year. All power supplied to the lights was in DC form, using a market converter with competitive efficiency (between 90-95%) to convert the AC from grid supply and wind turbines, to DC.

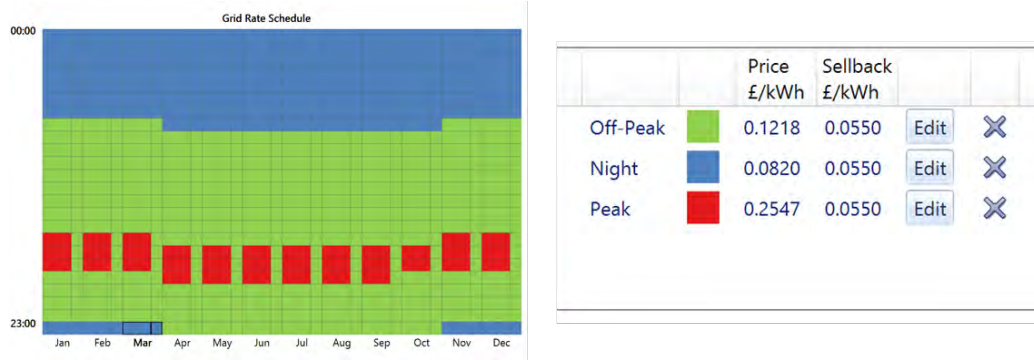


Figure 53: Hourly energy tariffs monthly for grid electricity from a UK energy company (10/2020), entered into HOMER simulations.

From section 4, using optimal light recipe for strawberry growth from the literature [86] and efficient Osram LED bulbs, the power demand was calculated to be 13.59 kW for the UoR case study system, with a calculated grow area of 36 m². This power is therefore used as the power requirement for simulations in HOMER for the small system size equal to the UoR system. Hourly and monthly loads can be inputted into HOMER, so the base 13.59 kW was entered for 16 hour photo-periods which made sure to overlap the daylight hours of each month, while where possible avoiding peak hour energy prices. Also, the dimming strategy from section 4 was also incorporated, as can be seen from the varied seasonal load profile in Figure 51 where less lighting is needed in summer months.

For later simulations involving larger systems, the same setup i.e. spatial density of plants & lights and the same row spacing as in the UoR system (from Figure 28) was used when scaling up to one hectare. The total growing area, number of LEDs required (and therefore the total price of LEDs), the power required for the lighting and the length (and cost) of cable required could then be calculated to be:

- Growth area: 5962 m²
- Lighting power required: 2252 kW
- LEDs cost: £790k
- Cable cost: £420k

For the two hectare system, the setup and input conditions for simulations were based on the one hectare system, so the power requirement, number of lights and cabling etc. was simply doubled:

- Growth area: 11,924 m²
- Lighting power required: 4504 kW
- LEDs cost: £1580k
- Cable cost: £840k

For the biomass CHP simulations in the final section of this chapter, an extra power demand was added in order to provide energy for heating and cooling as well as for the lighting, despite this project's focus being on lighting alone. It would indeed be possible to investigate incorporation of biomass for lighting solely and keep the power demand the same as in other simulations. However, biomass cogeneration has much higher efficiency when there is a thermal load as well as an electrical load. Given that any artificially lit CEA system in the UK would require heating and cooling throughout the year, it seems that including a heating and cooling power demand in simulations involving biomass would be more worthwhile. Energy demand for heating and cooling is typically estimated at around 40% of the total power consumption for artificially lit CEA facilities. Therefore, the total power requirement was scaled up appropriately from the other power demands calculated for the one hectare and two hectare systems without heating and cooling.

6.3 Results & Discussion

6.3.1 University of Reading System Model

From Figures 54-57 in the case of the UoR modelled system, it is clear that the best system for cost is a grid connected system with wind, PV and batteries installed. This gives the lowest cost, but also with relatively low emissions. Importantly, comparing Figure 54 to Figure 56, simulations calculate the grid, wind, PV and battery system to be cheaper, both the NPC and levelised cost of electricity (LCOE) values. Part of the cost saving comes from extra renewable energy generated and sold to the grid. From Figure 56, the grid purchases can be seen as 26,761 kWh/yr, but throughout the year 25,452 kWh/yr is sold back, meaning a low net grid energy purchased of 1,308 kWh/yr. Note, the monthly profile information for grid purchase and sell-back is detailed in the appendix

(see Figure A.13). There is also a significant reduction in CO₂ emissions (41% reduction) compared with the sole grid supplied system (compare Figure 55 to Figure 54).

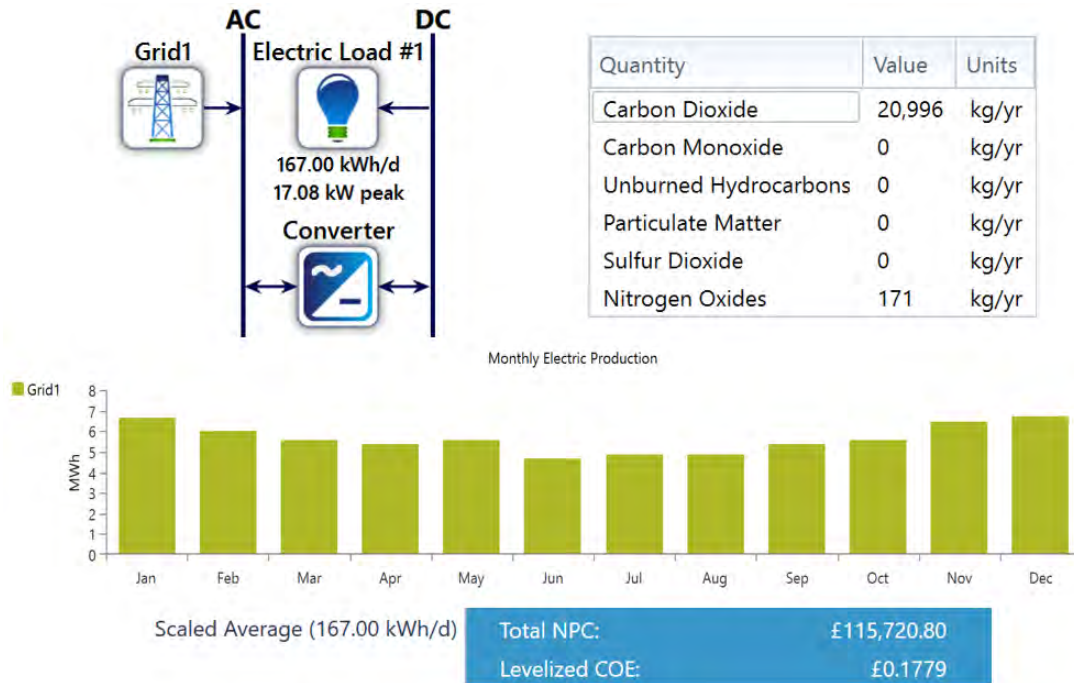


Figure 54: Power setup schematic, emissions data, monthly electric production, NPC and LCOE for the grid connected UoR case study sized system.

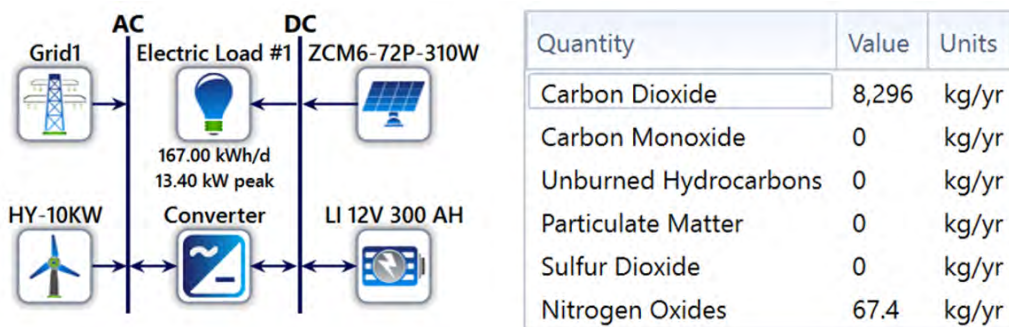


Figure 55: Power setup schematic and emissions data for the grid connected wind, PV and battery UoR case study sized system.

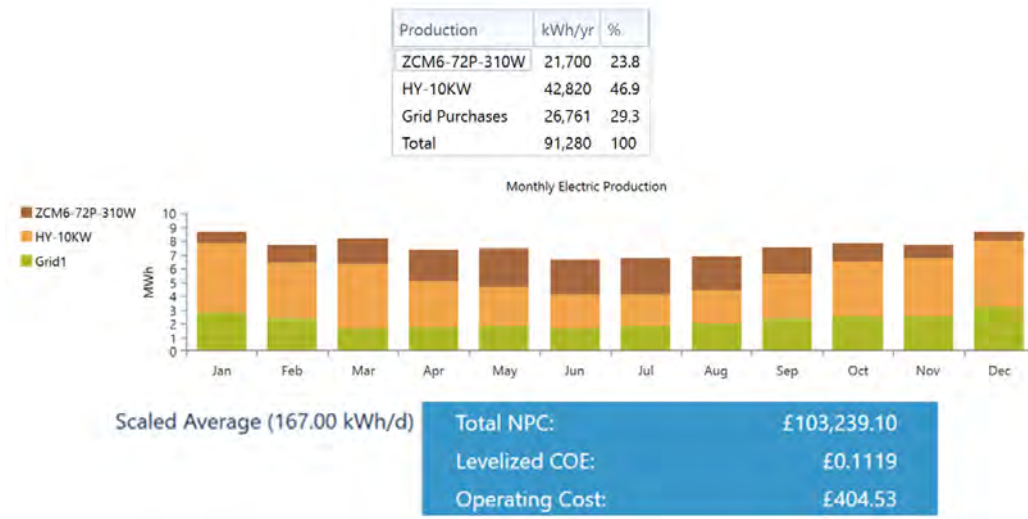


Figure 56: Yearly and monthly electric production by energy source, NPC, LCOE and operating costs for the grid connected wind, PV and battery UoR case study sized system.

Regarding the other feasible system configurations, the grid system with only PV also gives a competitive cost, graphic information of this is displayed in the appendix (Figures A.7 - A.9). This is firstly because PV produces DC electricity which is suitable for LED supply. Secondly, as grid prices are higher during the peak hours of the day and with LEDs having to work during peak times during summer (as discussed in the previous section), PV can supply electricity to the LEDs during the more expensive grid hours in the summer as it coincides with the times the PV panels produce significant amounts of electricity, thus saving on cost. PV also gives an even bigger CO₂ emission reduction (than the lowest cost system) of 45.5%.

For a system that is completely off-grid (Figure 57), the cost is high relative to the other feasible scenarios presented, both in the LCOE and the total NPC. However, emissions are zero, and there is no reliance on grid supply. This setup would therefore suit a project with a primary focus of environmental impact rather than cost. Information on the battery state of charge, PV power output and wind power output throughout the year can be found in the appendix (Figure A.14).

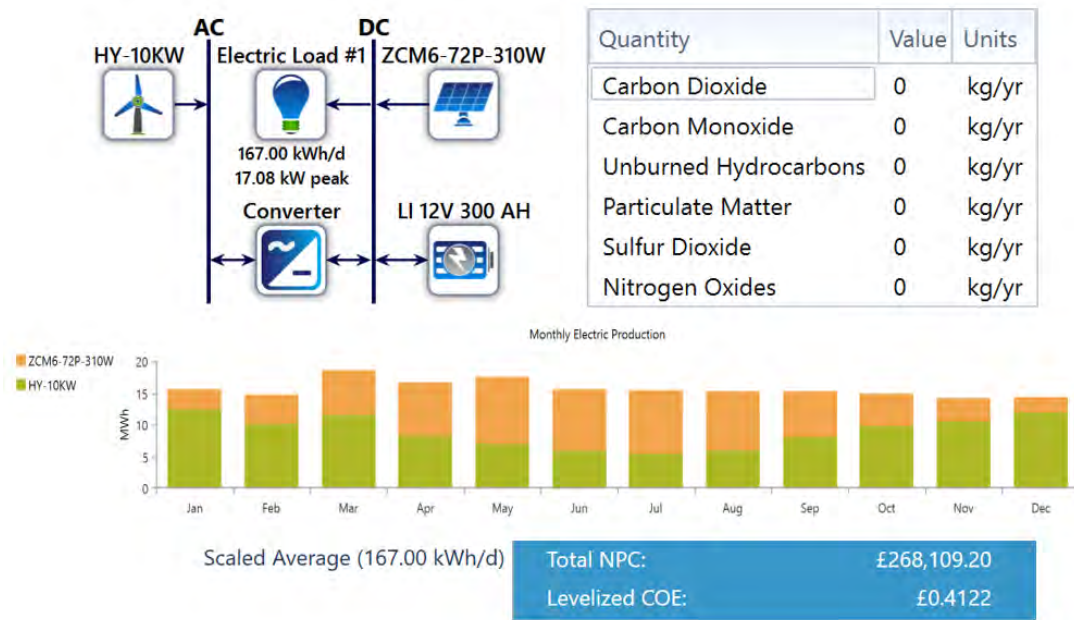


Figure 57: Power setup schematic, emissions data, monthly electric production, NPC and LCOE for the off-grid wind, PV and battery UoR case study sized system.

A comparison of total NPC, LCOE and CO₂ emissions for each optimised setup is given in Table 13, where results from an optimised grid connected PV & battery system and a grid connected wind & battery system are also included. More detailed results from these simulations can be found in the appendix (Figures A.7-A.12).

Table 13: Comparison of HOMER optimisation results for cost and emissions, between the pure grid supplied case and renewable cases for the case study UoR system.

Case	NPC (£)	LCOE (£)	CO ₂ Emissions (kg/yr)
Grid	115,720.80	0.1779	20,996
Grid + PV + Battery	114,970.10	0.1554	13,088
Grid + Wind + Battery	107,282.20	0.1329	12,280
Grid + Wind + PV + Battery	103,239.10	0.1119	8296
Wind + PV + Battery	268,109.20	0.4122	0

6.3.2 One Hectare System

After assessing different renewable power setups for the University of Reading case study strawberry growing facility, which is a relatively small system, a larger system is now considered separately for optimisation as the optimal power setup is likely to differ for systems of different sizes and scales. Conditions and input values for scaling up to the larger one hectare system were calculated as detailed in the methodology section. With these values determined, optimisations for various renewable power setups, both on and off-grid were done in the same way as for the small case study system.

Results from these optimisations are shown in Figures 58-63. Note that in each simulation, an added initial capital cost of £1m is included in the system to account for cables, installation costs and any other extra costs related to the power system's installation which have not explicitly been accounted for. The cost of LEDs (shown above) is not included directly in the optimisation results as it is the load and not linked with the power system or energy distribution itself. Setup schematic, emissions data, monthly energy consumption and total cost can be seen in the case of the sole grid connected one hectare system in Figure 58.

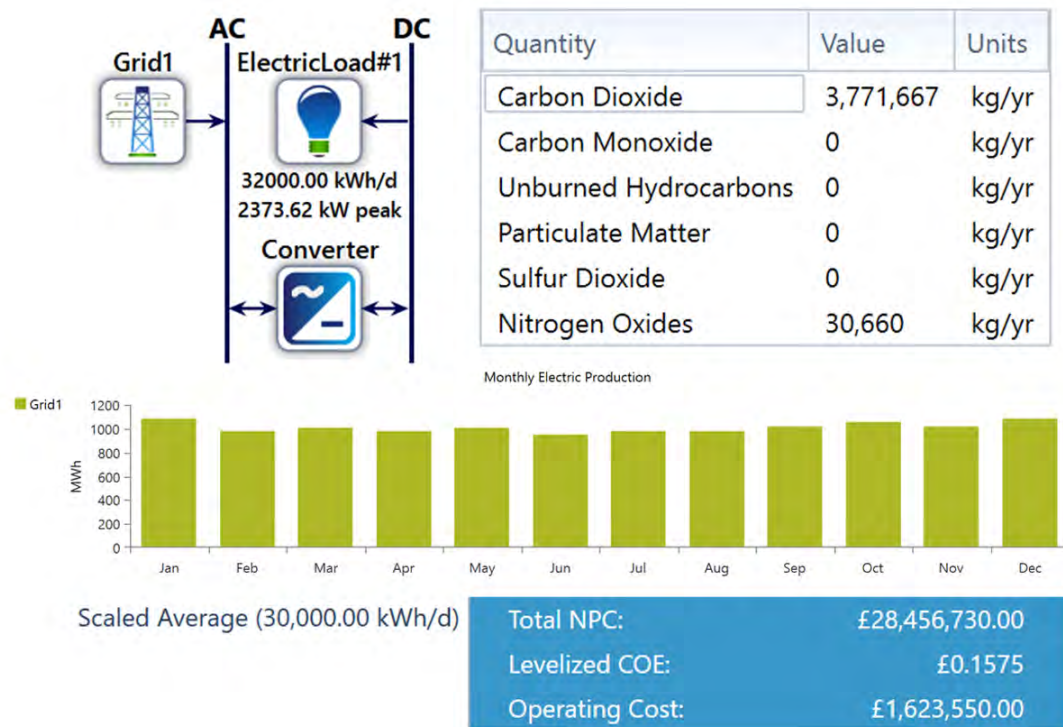


Figure 58: Power setup schematic, emissions data, monthly electric production, NPC, LCOE and operating cost for the grid connected one hectare system.

The power setup schematic and emissions data is shown for the grid connected wind and battery one hectare system in Figure 59. In Figure 60 the monthly electricity production, total cost, yearly operating cost (cost per year discounting initial investment), levelised cost of electricity and yearly wind electricity production and grid energy purchase is shown. Overall, this power system comprised of grid, wind and batteries performs best, with moderate CO₂ emissions and the lowest LCOE and NPC from all other systems. Also, as for the equivalent smaller UoR system case, there is some grid sell-back in times where the renewables are able to produce more electricity than is needed for consumption or storage. The total annual grid purchases are shown in Figure 60 as 8,112,332 kWh/yr, but there is also 3,328,361 kWh/yr sold back to the grid, meaning a net energy purchase of 4,783,971 kWh/yr. Monthly data on energy purchase and sell-back is detailed in the appendix (see Figure A.19).

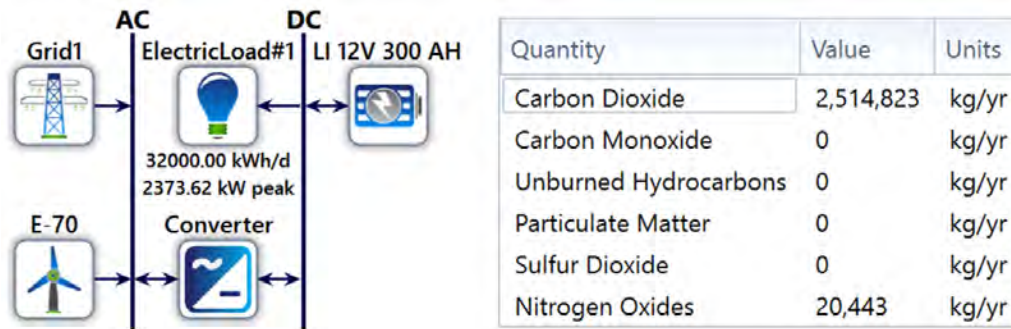


Figure 59: Power setup schematic and emissions data for the grid connected wind and battery one hectare system.

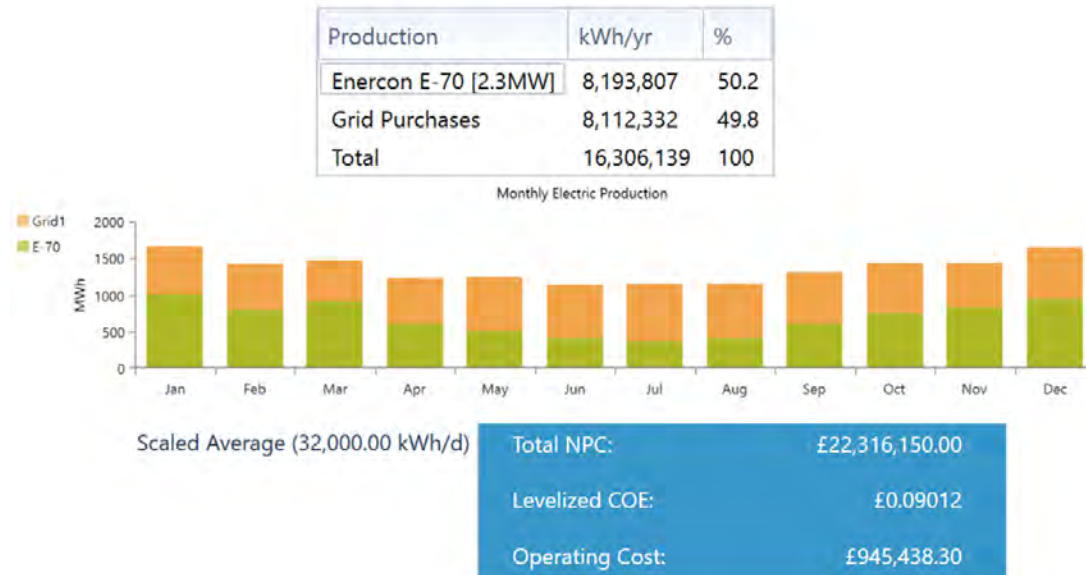


Figure 60: Yearly and monthly electric production by energy source, NPC, LCOE and operating costs for the grid connected wind and battery one hectare system.

More detailed economic analysis is shown in Figure 61, where the cost of the system is shown from the beginning to the end of the 15 years, with the initial capital cost being the intercept of the x axis and the gradient being the cost per year. From this graph's intercept between the two lines, the return on investment (ROI) time is shown (relative to the purely grid powered case).

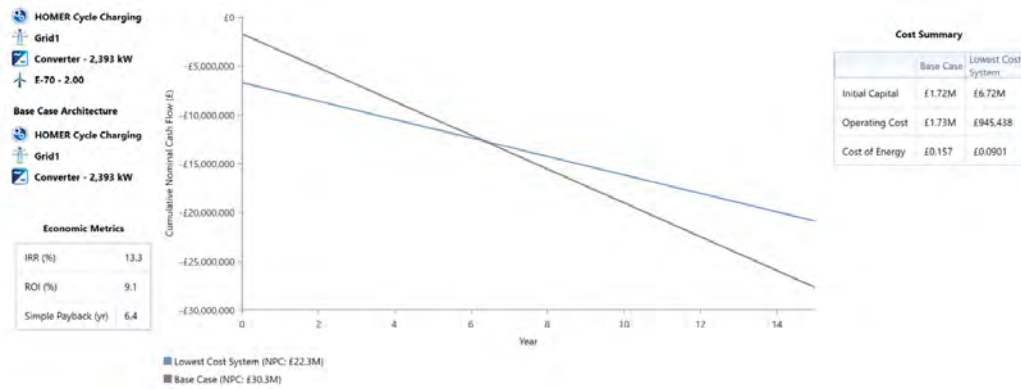


Figure 61: Economic analysis of the grid connected wind and battery one hectare system in comparison to the base grid system throughout the 15 year project length.

For a completely off-grid one hectare system using PV, wind and batteries, Figure 62 shows the power schematic, emissions data and energy production per year by PV and wind. The energy production per month breakdown and total cost, LCOE and operating cost can be seen in Figure 63. Although the grid connected wind and battery was deemed best overall, if instead carbon footprint reduction is valued above cost saving, then this off-grid PV, wind and battery system is best. The off-grid system has zero emissions, but a very high NPC due to the installed power requirement for the initial capital investment. However, this means that if the project time were to exceed the 15 year project length in this work, then the overall cost would begin to become comparable to the other cheaper grid connected scenarios. Battery charge profile data throughout the year is detailed in the appendix (see Figure A.23).

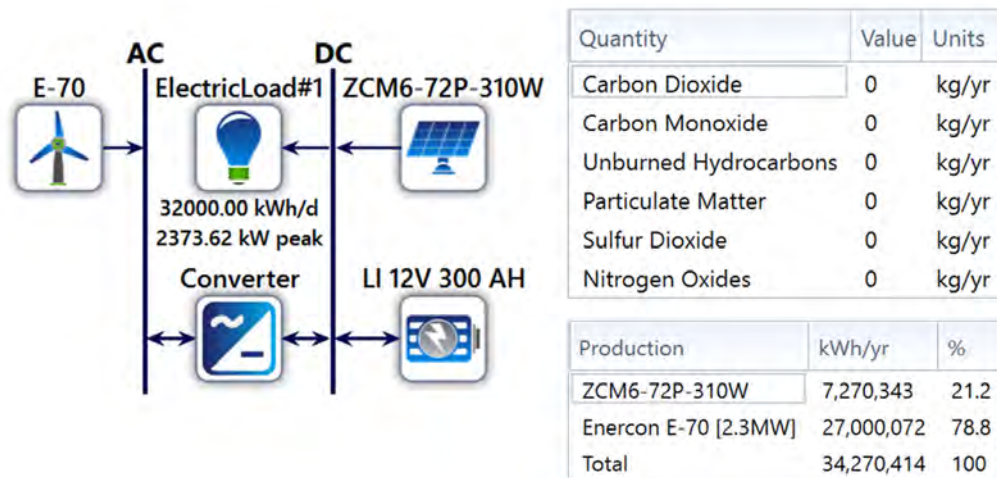


Figure 62: Power setup schematic, emissions data and yearly energy production by source for the off-grid wind, PV and battery one hectare system.



Figure 63: Monthly electric production by energy source, NPC, LCOE and operating costs for the off-grid wind, PV and battery one hectare system.

Results from the key setup optimisations have been directly included in this section, but more setup configurations were also optimised and the graphs from these systems can be seen in the appendix. The key results of all optimisations are summarised in Table 14.

Table 14: Comparison of HOMER simulation results for cost and emissions in the case of the one hectare system.

Case	NPC (£)	LCOE (£)	CO ₂ Emissions (kg/yr)
Grid	28,456,730	0.1575	3,771,667
Grid + PV + Battery	27,931,650	0.1340	2,666,750
Grid + Wind + Battery	22,316,150	0.0901	2,514,823
Grid + Wind + PV + Battery	22,823,450	0.1151	2,650,909
Wind + PV + Battery	46,364,640	0.2567	0

If the results for the small UoR system are compared to their equivalent optimised configuration in the one hectare system, differences can be seen in the most suitable renewable setups for small and large greenhouses using LEDs. This comparison is shown quantitatively in Table 15.

Table 15: Comparison of HOMER simulation results for the small UoR system and the larger one hectare system. Where each result's value is shown as a fraction of the solely grid connected (GC) case for the associated system size.

Case	NPC/GC	LCOE/GC	CO ₂ Emissions/GC
UoR System			
Grid + PV + Battery	0.99	0.87	0.62
Grid + Wind + Battery	0.93	0.75	0.58
Grid + Wind + PV + Battery	0.89	0.61	0.39
Wind + PV + Battery	2.32	2.32	0
One Hectare System			
Grid + PV + Battery	0.98	0.85	0.71
Grid + Wind + Battery	0.78	0.56	0.66
Grid + Wind + PV + Battery	0.80	0.73	0.70
Wind + PV + Battery	1.63	1.63	0

For the UoR system size, the grid with wind, PV and battery is the best system, with the grid, wind and battery system being slightly more expensive and having higher emissions. As the system size increases from the UoR system to the one hectare system, the preferred system becomes grid connected with wind and batteries, without PV, for the larger system. Wind energy seems the more prevalent renewable in both system sizes, but particularly so in the one hectare system.

6.3.3 Two Hectare System

The results of simulations for the two hectare case would not necessarily simply scale up directly from the one hectare case, because the efficiency, cost and practicality of different renewable generation technologies varies at different scales. Figure 64 shows the two hectare system for a grid connected system with no integrated renewable technologies. As this is grid only, the costs have effectively doubled from the one hectare case.

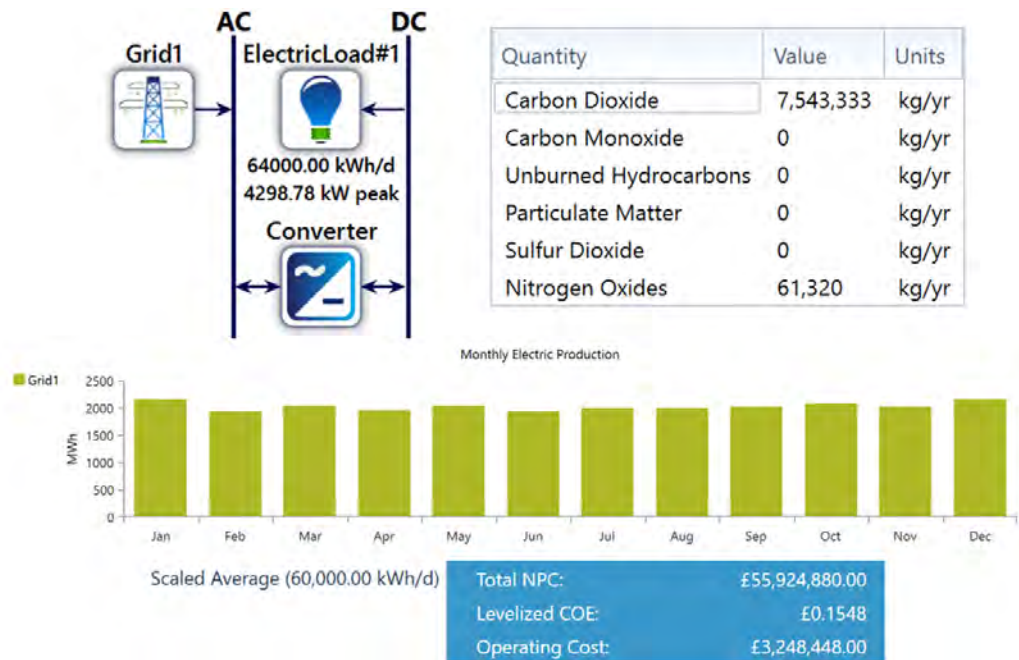


Figure 64: Power setup schematic, emissions data, monthly electric production, NPC, LCOE and operating cost for the grid connected two hectare system.

For the two hectare system simulations, setups with PV were not considered, this is because as discussed previously, PV becomes less favourable when scaling up from the small UoR system, to the one hectare system. PV also contributes fractionally less to the energy production in simulations for the one hectare case than in the UoR system case, further suggesting that it does not scale as well as wind. This is not surprising given that the efficiency of PV does not increase at larger scales, but wind turbines can due to choice of a larger capacity turbine in place of multiple lower efficiency smaller turbines. Beyond these reasons, if PV were to have a large share of the energy production for a two hectare or larger system, the space the PV panels would require itself would

be significantly higher than the space required for wind turbines.

Results from the most favourable system setup are displayed in Figure 65 with wind turbines and batteries connected to the grid showing a far more cost effective and low emission case than for solely grid connected. Also, as for the smaller systems, there is significant grid sell-back. The total annual grid purchases are 14,730,676 kWh/yr, with 6,454,144 kWh/yr sold back to the grid, meaning a net energy purchase of 8,276,531 kWh/yr. Monthly and daily data on energy purchase and sell-back is detailed in the appendix (see Figure A.24), where it can be seen that there is significant sell-back particularly during the night in winter when turbines are generating electricity while no electric load is needed.

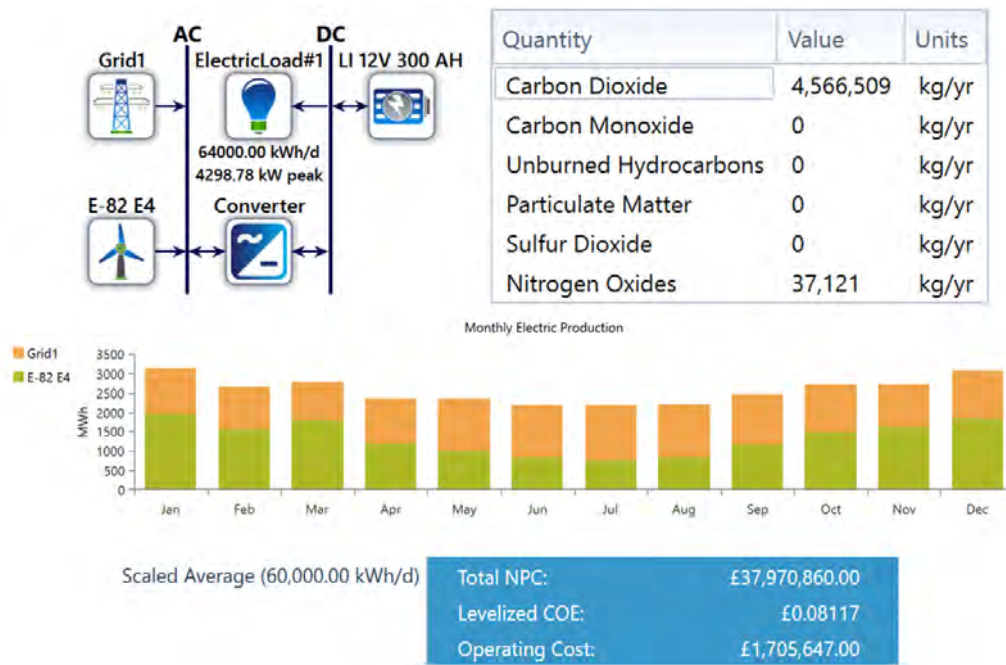


Figure 65: Power setup schematic, emissions data, monthly electric production, NPC, LCOE and operating cost for the grid connected wind and battery two hectare system.

If a comparison is made between the best systems of all sizes, i.e. of the small UoR system, the one hectare system and the two hectare system, differences can be seen in the cost effectiveness and emissions reductions at different scales. Comparison information is displayed in Table 16. As realised previously in Table 15, the smaller scale UoR system favours inclusion of grid, wind, PV

and battery, but at larger scales, wind without PV dominates. Quantitatively from Table 16, we see that when scaling up from one hectare to two hectares, NPC, LCOE and CO₂ emissions are all reduced relative to their sole grid connected base case. This means that the larger the system is, the higher the proportional cost saving and emissions cutting the system has under a wind and battery enhanced CEA system. The only value in Table 16 that does not fit the trend of improvement at larger scale is the CO₂ emission reduction relative to the sole grid connected for the UoR sized system, which is 0.39, lower than both the one hectare system (0.66) and the two hectare system (0.61). This apparent anomaly is probably because the system is small enough to effectively incorporate both PV and wind, such that grid purchases only account for less than 30% of the energy used. The larger systems take around half of their energy from the grid and half from wind, none from PV as it does not scale up as well as wind.

Table 16: Comparison of HOMER simulation results for the optimal power setups for the UoR case study system, the one hectare system and the two hectare system. Where each result's value is shown as a fraction of the solely grid connected (GC) case for the associated system size.

Case	NPC/GC	LCOE/GC	CO ₂ Emissions/GC
Reading System			
Grid + Wind + PV + Battery	0.89	0.61	0.39
One Hectare System			
Grid + Wind + Battery	0.78	0.56	0.66
Two Hectare System			
Grid + Wind + Battery	0.68	0.52	0.61

6.3.4 Biomass CHP Incorporation

The following simulations involve biomass CHP energy and include an added thermal load, as discussed in the methodology, to the existing electrical lighting load in order to assess the performance of biomass CHP in large one hectare and two hectares systems where cogeneration may be feasible.

For the previously investigated one hectare system with a purely electrical load and no biomass CHP, the most favourable setup involved a grid connected system with wind turbines and batteries. In the one hectare biomass CHP simulation therefore, the biomass CHP is integrated and added to

this system, with the 40% extra thermal load to account for the heating and cooling.

Two optimisations have been performed for the one hectare case using biomass CHP. They are identical in load and renewable setup, the difference is in the choice of biogas. HOMER has two preset biogas fuel options, one of which has a higher calorific value, but at the expense of being more greenhouse gas emitting. The other being more environmentally friendly, but less energy efficient, details of both are given in Table 17.

Table 17: Comparison of properties of the available biogas resources in the HOMER software.

Properties	Biogas 1	Biogas 2
Lower Heating Value (MJ/kg):	5.50	45.00
Density (kg/m ³)	0.72	0.79
Carbon Content (%)	2.00	67.00
Sulfur Content (%)	0.00	0.00

Note also that a primary argument for the sustainability of biomass energy production is that although energy production emits CO₂, it is argued that the biomass would have emitted these gases whether it is used or not (in the case of agricultural waste biomass). For the case of biomass retrieved from forest wood, it is argued that any CO₂ released in the burning of the wood is replenished by regrowth of the replanted tree in the sustainable forest from which the tree wood was sourced. Therefore, the emissions data from these simulations which does not account for this point are possibly an overestimate of the real emissions for the supposed system.

The results in Figure 66 show that in the case of biogas 1, using biomass CHP technology for cogeneration alongside grid, wind and batteries yields a relatively low carbon footprint. The emissions are more than one million kg/yr of carbon dioxide and nearly one hundred thousand kg/yr of nitrogen oxides, but this is not so high when compared to the common values in the previous section (Table 14) which were mostly above two million kg/yr. Also, accounting for the fact that the CHP system has a 67% higher energy demand due to accounting for heating and cooling as well as lighting, the carbon emissions are low.

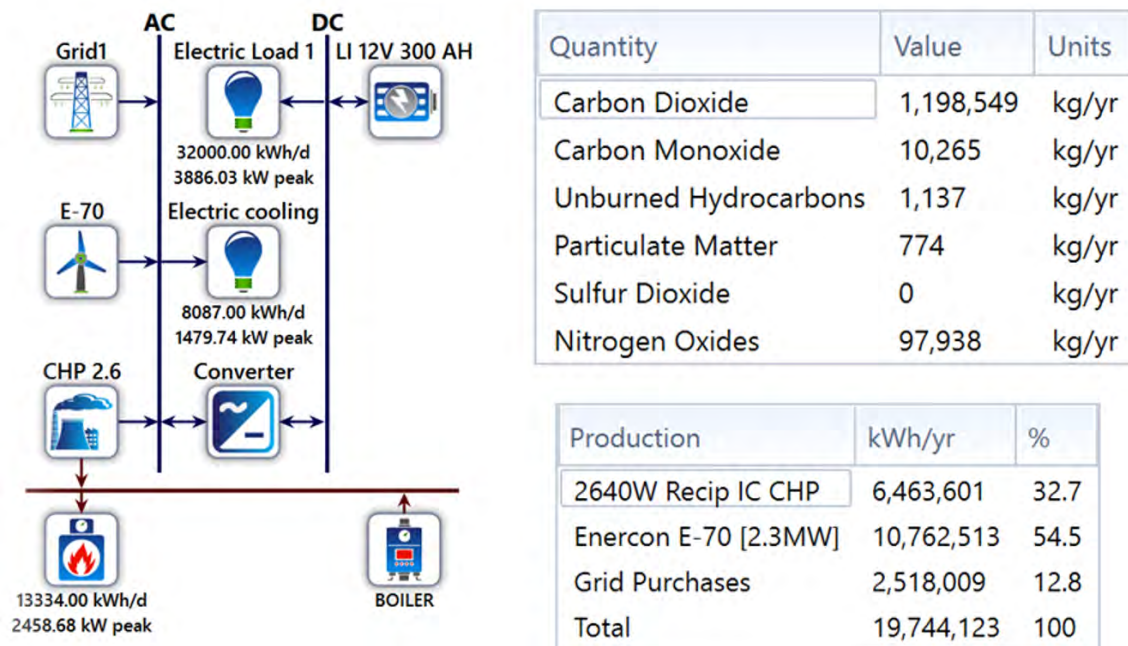


Figure 66: Power setup schematic, emissions data and yearly electric production by source for the grid connected biomass CHP, wind and battery one hectare system with biogas 1.

Regarding cost, although the NPC seems high for the lower emitting biogas 1 system, the CHP cases represent a more comprehensive scenario where power can be supplied mostly on-site, purchasing additional power for heating/cooling from grid for other cases would increase the NPC considerably. In Figure 67, the total cost, LCOE and operating costs are shown, as well as the monthly energy production in terms of production source. From the monthly production graph it is clear that majority of the energy is coming from renewable production and only supplemented by the grid. Further economic information is given in Figure 68, where if compared to a purely grid supplied system with the same power demand, the biomass CHP, wind and battery case although requiring more initial capital, is far cheaper over the 15 year project time, with a payback time of 7.1 years.

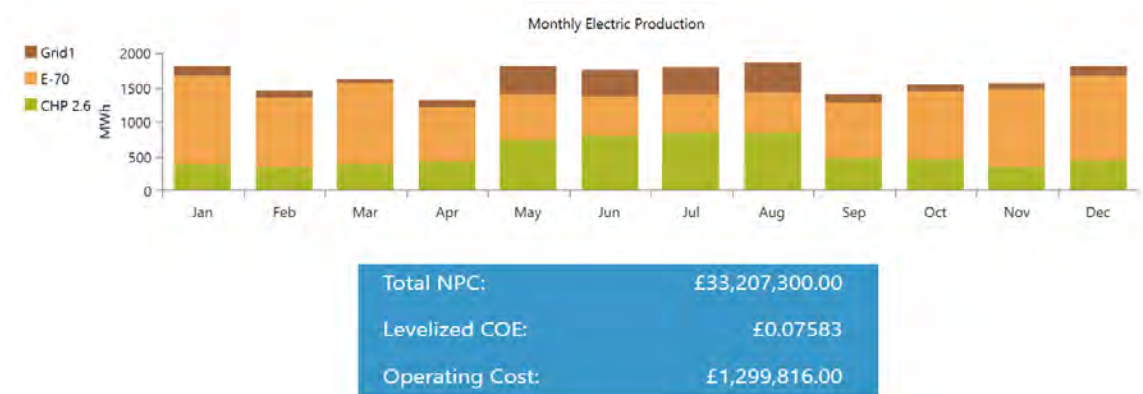


Figure 67: Monthly electric production by energy source, NPC, LCOE and operating costs for the grid connected biomass CHP, wind and battery one hectare system with biogas 1.

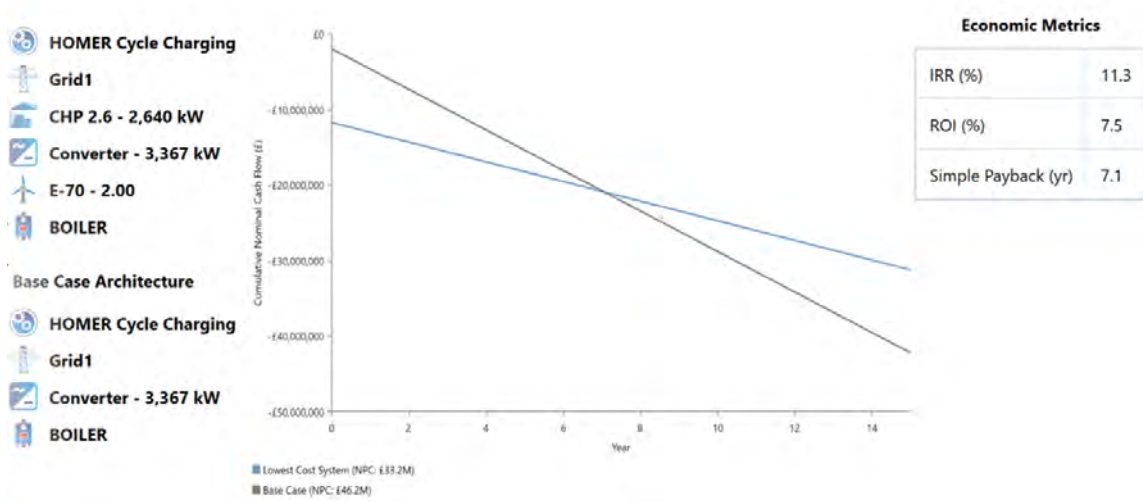


Figure 68: Economic analysis of the grid connected biomass CHP, wind and battery one hectare system with biogas 1 in comparison to the base grid system throughout the 15 year project length.

From Table 18 there is quite a significant difference between the optimisation results for the two preset biogas options on HOMER. Though biogas 2 yields a less costly system, it is at the expense of much higher emissions. It is for that reason that for the following biomass CHP simulation in a two hectare system, the less emitting biogas 1 was chosen. Graphs from the simulation of the same system with biogas 2 can be seen in the appendix (see Figures A.26-A.28).

Table 18: Comparison of HOMER simulation results for cost and emissions in the case of the one hectare system.

Case	NPC (£)	LCOE (£)	CO ₂ Emissions (kg/yr)
Biogas 1	33,207,300	0.07583	1,198,549
Biogas 2	21,200,140	0.03186	10,991,759

Similarly to the one hectare case, a simulation which allows for integration of a biomass CHP system was considered for a two hectare system, this was based on the optimal system without biomass, which includes a grid connected system with wind turbines and batteries. Again, this includes an added thermal load in comparison to the non-CHP systems, which must be considered when comparing cost and emissions results from both.

Figure 69 shows the power schematic, emissions data and yearly electric production by source for the optimised grid connected biomass CHP, wind and battery two hectare system. The monthly breakdown for electric production along with total cost, LCOE and operating costs are shown in Figure 70. Grid use in this configuration is very low but still present. Given that HOMER optimises cost with respect to variation in production share of wind, CHP and grid electricity, the fact that the optimum scenario involves little grid share suggests that renewables are much more cost efficient.

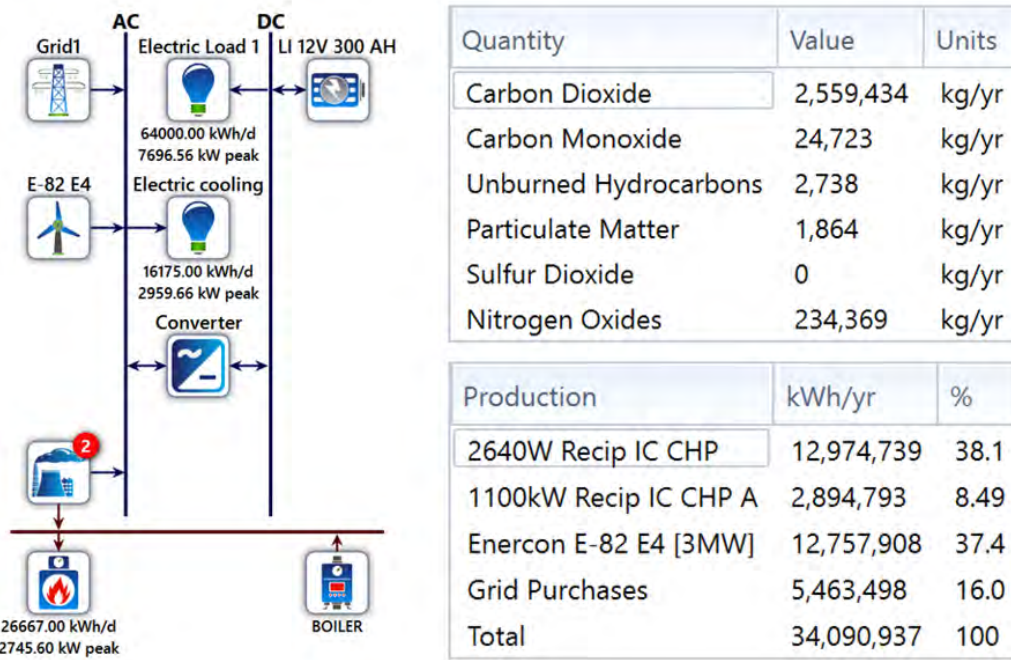


Figure 69: Power setup schematic, emissions data and yearly electric production by source for the grid connected biomass CHP, wind and battery two hectare system.

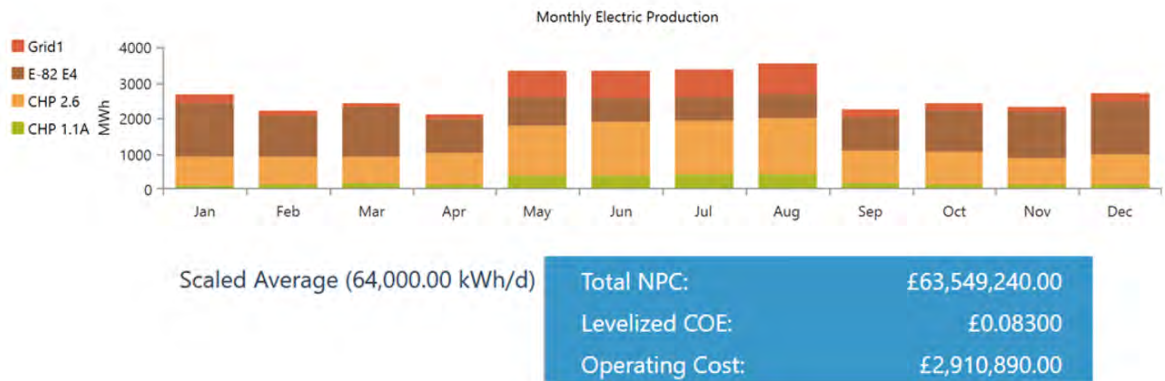


Figure 70: Monthly electric production by energy source, NPC, LCOE and operating costs for the grid connected biomass CHP, wind and battery two hectare system.

If one compares the cost difference between this case and the sole grid case, as shown in Figure 71, it is clear that again (as for previous systems in this chapter) the initial cost is higher for the renewable case, but when considering the whole project cost the renewable system is much cheaper.

The payback time is only 5.1 years in this case with a return on investment of 12.9%. Overall, not only is the cost significantly cheaper, but also the emissions and environmental footprint is much lower than for a solely grid supplied system.

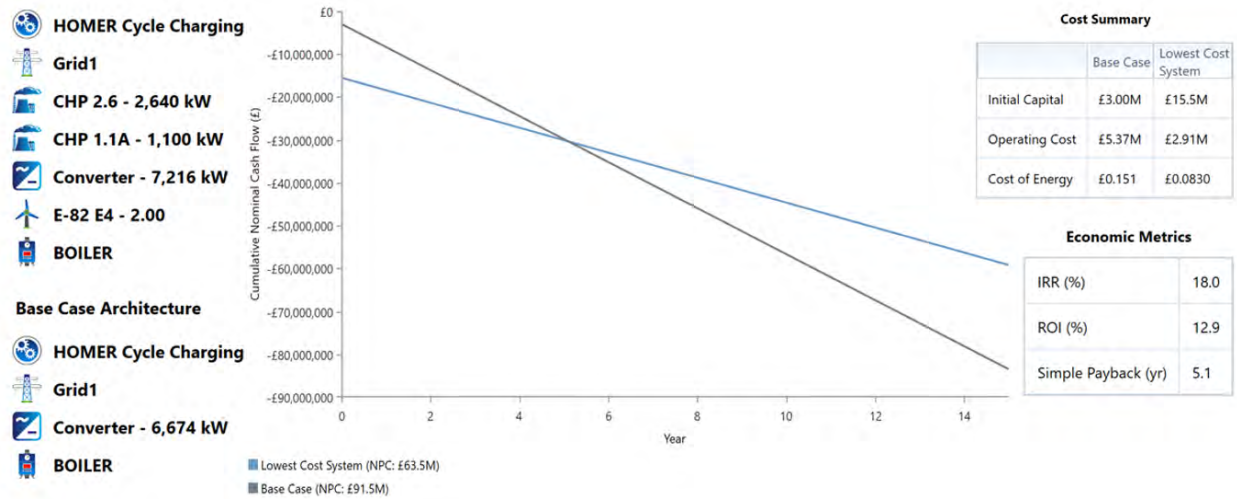


Figure 71: Economic analysis of the grid connected biomass CHP, wind and battery two hectare system in comparison to the base grid system throughout the 15 year project length.

6.4 Section Summary

The other sections in the project have assessed strategies to reduce energy consumption while maintaining optimal plant growth. This section has aimed instead to evaluate and compare different renewable energy supply options in order to try and lower the system's carbon footprint and cost, in comparison to a solely grid supplied system.

The HOMER software has been used to simulate different renewable grid and off-grid power supply systems, both for the case study strawberry growing system in section 4 and for scaled up one and two hectare systems based on the case study system (i.e. vertical greenhouses with supplemental LED lighting). Various combinations of grid, wind and solar energy coupled with lithium ion batteries were considered to supply the electricity for the lighting of the greenhouse.

For a small system based on the UoR case study, a grid connected setup with wind, PV and

batteries gave the optimum cost with high emission cuts. Compared to the solely grid supplied system, the total NPC was 89%, LCOE was 61% and CO₂ emissions were 39%. For the one hectare system, a grid connected setup with wind and batteries was optimum, with 78% of the NPC, 56% of the LCOE and 66% of the CO₂ emissions compared with a solely grid supplied setup. For the two hectare system, a grid connected setup with wind generation and batteries gave 68% NPC, 52% LCOE and 61% CO₂ emissions compared with a solely grid supplied setup.

Following on from these results, biomass CHP has been considered, to benefit fully from the high efficiency potential of cogeneration and utilise likely biomass resources on a CEA crop growing facility. Extra power demand (thermal) was introduced to the greenhouse system to account for the heating/cooling power required on top of the lighting power. Considering two different biogases for a one hectare system, integration of biomass CHP with grid, wind and batteries gave favourable results in both cases, compared to a solely grid supplied system. Biogas 1 was chosen moving forward to a two hectare system, due to its much lower emission data, and despite being more costly than biogas 2, it still gave a much lower cost than the pure grid supplied equivalent system. This was the case for both the one and two hectare systems, but with the two hectare system benefiting more from the use of biomass CHP.

7 Concluding Remarks & Future Work

7.1 Summary

Firstly, an LED lit Little Gem lettuce growing experiment was designed and built from scratch in order to test the effectiveness of various spectral compositions on the growth of Little Gem lettuce, finding that (similarly to the literature on other lettuce variants) a mixture of blue & red light gives the best yield after 21 days. Boards with only blue light also gave crops with good leaf shape and colour as well as reasonably high weight. The purely red board gave the third biggest yield by weight, but shoots were too long and leaf width was low. The purely green LED board and the greenhouse reference tray gave the weakest growth results.

Neural network analysis on LED lighting for lettuce was then investigated. A series of data sets from various literature on lettuce growth using LEDs was collected and normalised such that the data was maximally compatible. A deep neural network was then fit to the data using MATLAB's neural network tool to test performance. Fitting results show that there is a general tendency for the neural network to fit to the target data, with an R value of around 0.8 for all data sets and an error histogram which is significantly better than one which would represent random prediction data. There is however significant variation in the error, with some large errors in neural network predicted vs target data. This was thought to be due to the incoherence between the different studies in the literature. Not only were many of the studies looking at different varieties of lettuce, but they also had different experimental conditions and approaches beyond the lighting input data. As Ozawa *et al.* stated in their work comparing two studies with very similar conditions two years apart, there was significant difference in output data even in identical lighting conditions for the same crop [85]. Overall, it seems that though neural networks could prove to be very useful for this application, the difficulty comes when collating data from different studies. If enough data on growth of a species under several LED light recipes was available from a single source with identical experimental conditions and procedure, fitting of data using neural networks could potentially give considerably better results.

Next, a model system was built based on the three vertical tier LED lit strawberry growing facility at the University of Reading. A series of the following CEA power saving considerations were investigated in a simplified conservative approach to be combined and quantitatively analysed for

energy saving potential:

1. Careful choice of the most efficient LED devices available for setup. For the UoR system used as a case study the newest Osram lights were compared to the currently used Sulis LED boards:

Calculated Energy Saving: **14%**

2. Energy saving from appropriate choice of the spectral recipes based on the literature. A comparison of purely white Osram LED boards vs an optimal (for strawberries) [86] red/blue/white mixture with the same PPFD output value gives:

Calculated Energy Saving: **21%**

3. Calculations based on dimming LED boards during sunlight hours on clear days where appropriate for a 3-tiered greenhouse as at the UoR gives:

Calculated Energy Saving: **8%**

4. DC rectifier use in place of AC could increase efficiency. Additionally, it would be less prone to faults since there are fewer components and would therefore increase the average lifetime of modules (this point forms the basis of the work in section 5, where further investigation of this is looked at).

Estimated Energy Saving: **10%**

5. Operating LEDs at half the forward current increases power output efficiency and also lowers LED junction temperature and therefore increase lifetime, while making the modules more compact by reducing heat-sink requirements; so higher investment of LED number is balanced by energy saving and increased time before replacement.

Estimated Energy Saving: **6%**

These savings have been calculated to give a significant combined total estimated energy savings of approximately **47%** when compared with a system which does not employ any of the energy saving methods investigated.

In section 5, power distribution to lighting setup was considered. Arguments for DC grid supply in place of AC grid supply to LEDs were discussed, referring to existing literature on other DC grid application areas and electricity savings. Schematics of a DC based greenhouse system were discussed followed by modelling of both DC-DC buck converter and rectifier coupled with buck converter in MATLAB Simulink.

In section 6, the HOMER software was used to find optimum power generation setups involving a variety of renewable options, with and without grid connection, for a UK LED CEA facility. System input load requirements were calculated based on the UoR case study from section 4, energy cost tariffs taken from a UK energy company and installation costs along with different grid connected and off-grid supply setup regimes realised from the HOMER software. Energy production, use and storage information was calculated using the software, it was then optimised by varying the share of power production from different technologies in order to minimise overall cost while meeting power demand. Net present cost and cost of electricity was calculated, as was emissions data. This process was done for three system sizes: a small system the size of the UoR case study system, then a scaled up one hectare system, then a two hectare system.

Optimisation results show that a grid connected system with wind turbines, PV and lithium ion batteries installed would be the cheapest and most environmentally sustainable option for a small system comparable in size with the UoR case study system, offering an 11% saving on NPC and a 61% saving on CO₂ emissions. For larger systems, wind energy becomes dominant, with a grid connected wind turbine system being the overall favourable setup, offering a 22% saving on NPC and a 34% saving on CO₂ emissions in the case of the one hectare system. For the case of the larger two hectare system, the wind and battery grid system offered a 32% saving on NPC and 39% saving on CO₂ emissions relative to a conventional grid powered system. In all of the optimal setups, initial investment is higher than for the standard grid case, but within the lifetime of the project, the lowered operating costs render the project less expensive overall, with an associated simple payback time (yr) as seen in this section's figures. This combined with the large emission decreases means that for LED CEA systems in the UK, small and large, integration with renewables cuts both cost and emissions, requiring only a higher initial investment.

Lastly, biomass CHP was considered as an extra renewable technology on top of the ones previously included in optimisations, with an extra thermal load added accounting for the heating and cooling of the greenhouse. Optimisations were performed with a one hectare system using two preset biogas options from the HOMER software, both of which gave lower cost and emissions than a purely grid supplied case. Biogas 1 was chosen to progress to a two hectare system, as the emissions were significantly lower than for biogas 2, where the cost was proportionally less high. Results for these optimisations show that biomass CHP systems could cut costs and emissions by utilising available waste biomass on site. They also show that as the system size increases, the cost effectiveness does as well; large biomass CHP, wind, battery and grid LED lit and heated and cooled CEA systems in the UK are significantly more cost effective and environmentally friendly than conventional grid supplied systems.

7.2 Future Work

Regarding future work, there are many potential avenues which could be explored based on this project's topics. Firstly, regarding the Little Gem lettuce growth experiments, as discussed in section 2.3.3, if a future experiment were to take place, a much higher level of resources would be needed in order to generate high amounts of good quality reliable data on spectral response of Little Gem lettuce. A significantly higher number of LED boards should be tested, and all including some levels of both red and blue light. These should use a higher performance LED such as the Osram bulbs discussed and also PPFD data should be available at the beginning of the experiment and boards designed with enough lights on them to supply an ideal level of PPFD. Experiments should also operate within an environment with optimised CO₂ concentration, humidity and temperature so that crop growth from spectral response is not in any way impeded by lack of ideal conditions outside lighting. In terms of output variables measured, more devices could be used to measure more quantities, which could be useful for modelling in neural networks.

Secondly, as concluded in section 3, there needs to be a much larger data set from experiments with identical conditions (aside from lighting) in order for deep neural networks to potentially work. If this can be either supplied by potential prospective experimental collaborators or generated from future experiments as detailed in the previous paragraph, then the same methodology could be better tested in order to evaluate the feasibility of deep neural networks for predicting optimal LED

light recipes for maximum yield.

In terms of expanding on the work in section 4, more technical analysis of a holistic approach to energy saving in LED CEA systems could be conducted. This would be similar to the work in section 4, but instead of a small number of strategies considered with simplified and generally conservative estimates for energy saving being predicted and combined, a more in depth quantitative analysis of the literature could be considered to give a more accurate and ambitious estimate of the combined energy saving potential. For example, this could include real-time modelling of adaptive LED light dimming with sunlight. It could also include experimental measurement of efficacy vs forward current for chosen LED bulbs, in order to gain insight on optimal operating current. Investigating the use of the Trace Pro software to model reflectors to maximise light received by the plant surface could be done. Methods such as pulsing light to save energy whilst maintaining optimal yield could also be considered. There are a significant number of these individual energy saving strategies, many of which could theoretically be incorporated simultaneously.

Modelling of AC-DC rectifier and DC-DC converter in MATLAB Simulink from section 5 could be completed, and power losses and energy efficiency calculated and compared with the standard AC grid LED system case. These simulated devices can then be incorporated directly into HOMER simulations to model energy consumption and cost for various different DC grid setups. These could also incorporate the other discussed energy saving strategies to combine and give total energy saving analysis incorporating all sections of this work.

Finally, regarding section 6, the same methodology using HOMER could be applied to different geographical areas of interest and case study candidate systems. Additionally, if information and power saving/optimisation techniques gathered in the future work from other sections was incorporated once conducted, the updated load profile and initial-cost implications could give new simulation results which would reflect a more all encompassing indication of how low energy consumption and greenhouse gas emissions could potentially be for high performance LED lit CEA systems.

8 References

- [1] P. Ponce, A. Molina, P. Cepeda, E. Lugo, and B. MacCleery, *Greenhouse design and control*. CRC Press, 2014.
- [2] X. Zhu, R. Clements, J. Hagggar, A. Quezada, and J. Torres, “Technologies for climate change adaptation-agriculture sector,” 2011.
- [3] W. R. Briggs and M. A. Olney, “Photoreceptors in plant photomorphogenesis to date. five phytochromes, two cryptochromes, one phototropin, and one superchrome,” *Plant Physiology*, vol. 125, no. 1, pp. 85–88, 2001.
- [4] J. J. Casal, “Phytochromes, cryptochromes, phototropin: photoreceptor interactions in plants,” *Photochemistry and Photobiology*, vol. 71, no. 1, pp. 1–11, 2000.
- [5] C. Fankhauser and J. Chory, “Light control of plant development,” *Annual review of cell and developmental biology*, vol. 13, no. 1, pp. 203–229, 1997.
- [6] H. Poorter, Ü. Niinemets, N. Ntagkas, A. Siebenkäs, M. Mäenpää, S. Matsubara, and T. Pons, “A meta-analysis of plant responses to light intensity for 70 traits ranging from molecules to whole plant performance,” *New Phytologist*, vol. 223, no. 3, pp. 1073–1105, 2019.
- [7] S. Adams and F. Langton, “Photoperiod and plant growth: a review,” *The Journal of Horticultural Science and Biotechnology*, vol. 80, no. 1, pp. 2–10, 2005.
- [8] G. Verhoeven, “The reflection of two fields – electromagnetic radiation and its role in (aerial) imaging,” vol. 55, pp. 13–18, 10 2017.
- [9] P. A. Davis and C. Burns, “Photobiology in protected horticulture,” *Food and Energy Security*, vol. 5, no. 4, pp. 223–238, 2016.
- [10] K. J. McCree, “The action spectrum, absorptance and quantum yield of photosynthesis in crop plants,” *Agricultural Meteorology*, vol. 9, pp. 191–216, 1971.
- [11] P. D. Cerdán and J. Chory, “Regulation of flowering time by light quality,” *Nature*, vol. 423, no. 6942, pp. 881–885, 2003.
- [12] G. D. Massa, H.-H. Kim, R. M. Wheeler, and C. A. Mitchell, “Plant productivity in response to led lighting,” *HortScience*, vol. 43, no. 7, pp. 1951–1956, 2008.

- [13] T. Ouzounis, E. Rosenqvist, and C.-O. Ottosen, "Spectral effects of artificial light on plant physiology and secondary metabolism: a review," *HortScience*, vol. 50, no. 8, pp. 1128–1135, 2015.
- [14] K. M. Folta and K. S. Childers, "Light as a growth regulator: controlling plant biology with narrow-bandwidth solid-state lighting systems," *HortScience*, vol. 43, no. 7, pp. 1957–1964, 2008.
- [15] R. J. Bula, R. C. Morrow, T. Tibbitts, D. Barta, R. Ignatius, and T. Martin, "Light-emitting diodes as a radiation source for plants," *HortScience*, vol. 26, no. 2, pp. 203–205, 1991.
- [16] A. Zukauskas, Z. Bliznikas, K. Breivė, A. Novičkovas, G. Samuolienė, A. Urbonavičiūtė, A. Brazaitytė, J. Jankauskienė, and P. Duchovskis, "Effect of supplementary pre-harvest led lighting on the antioxidant properties of lettuce cultivars," in *VI International Symposium on Light in Horticulture 907*, pp. 87–90, 2009.
- [17] M. LIU and X. ZHU, "Points of several key issues on agricultural lighting," *CHINA LIGHT & LIGHTING*, pp. 1–4, 2015.
- [18] N. Yeh and J.-P. Chung, "High-brightness leds—energy efficient lighting sources and their potential in indoor plant cultivation," *Renewable and Sustainable Energy Reviews*, vol. 13, no. 8, pp. 2175–2180, 2009.
- [19] "Control flowering with leds. lighting research. growers talk 62." <http://www.ballpublishing.com/GrowerTalks/ViewArticle.aspx?articleid=20604>.
- [20] D. Singh, C. Basu, M. Meinhardt-Wollweber, and B. Roth, "Leds for energy efficient greenhouse lighting," *Renewable and Sustainable Energy Reviews*, vol. 49, pp. 139–147, 2015.
- [21] H. Watanabe, "Light-controlled plant cultivation system in japan-development of a vegetable factory using leds as a light source for plants," in *VI International Symposium on Light in Horticulture 907*, pp. 37–44, 2009.
- [22] T. Kozai, "Resource use efficiency of closed plant production system with artificial light: Concept, estimation and application to plant factory," *Proceedings of the Japan Academy, Series B*, vol. 89, no. 10, pp. 447–461, 2013.

- [23] W. Van Ieperen and G. Trouwborst, "The application of leds as assimilation light source in greenhouse horticulture: a simulation study," in *International Symposium on High Technology for Greenhouse System Management: Greensys2007 801*, pp. 1407–1414, 2007.
- [24] E. F. Schubert, *Light-emitting diodes*. E. Fred Schubert, 2018.
- [25] E. F. Schubert, T. Gessmann, and J. K. Kim, "Light emitting diodes," *Kirk-Othmer Encyclopedia of Chemical Technology*, 2000.
- [26] "Led fundamental series by osram opto semiconductor." https://www.osram.com/os/products/illumination-applications/tools-and-service/led-fundamentals/leds_basics.jsp.
- [27] C. Lenk and R. Lenk, "Practical lighting design with leds (ed.) john wiley & sons," 2011.
- [28] M. Pietrzykowska, *The roles of Lhcb1 och Lhcb2 in regulation of photosynthetic light harvesting*. PhD thesis, Umeå University, 2015.
- [29] T. Yanagi, K. Okamoto, and S. Takita, "Effect of blue and red light intensity on photosynthetic rate of strawberry leaves," in *International Symposium on Plant Production in Closed Ecosystems 440*, pp. 371–376, 1996.
- [30] C. S. Brown, A. C. Schuerger, and J. C. Sager, "Growth and photomorphogenesis of pepper plants under red light-emitting diodes with supplemental blue or far-red lighting," *Journal of the American Society for Horticultural Science*, vol. 120, no. 5, pp. 808–813, 1995.
- [31] G. D. Goins, N. C. Yorio, M. Sanwo, and C. Brown, "Photomorphogenesis, photosynthesis, and seed yield of wheat plants grown under red light-emitting diodes (leds) with and without supplemental blue lighting," *Journal of experimental botany*, vol. 48, no. 7, pp. 1407–1413, 1997.
- [32] B. C. Tripathy and C. S. Brown, "Root-shoot interaction in the greening of wheat seedlings grown under red light," *Plant Physiology*, vol. 107, no. 2, pp. 407–411, 1995.
- [33] M.-J. Lee, K.-H. Son, and M.-M. Oh, "Increase in biomass and bioactive compounds in lettuce under various ratios of red to far-red led light supplemented with blue led light," *Horticulture, Environment, and Biotechnology*, vol. 57, no. 2, pp. 139–147, 2016.

- [34] M. Koornneef and R. E. Kendrick, “Photomorphogenic mutants of higher plants,” in *Photomorphogenesis in plants*, pp. 601–628, Springer, 1994.
- [35] R. Paradiso and S. Proietti, “Light-quality manipulation to control plant growth and photomorphogenesis in greenhouse horticulture: The state of the art and the opportunities of modern led systems,” *Journal of Plant Growth Regulation*, pp. 1–39, 2021.
- [36] J. W. Reed, P. Nagpal, D. S. Poole, M. Furuya, and J. Chory, “Mutations in the gene for the red/far-red light receptor phytochrome b alter cell elongation and physiological responses throughout arabidopsis development.,” *The Plant Cell*, vol. 5, no. 2, pp. 147–157, 1993.
- [37] S. Demotes-Mainard, T. Péron, A. Corot, J. Bertheloot, J. Le Gourrierec, S. Pelleschi-Travier, L. Crespel, P. Morel, L. Huché-Thélier, R. Boumaza, *et al.*, “Plant responses to red and far-red lights, applications in horticulture,” *Environmental and experimental Botany*, vol. 121, pp. 4–21, 2016.
- [38] G. W. Stutte, S. Edney, and T. Skerritt, “Photoregulation of bioprotectant content of red leaf lettuce with light-emitting diodes,” *HortScience*, vol. 44, no. 1, pp. 79–82, 2009.
- [39] G. D. Goins, L. M. Ruffe, N. A. Cranston, N. C. Yorio, R. M. Wheeler, and J. C. Sager, “Salad crop production under different wavelengths of red light-emitting diodes (leds),” tech. rep., SAE Technical Paper, 2001.
- [40] D. S. Craig and E. S. Runkle, “A moderate to high red to far-red light ratio from light-emitting diodes controls flowering of short-day plants,” *Journal of the American Society for Horticultural Science*, vol. 138, no. 3, pp. 167–172, 2013.
- [41] T. Mizuno, W. Amaki, and H. Watanabe, “Effects of monochromatic light irradiation by led on the growth and anthocyanin contents in leaves of cabbage seedlings,” in *VI International Symposium on Light in Horticulture 907*, pp. 179–184, 2009.
- [42] S. Nakamura, T. Mukai, and M. Senoh, “Candela-class high-brightness ingan/algan double-heterostructure blue-light-emitting diodes,” *Applied Physics Letters*, vol. 64, no. 13, pp. 1687–1689, 1994.
- [43] N. C. Yorio, G. D. Goins, H. R. Kagie, R. M. Wheeler, and J. C. Sager, “Improving spinach, radish, and lettuce growth under red light-emitting diodes (leds) with blue light supplementation,” *HortScience*, vol. 36, no. 2, pp. 380–383, 2001.

- [44] G. Akoyunoglou and H. Anni, “Blue light effect on chloroplast development in higher plants,” in *Blue light effects in biological systems*, pp. 397–406, Springer, 1984.
- [45] A. Sæbø, T. Krekling, and M. Appelgren, “Light quality affects photosynthesis and leaf anatomy of birch plantlets in vitro,” *Plant Cell, Tissue and Organ Culture*, vol. 41, no. 2, pp. 177–185, 1995.
- [46] H. Senger, “The effect of blue light on plants and microorganisms,” *Photochem. Photobiol.*, vol. 35, no. 6, pp. 911–920, 1982.
- [47] W. R. Briggs and E. Huala, “Blue-light photoreceptors in higher plants,” *Annual review of cell and developmental biology*, vol. 15, no. 1, pp. 33–62, 1999.
- [48] Z. H. Bian, Q. C. Yang, and W. K. Liu, “Effects of light quality on the accumulation of phytochemicals in vegetables produced in controlled environments: a review,” *Journal of the Science of Food and Agriculture*, vol. 95, no. 5, pp. 869–877, 2015.
- [49] H. Li, C. Tang, Z. Xu, X. Liu, and X. Han, “Effects of different light sources on the growth of non-heading chinese cabbage (*brassica campestris* l.),” *Journal of Agricultural Science*, vol. 4, no. 4, p. 262, 2012.
- [50] M. G. Lefsrud, D. A. Kopsell, and C. E. Sams, “Irradiance from distinct wavelength light-emitting diodes affect secondary metabolites in kale,” *HortScience*, vol. 43, no. 7, pp. 2243–2244, 2008.
- [51] M. Johkan, K. Shoji, F. Goto, S.-n. Hahida, and T. Yoshihara, “Effect of green light wavelength and intensity on photomorphogenesis and photosynthesis in *lactuca sativa*,” *Environmental and Experimental Botany*, vol. 75, pp. 128–133, 2012.
- [52] P. Chen, “Chlorophyll and other photosensitive,” *LED Grow Lights, Absorption Spectrum for Plant Photosensitive Pigments*. <http://www.ledgrowlightshq.co.uk/chlorophyllplant-pigments/>. Accessed, vol. 12, 2014.
- [53] A. C. Schuerger, C. S. Brown, and E. C. Stryjewski, “Anatomical features of pepper plants (*capsicum annuum*l.) grown under red light-emitting diodes supplemented with blue or far-red light,” *Annals of Botany*, vol. 79, no. 3, pp. 273–282, 1997.

- [54] A. Novičkovas, A. Brazaitytė, P. Duchovskis, J. Jankauskienė, G. Samuolienė, A. Virsilė, R. Sirtautas, Z. Bliznikas, and A. Zukauskas, “Solid-state lamps (leds) for the short-wavelength supplementary lighting in greenhouses: experimental results with cucumber,” in *XXVIII International Horticultural Congress on Science and Horticulture for People (IHC2010): International Symposium on 927*, pp. 723–730, 2010.
- [55] K. M. Folta, “Green light stimulates early stem elongation, antagonizing light-mediated growth inhibition,” *Plant Physiology*, vol. 135, no. 3, pp. 1407–1416, 2004.
- [56] H.-H. Kim, G. D. Goins, R. M. Wheeler, and J. C. Sager, “Green-light supplementation for enhanced lettuce growth under red-and blue-light-emitting diodes,” *HortScience*, vol. 39, no. 7, pp. 1617–1622, 2004.
- [57] A. E. Stapleton, “Ultraviolet radiation and plants: burning questions,” *The Plant Cell*, vol. 4, no. 11, p. 1353, 1992.
- [58] C. M. Bourget, “An introduction to light-emitting diodes,” *HortScience*, vol. 43, no. 7, pp. 1944–1946, 2008.
- [59] I. Voipio and J. Autio, “Responses of red-leaved lettuce to light intensity, uv-a radiation and root zone temperature,” *Greenhouse Environment Control and Automation 399*, pp. 183–190, 1994.
- [60] E. Tsormpatsidis, R. Henbest, F. J. Davis, N. Battey, P. Hadley, and A. Wagstaffe, “Uv irradiance as a major influence on growth, development and secondary products of commercial importance in lollo rosso lettuce ‘revolution’ grown under polyethylene films,” *Environmental and Experimental Botany*, vol. 63, no. 1-3, pp. 232–239, 2008.
- [61] J. Rozema, J. van de Staaij, L. O. Björn, and M. Caldwell, “Uv-b as an environmental factor in plant life: stress and regulation,” *Trends in Ecology & Evolution*, vol. 12, no. 1, pp. 22–28, 1997.
- [62] X. Liu, T. Chang, S. Guo, Z. Xu, and J. Li, “Effect of different light quality of led on growth and photosynthetic character in cherry tomato seedling,” in *VI International Symposium on Light in Horticulture 907*, pp. 325–330, 2009.
- [63] R. Wheeler, J. Sager, G. Goins, and H.-H. Kim, “A comparison of growth and photosynthetic characteristics of lettuce grown under red and blue light-emitting diodes (leds) with and

- without supplemental green leds,” in *VII International Symposium on Protected Cultivation in Mild Winter Climates: Production, Pest Management and Global Competition 659*, pp. 467–475, 2004.
- [64] T. Yanagi, K. Okamoto, and S. Takita, “Effects of blue, red, and blue/red lights of two different ppf levels on growth and morphogenesis of lettuce plants,” in *International Symposium on Plant Production in Closed Ecosystems 440*, pp. 117–122, 1996.
- [65] H.-H. Kim, R. M. Wheeler, J. C. Sager, N. C. Yorio, and G. D. Goins, “Light-emitting diodes as an illumination source for plants: A review of research at kennedy space center,” *Habitation*, vol. 10, no. 2, pp. 71–78, 2005.
- [66] M. O. Ojo and A. Zahid, “Deep learning in controlled environment agriculture: A review of recent advancements, challenges and prospects,” *Sensors*, vol. 22, no. 20, p. 7965, 2022.
- [67] B. Alhnaity, S. Pearson, G. Leontidis, and S. Kollias, “Using deep learning to predict plant growth and yield in greenhouse environments,” *arXiv preprint arXiv:1907.00624*, 2019.
- [68] M. T. Hagan, H. B. Demuth, and M. Beale, *Neural network design*. PWS Publishing Co., 1997.
- [69] L. Shukla, “Fundamentals of neural networks.” <https://www.wandb.com/articles/fundamentals-of-neural-networks>.
- [70] F. Rosenblatt, “The perceptron: a probabilistic model for information storage and organization in the brain,” *Psychological review*, vol. 65, no. 6, p. 386, 1958.
- [71] S. Marsland, *Machine learning: an algorithmic perspective*. Chapman and Hall/CRC, 2011.
- [72] H.-H. Kim, G. D. Goins, R. M. Wheeler, and J. C. Sager, “Stomatal conductance of lettuce grown under or exposed to different light qualities,” *Annals of Botany*, vol. 94, no. 5, pp. 691–697, 2004.
- [73] K. Son, J. Park, D. Kim, M. Oh, *et al.*, “Leaf shape index, growth, and phytochemicals in two leaf lettuce cultivars grown under monochromatic light-emitting diodes,” *Korean Journal of Horticultural Science & Technology*, vol. 30, no. 6, pp. 664–672, 2012.

- [74] K.-H. Son and M.-M. Oh, “Leaf shape, growth, and antioxidant phenolic compounds of two lettuce cultivars grown under various combinations of blue and red light-emitting diodes,” *HortScience*, vol. 48, no. 8, pp. 988–995, 2013.
- [75] J. H. Kang, S. KrishnaKumar, S. L. S. Atulba, B. R. Jeong, and S. J. Hwang, “Light intensity and photoperiod influence the growth and development of hydroponically grown leaf lettuce in a closed-type plant factory system,” *Horticulture, Environment, and Biotechnology*, vol. 54, no. 6, pp. 501–509, 2013.
- [76] K.-H. Lin, M.-Y. Huang, W.-D. Huang, M.-H. Hsu, Z.-W. Yang, and C.-M. Yang, “The effects of red, blue, and white light-emitting diodes on the growth, development, and edible quality of hydroponically grown lettuce (*lactuca sativa* l. var. capitata),” *Scientia Horticulturae*, vol. 150, pp. 86–91, 2013.
- [77] S. Muneer, E. J. Kim, J. S. Park, and J. H. Lee, “Influence of green, red and blue light emitting diodes on multiprotein complex proteins and photosynthetic activity under different light intensities in lettuce leaves (*lactuca sativa* l.),” *International journal of molecular sciences*, vol. 15, no. 3, pp. 4657–4670, 2014.
- [78] K. R. Cope, M. C. Snowden, and B. Bugbee, “Photobiological interactions of blue light and photosynthetic photon flux: Effects of monochromatic and broad-spectrum light sources,” *Photochemistry and photobiology*, vol. 90, no. 3, pp. 574–584, 2014.
- [79] K.-H. Son and M.-M. Oh, “Growth, photosynthetic and antioxidant parameters of two lettuce cultivars as affected by red, green, and blue light-emitting diodes,” *Horticulture, Environment, and Biotechnology*, vol. 56, no. 5, pp. 639–653, 2015.
- [80] M. Urrestarazu, C. Nájera, and M. del Mar Gea, “Effect of the spectral quality and intensity of light-emitting diodes on several horticultural crops,” *HortScience*, vol. 51, no. 3, pp. 268–271, 2016.
- [81] X.-l. Chen, X.-z. Xue, W.-z. Guo, L.-c. Wang, and X.-j. Qiao, “Growth and nutritional properties of lettuce affected by mixed irradiation of white and supplemental light provided by light-emitting diode,” *Scientia horticulturae*, vol. 200, pp. 111–118, 2016.

- [82] W. H. Kang, J. S. Park, K. S. Park, and J. E. Son, "Leaf photosynthetic rate, growth, and morphology of lettuce under different fractions of red, blue, and green light from light-emitting diodes (leds)," *Horticulture, Environment, and Biotechnology*, vol. 57, no. 6, pp. 573–579, 2016.
- [83] H. Liu, Y. Fu, and M. Wang, "Green light enhances growth, photosynthetic pigments and co₂ assimilation efficiency of lettuce as revealed by 'knock out' of the 480–560 nm spectral waveband," *Photosynthetica*, vol. 55, no. 1, pp. 144–152, 2017.
- [84] T. Han, V. Vaganov, S. Cao, Q. Li, L. Ling, X. Cheng, L. Peng, C. Zhang, A. N. Yakovlev, Y. Zhong, *et al.*, "Improving "color rendering" of led lighting for the growth of lettuce," *Scientific Reports*, vol. 7, p. 45944, 2017.
- [85] M. OZAWA, Y. SANO, Y. NAKANO, and M. AKUTSU, "Growth differences among eight leaf lettuces cultivated under led light and comparison of two leaf lettuces grown in 2016 and in 2018," *ICIC express letters. Part B, Applications: an international journal of research and surveys*, vol. 10, no. 11, pp. 985–993, 2019.
- [86] C. Piovene, F. Orsini, S. Bosi, R. Sanoubar, V. Bregola, G. Dinelli, and G. Gianquinto, "Optimal red: blue ratio in led lighting for nutraceutical indoor horticulture," *Scientia Horticulturae*, vol. 193, pp. 202–208, 2015.
- [87] Philips, "Understanding power led lifetime analysis." http://www.climateaction.org/images/uploads/documents/Philips_Understanding-Power-LED-Lifetime-Analysis.pdf.
- [88] A. Varella, D. J. Moot, K. Pollock, P. L. Peri, and R. J. Lucas, "Do light and alfalfa responses to cloth and slatted shade represent those measured under an agroforestry system?," *Agroforestry systems*, vol. 81, no. 2, pp. 157–173, 2011.
- [89] J. Bright, C. Smith, P. Taylor, and R. Crook, "Stochastic generation of synthetic minutely irradiance time series derived from mean hourly weather observation data," *Solar Energy*, vol. 115, pp. 229–242, 2015.
- [90] H.-J. Tantau, J. Hinken, B. von Elsner, J. Max, A. Ulbrich, U. Schurr, T. Hofmann, and G. Reisinger, "Solar transmittance of greenhouse covering materials," in *VII International Symposium on Light in Horticultural Systems 956*, pp. 441–448, 2012.

- [91] R. T. Watson, M.-C. Boudreau, and M. W. van Iersel, "Simulation of greenhouse energy use: An application of energy informatics," *Energy Informatics*, vol. 1, no. 1, p. 1, 2018.
- [92] V. Vossos, K. Johnson, M. Kloss, M. Khattar, and R. Brown, "A market assessment for dc distribution systems in buildings," *Lawrence Berkeley National Laboratory, Berkeley, CA*, 2017.
- [93] V. Vossos, K. Johnson, M. Kloss, M. Khattar, D. Gerber, and R. Brown, "Review of dc power distribution in buildings: A technology and market assessment," *LBNL Report, Berkeley*, 2017.
- [94] E. Vossos, S. Pantano, R. Heard, and R. Brown, "Dc appliances and dc power distribution: A bridge to the future net zero energy homes," 2017.
- [95] P. Wang, L. Goel, X. Liu, and F. H. Choo, "Harmonizing ac and dc: A hybrid ac/dc future grid solution," *IEEE Power and Energy Magazine*, vol. 11, no. 3, pp. 76–83, 2013.
- [96] M. Starke, L. M. Tolbert, and B. Ozpineci, "Ac vs. dc distribution: A loss comparison," in *2008 IEEE/PES Transmission and Distribution Conference and Exposition*, pp. 1–7, IEEE, 2008.
- [97] S. Willems and W. Aerts, "Study and simulation of a dc micro grid with focus on efficiency, use of materials and economic constraints," *University of Leuven, Leuven, Belgium*, 2014.
- [98] D. L. Gerber, V. Vossos, W. Feng, A. Khandekar, C. Marnay, and B. Nordman, "A simulation based comparison of ac and dc power distribution networks in buildings," in *2017 IEEE Second International Conference on DC Microgrids (ICDCM)*, pp. 588–595, IEEE, 2017.
- [99] D. L. Gerber, V. Vossos, W. Feng, C. Marnay, B. Nordman, and R. Brown, "A simulation-based efficiency comparison of ac and dc power distribution networks in commercial buildings," *Applied Energy*, vol. 210, pp. 1167–1187, 2018.
- [100] V. Vossos, D. Gerber, Y. Bennani, R. Brown, and C. Marnay, "Techno-economic analysis of dc power distribution in commercial buildings," *Applied energy*, vol. 230, pp. 663–678, 2018.
- [101] S. M. Frank and S. Rebennack, "Optimal design of mixed ac–dc distribution systems for commercial buildings: A nonconvex generalized benders decomposition approach," *European Journal of Operational Research*, vol. 242, no. 3, pp. 710–729, 2015.

- [102] R. Weiss, L. Ott, and U. Boeke, “Energy efficient low-voltage dc-grids for commercial buildings,” in *2015 IEEE First International Conference on DC Microgrids (ICDCM)*, pp. 154–158, IEEE, 2015.
- [103] U. Boeke and M. Wendt, “Dc power grids for buildings,” in *2015 IEEE First International Conference on DC Microgrids (ICDCM)*, pp. 210–214, IEEE, 2015.
- [104] D. Fregosi, S. Ravula, D. Brhlik, J. Saussele, S. Frank, E. Bonnema, J. Scheib, and E. Wilson, “A comparative study of dc and ac microgrids in commercial buildings across different climates and operating profiles,” in *2015 IEEE First International Conference on DC Microgrids (ICDCM)*, pp. 159–164, IEEE, 2015.
- [105] S. N. Backhaus, G. W. Swift, S. Chatzivasileiadis, W. Tschudi, S. Glover, M. Starke, J. Wang, M. Yue, and D. Hammerstrom, “Dc microgrids scoping study. estimate of technical and economic benefits,” tech. rep., Los Alamos National Lab.(LANL), Los Alamos, NM (United States), 2015.
- [106] P. Savage, R. Nordhaus, and S. Jamieson, “Dc microgrids: Benefits and barriers,|| from silos to systems: Issues in clean energy and climate change,” 2010.
- [107] K. Garbesi, “Catalog of dc appliances and power systems,” 2012.
- [108] V. Vossos, K. Garbesi, and H. Shen, “Energy savings from direct-dc in us residential buildings,” *Energy and Buildings*, vol. 68, pp. 223–231, 2014.
- [109] D. J. Hammerstrom, “Ac versus dc distribution systemsdid we get it right?,” in *2007 IEEE Power Engineering Society General Meeting*, pp. 1–5, IEEE, 2007.
- [110] B. Nordman, “What the real world tells us about saving energy in electronics,” in *presentation, at the 1st Berkeley Symposium on Energy Efficient Electronic Systems (E3S)*, 2009.
- [111] A. Gago-Calderón, R. D. Orejón-Sánchez, and M. J. Hermoso-Orzáez, “Dc network indoor and outdoor led lighting,” *Light-Emitting Diode: An Outlook On the Empirical Features and Its Recent Technological Advancements*, p. 15, 2018.
- [112] S. Thielemans, D. Di Zenobio, A. Touhafi, P. Lataire, and K. Steenhaut, “Dc grids for smart led-based lighting: The edison solution,” *Energies*, vol. 10, no. 10, p. 1454, 2017.

- [113] D. Salomonsson and A. Sannino, “Low-voltage dc distribution system for commercial power systems with sensitive electronic loads,” *IEEE Transactions on Power Delivery*, vol. 22, no. 3, pp. 1620–1627, 2007.
- [114] T. Lambert, P. Gilman, and P. Lilienthal, “Micropower system modeling with homer,” *Integration of alternative sources of energy*, vol. 1, no. 1, pp. 379–385, 2006.
- [115] M. K. Shahzad, A. Zahid, T. ur Rashid, M. A. Rehan, M. Ali, and M. Ahmad, “Techno-economic feasibility analysis of a solar-biomass off grid system for the electrification of remote rural areas in pakistan using homer software,” *Renewable energy*, vol. 106, pp. 264–273, 2017.
- [116] G. Onbaşı, A. Williams, and S. Dhundhara, “Storage for community electricity: A comparison between batteries and mini pumped hydro,” in *Renewable Energy and Sustainable Buildings*, pp. 281–292, Springer, 2020.
- [117] S. Vendoti, M. Muralidhar, and R. Kiranmayi, “Techno-economic analysis of off-grid solar/wind/biogas/biomass/fuel cell/battery system for electrification in a cluster of villages by homer software,” *Environment, Development and Sustainability*, vol. 23, no. 1, pp. 351–372, 2021.
- [118] N. Kennedy, C. Miao, Q. Wu, Y. Wang, J. Ji, and T. Roskilly, “Optimal hybrid power system using renewables and hydrogen for an isolated island in the uk,” *Energy Procedia*, vol. 105, pp. 1388–1393, 2017.
- [119] Z. Chmiel and S. C. Bhattacharyya, “Analysis of off-grid electricity system at isle of eigg (scotland): Lessons for developing countries,” *Renewable Energy*, vol. 81, pp. 578–588, 2015.
- [120] M. T. Chaichan, H. A. Kazem, A. M. Mahdy, and A. A. Al-Waeely, “Optimal sizing of a hybrid system of renewable energy for lighting street in salalah-oman using homer software,” *International Journal of Scientific Engineering and Applied Science (IJSEAS)*, vol. 2, no. 5, pp. 157–164, 2016.
- [121] S. Ebrahimi, M. Jahangiri, H. A. Raiesi, and A. R. Ariae, “Optimal planning of on-grid hybrid microgrid for remote island using homer software, kish in iran,” *International Journal of Energy*, vol. 3, no. 2, pp. 13–21, 2019.

- [122] H. Shahinzadeh, M. Moazzami, S. H. Fathi, and G. B. Gharehpetian, "Optimal sizing and energy management of a grid-connected microgrid using homer software," in *2016 Smart Grids Conference (SGC)*, pp. 1–6, IEEE, 2016.
- [123] M. Nurunnabi and N. Roy, "Grid connected hybrid power system design using homer," in *2015 International Conference on Advances in Electrical Engineering (ICAEE)*, pp. 18–21, IEEE, 2015.
- [124] A. Tursi, "A review on biomass: importance, chemistry, classification, and conversion," *Biofuel Research Journal*, vol. 6, no. 2, pp. 962–979, 2019.
- [125] P. J. Verkerk, J. B. Fitzgerald, P. Datta, M. Dees, G. M. Hengeveld, M. Lindner, and S. Zudin, "Spatial distribution of the potential forest biomass availability in europe," *Forest Ecosystems*, vol. 6, no. 1, pp. 1–11, 2019.
- [126] M. Parikka, "Global biomass fuel resources," *Biomass and bioenergy*, vol. 27, no. 6, pp. 613–620, 2004.
- [127] J. Van Dam, A. Faaij, I. Lewandowski, and G. Fischer, "Biomass production potentials in central and eastern europe under different scenarios," *Biomass and Bioenergy*, vol. 31, no. 6, pp. 345–366, 2007.
- [128] K. Ericsson and L. J. Nilsson, "Assessment of the potential biomass supply in europe using a resource-focused approach," *Biomass and bioenergy*, vol. 30, no. 1, pp. 1–15, 2006.
- [129] Z. Wang *et al.*, "Does biomass energy consumption help to control environmental pollution? evidence from brics countries," *Science of the total environment*, vol. 670, pp. 1075–1083, 2019.
- [130] H. L. Chum, F. Nigro, R. McCormick, G. Beckham, J. Seabra, J. Saddler, L. Tao, E. Warner, and R. Overend, "Conversion technologies for biofuels and their use," *Bioenergy & Sustainability: Bridging the Gaps*, vol. 72, pp. 374–467, 2015.
- [131] K. Sartor, S. Quoilin, and P. Dewallef, "Simulation and optimization of a chp biomass plant and district heating network," *Applied Energy*, vol. 130, pp. 474–483, 2014.
- [132] N. T. Raj, S. Iniyan, and R. Goic, "A review of renewable energy based cogeneration technologies," *Renewable and Sustainable Energy Reviews*, vol. 15, no. 8, pp. 3640–3648, 2011.

A.2 Power Distribution to Lighting Setup - DC vs. AC

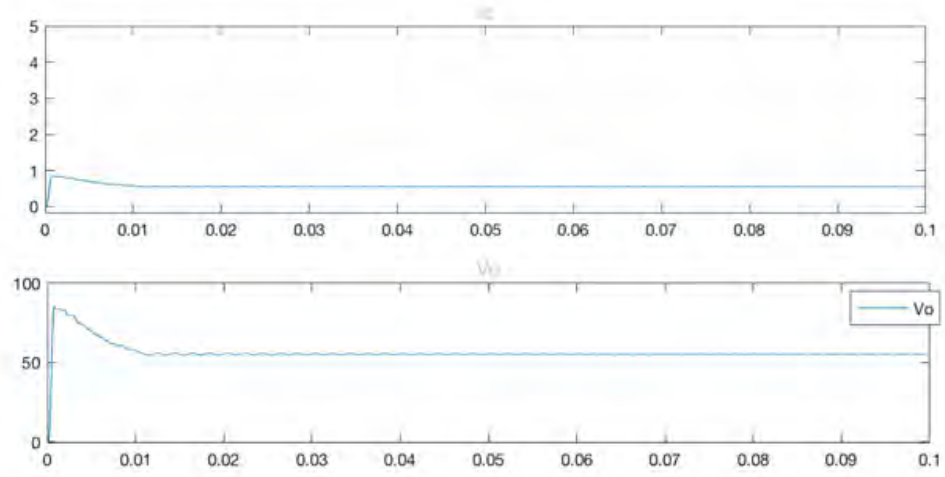


Figure A.1: Current vs time and Voltage vs time graph for the buck DC-DC converter.

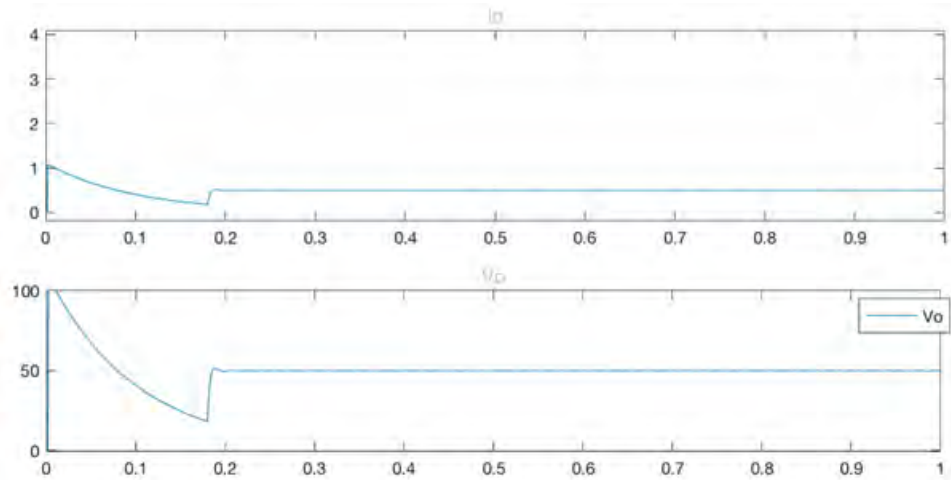


Figure A.2: Current vs time and Voltage vs time graph for the single phase rectifier and buck converter.

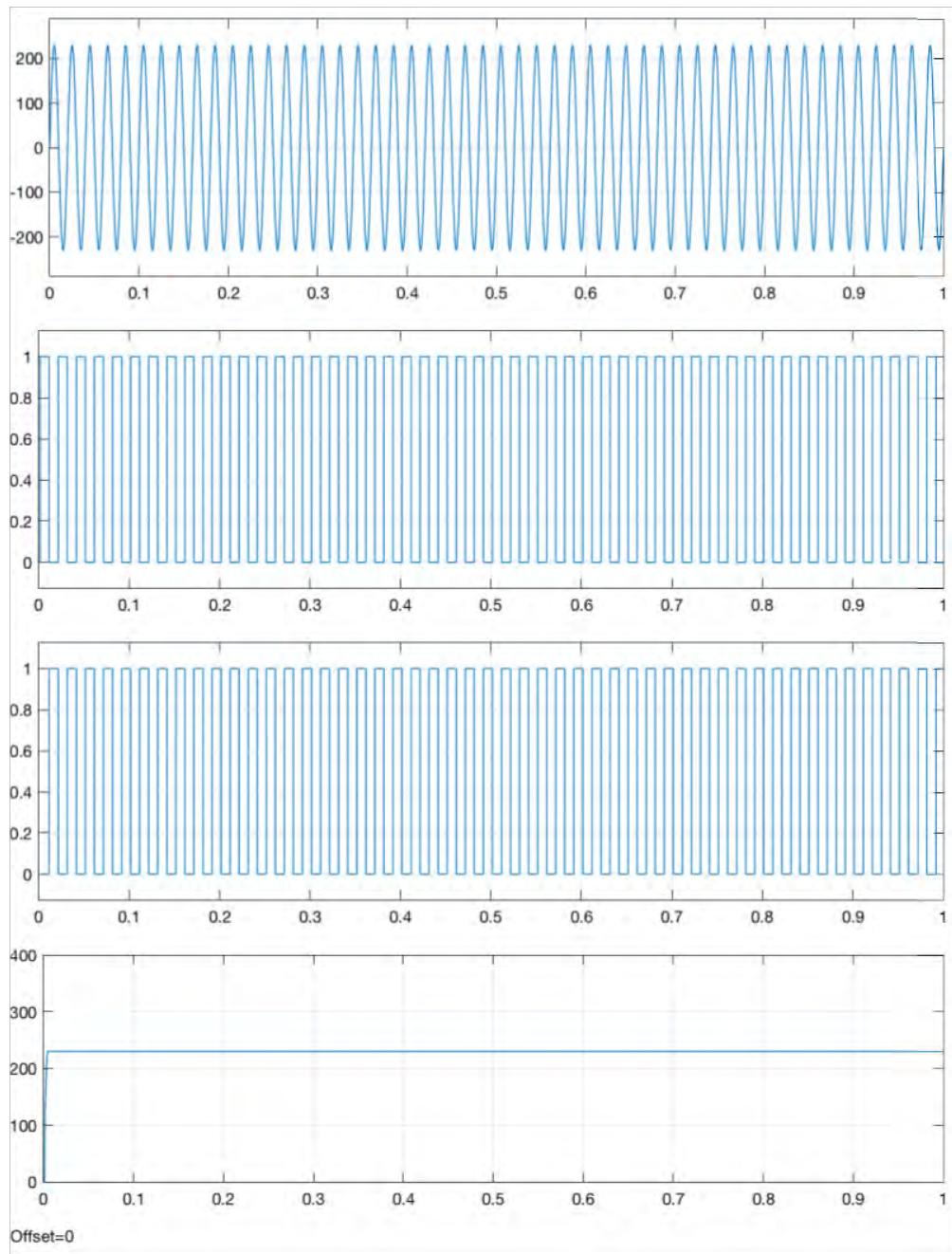


Figure A.3: Rectifier inputs, control signals, output.

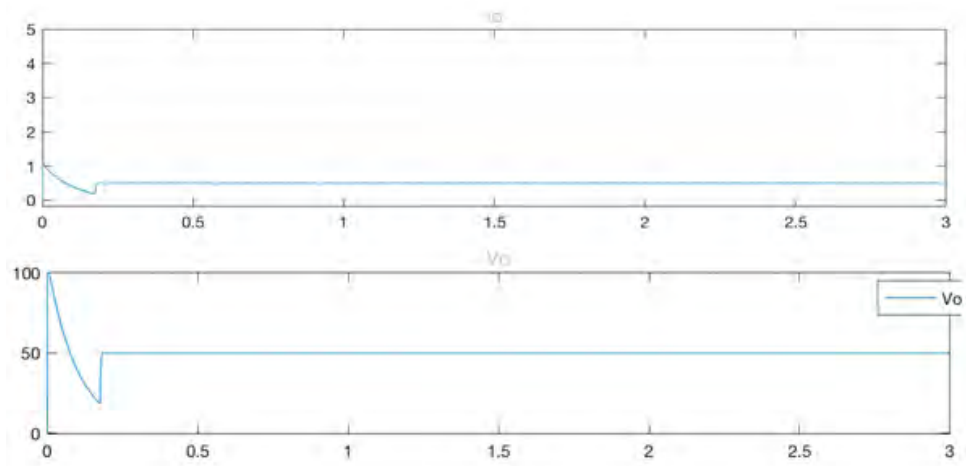


Figure A.4: Current vs time and Voltage vs time graph for the three phase rectifier and buck converter.

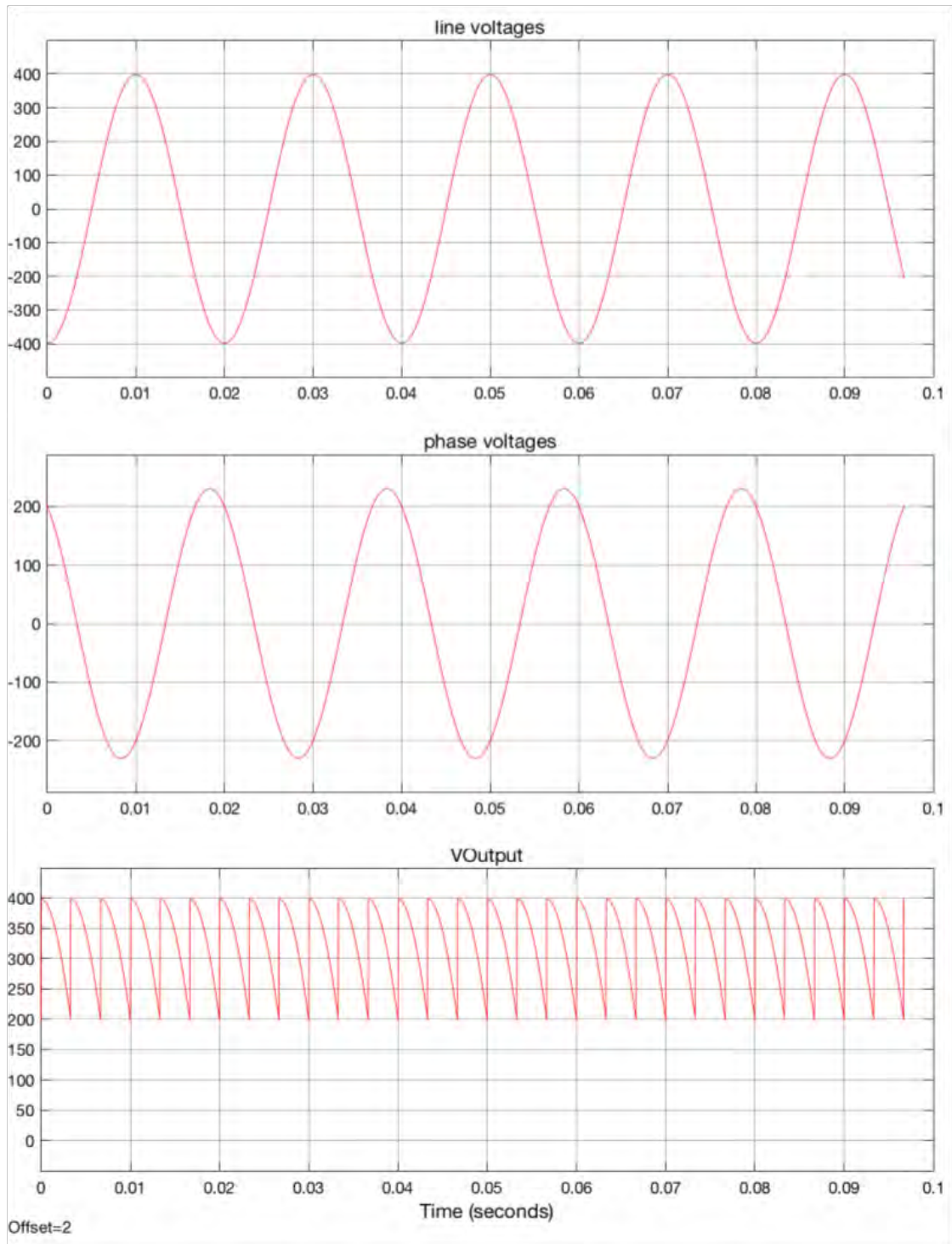


Figure A.5: Line to line, phase and output voltage of the three phase rectifier.

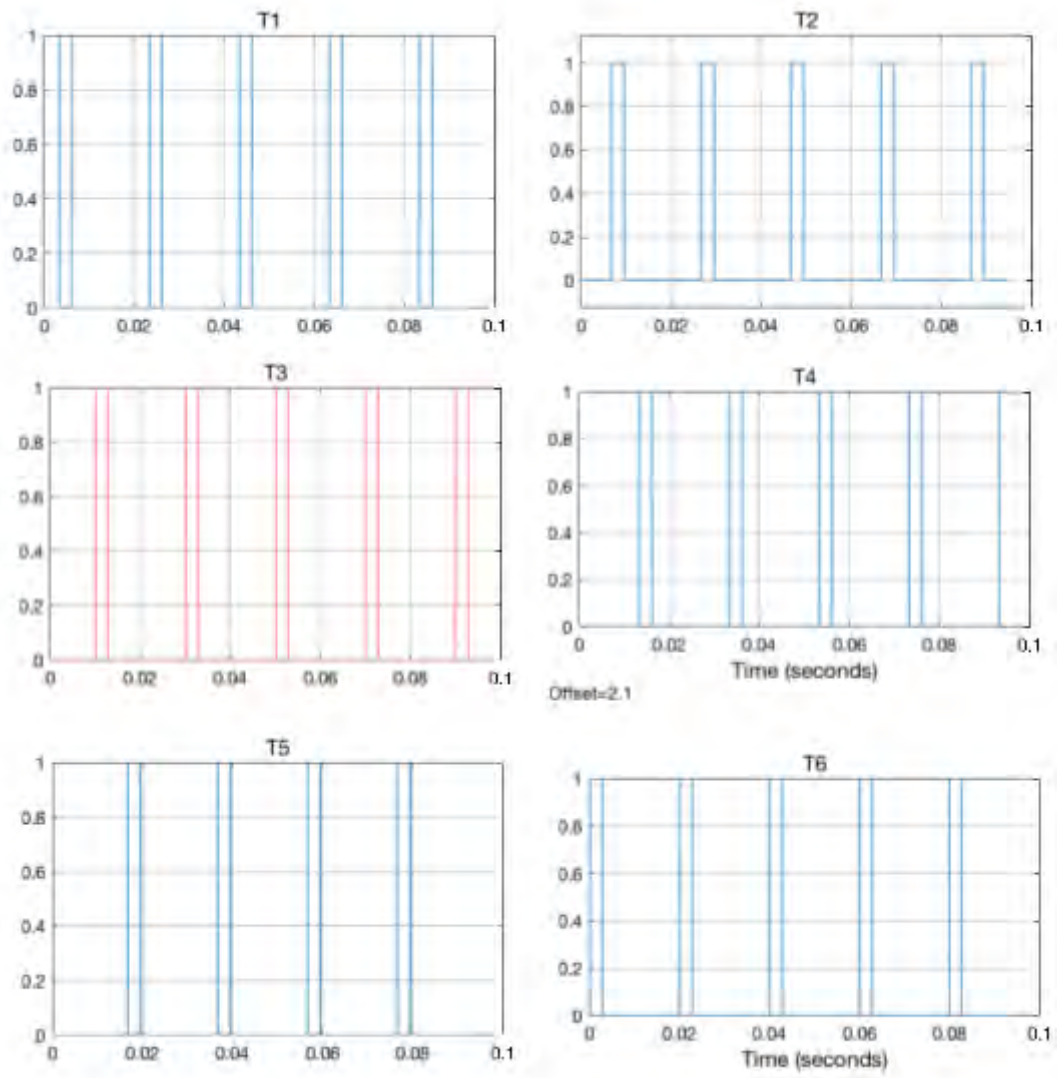


Figure A.6: Thyristor gate pulses for the three phase rectifier with buck converter.

A.3 Modelling Renewable Technology Integration into LED lit CEA systems

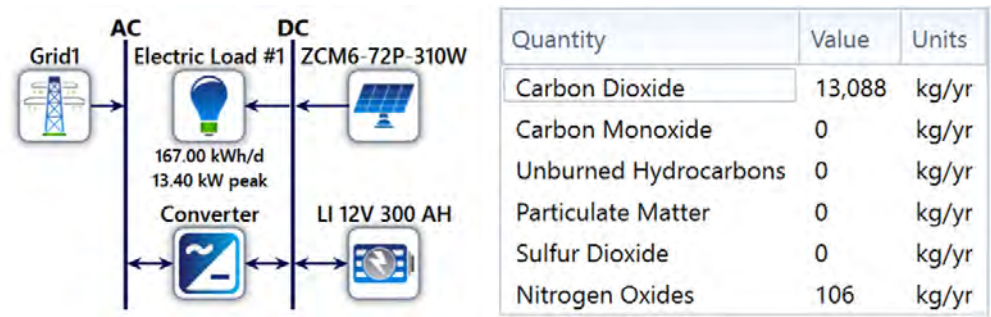


Figure A.7: Power setup schematic and emissions data for the grid connected PV and battery UoR case study sized system.

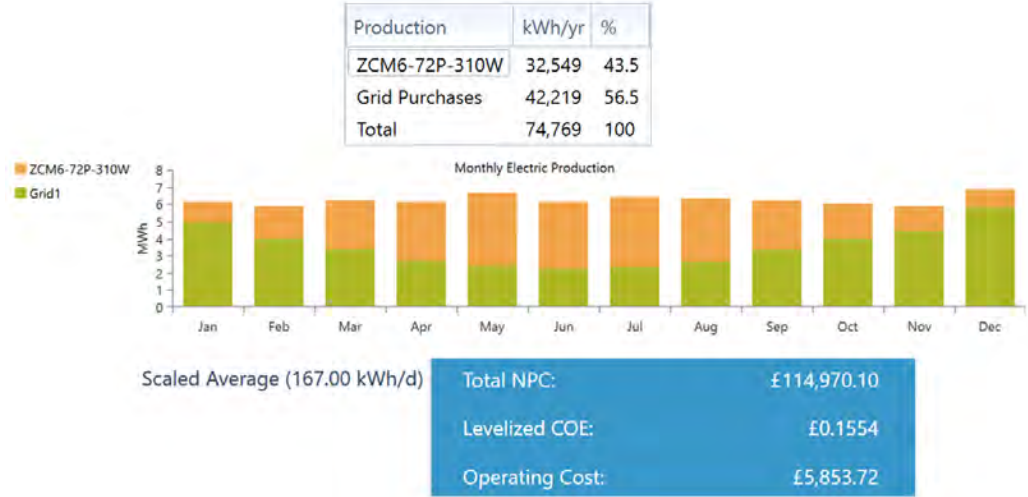


Figure A.8: Yearly and monthly electric production by energy source, NPC, LCOE and operating costs for the grid connected PV and battery UoR case study sized system.

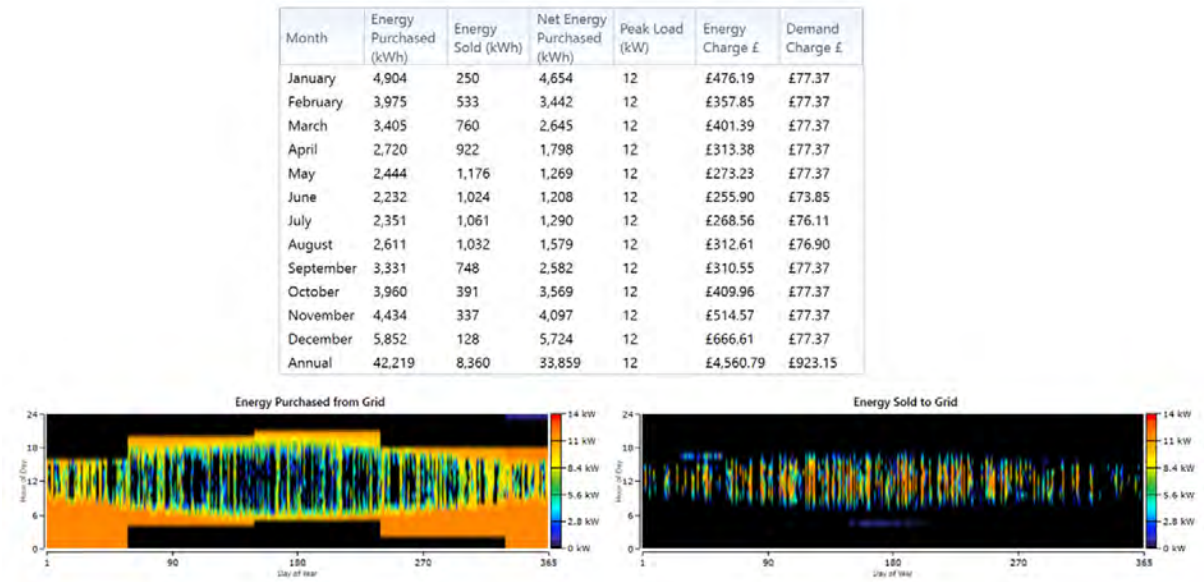


Figure A.9: Grid energy purchase and sell back information for the grid connected PV and battery UoR case study sized system.

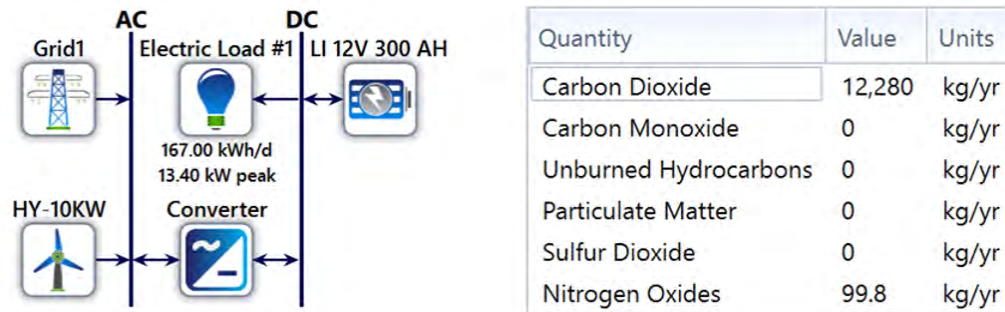


Figure A.10: Power setup schematic and emissions data for the grid connected wind and battery UoR case study sized system.

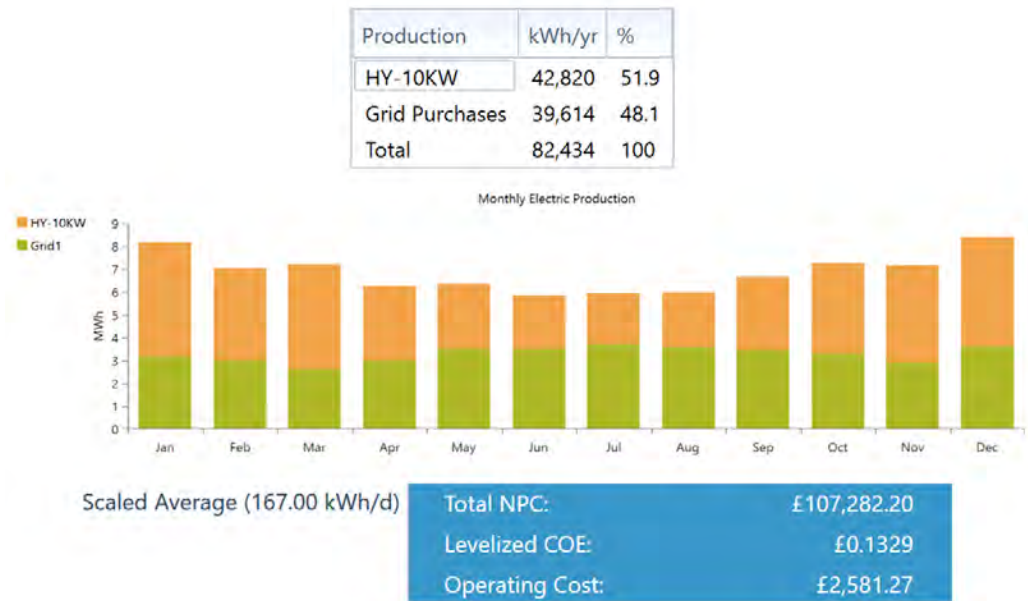


Figure A.11: Yearly and monthly electric production by energy source, NPC, LCOE and operating costs for the grid connected wind and battery UoR case study sized system.

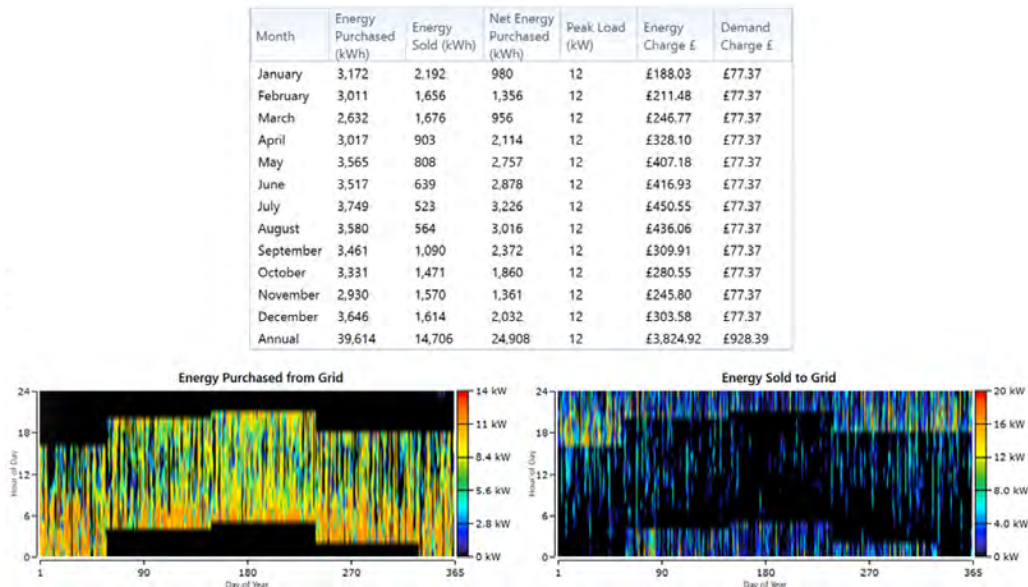


Figure A.12: Grid energy purchase and sell back information for the grid connected wind and battery UoR case study sized system.

Month	Energy Purchased (kWh)	Energy Sold (kWh)	Net Energy Purchased (kWh)	Peak Load (kW)	Energy Charge £	Demand Charge £
January	2,810	2,734	76	12	£114.04	£77.37
February	2,388	2,392	-4	12	£95.06	£77.37
March	1,691	2,767	-1,076	12	£63.60	£77.37
April	1,772	2,151	-379	12	£107.27	£77.37
May	1,803	2,076	-273	12	£124.04	£77.37
June	1,714	1,655	59	12	£137.49	£71.90
July	1,877	1,556	321	12	£161.24	£76.53
August	2,038	1,711	326	12	£183.86	£76.21
September	2,390	2,114	276	12	£125.32	£77.37
October	2,532	2,188	344	12	£146.24	£77.37
November	2,521	2,198	323	12	£161.36	£77.37
December	3,227	1,911	1,316	12	£236.13	£77.37
Annual	26,761	25,452	1,308	12	£1,655.65	£920.93

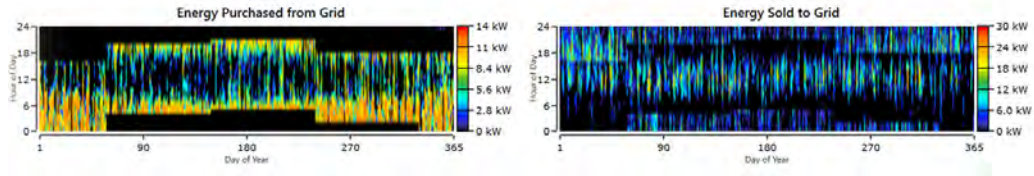


Figure A.13: Grid energy purchase and sell back information for the grid connected wind, PV and battery UoR case study sized system.

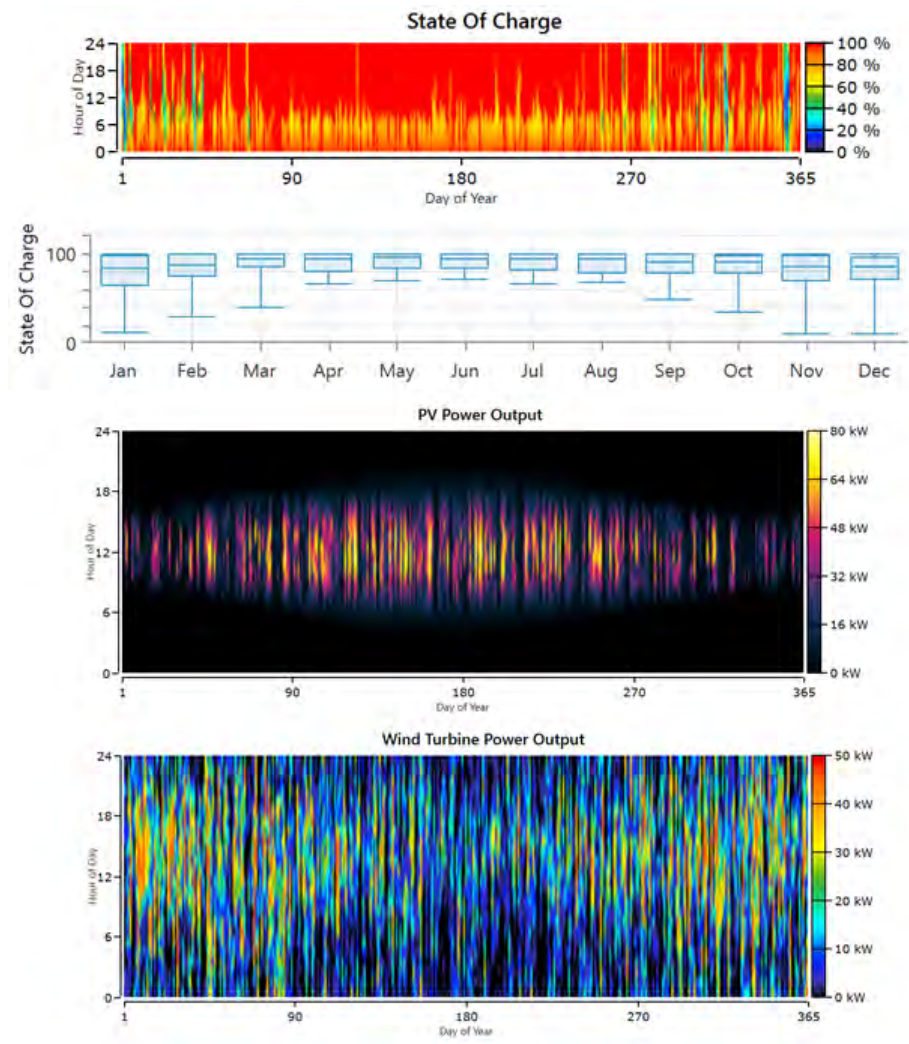


Figure A.14: Battery state of charge, PV power output and wind power output throughout the year for the off-grid wind, PV and battery UoR case study sized system.

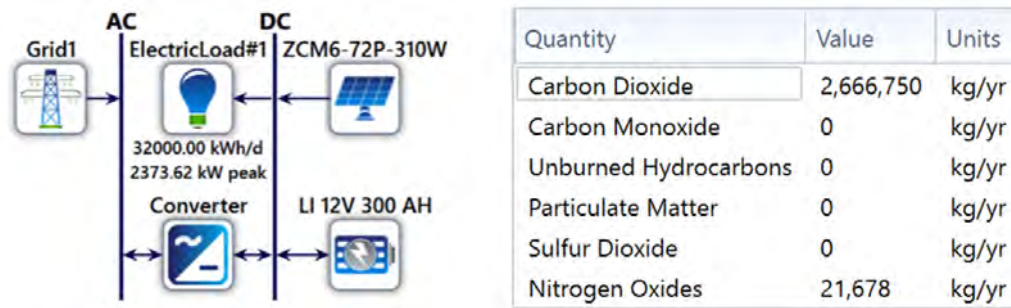


Figure A.15: Power setup schematic and emissions data for the grid connected PV and battery one hectare system.

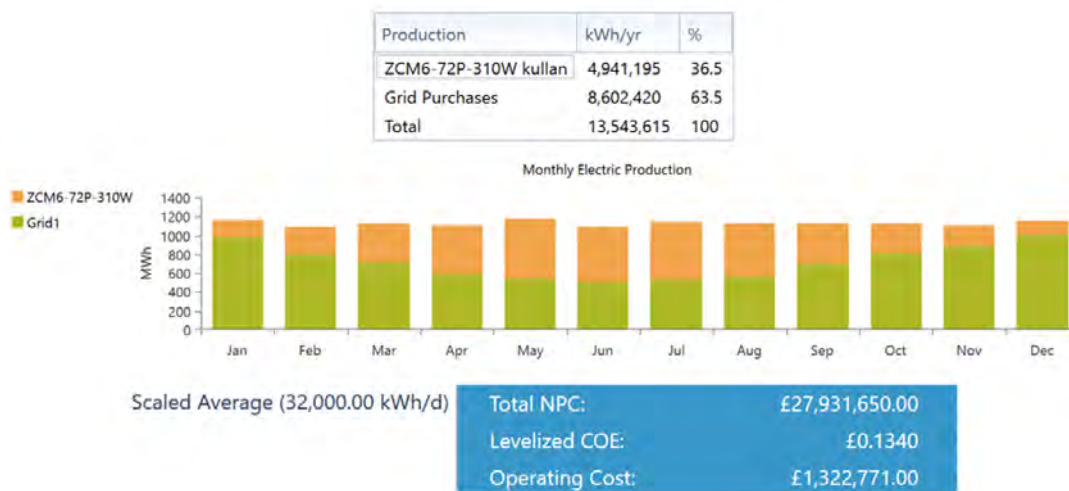


Figure A.16: Yearly and monthly electric production by energy source, NPC, LCOE and operating costs for the grid connected PV and battery one hectare system.

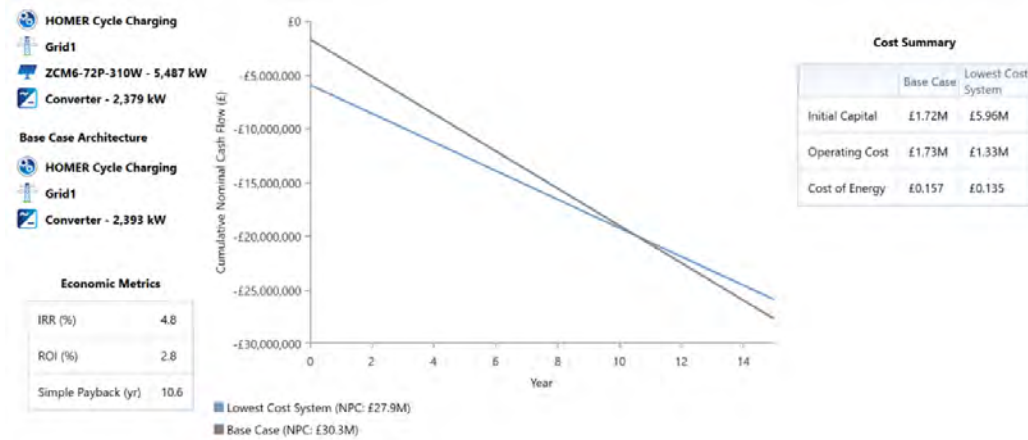


Figure A.17: Economic analysis of the grid connected PV and battery one hectare system in comparison to the base grid system throughout the 15 year project length.

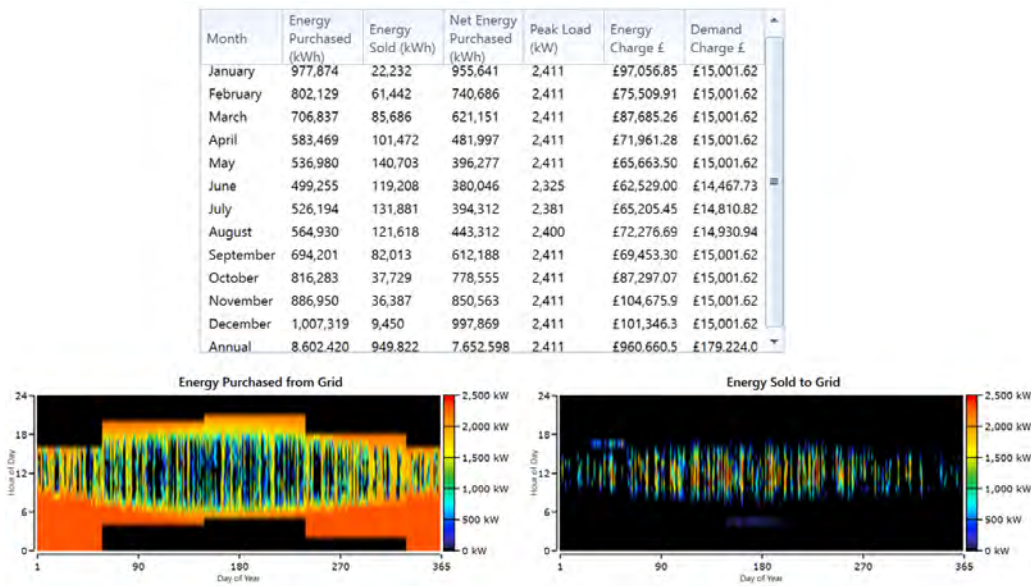


Figure A.18: Grid energy purchase and sell back information for the grid connected PV and battery one hectare system.

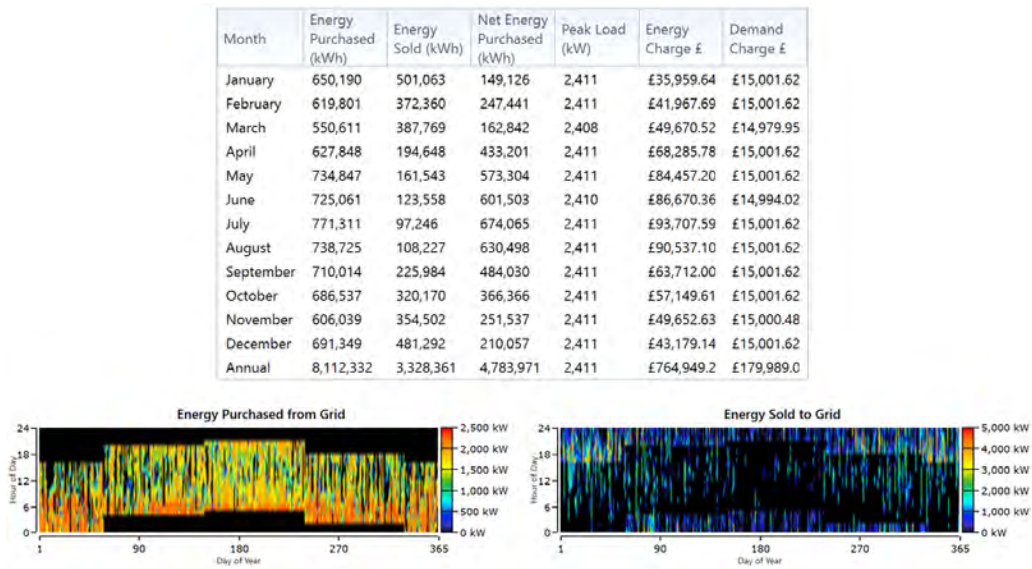


Figure A.19: Grid energy purchase and sell back information for the grid connected wind and battery one hectare system.

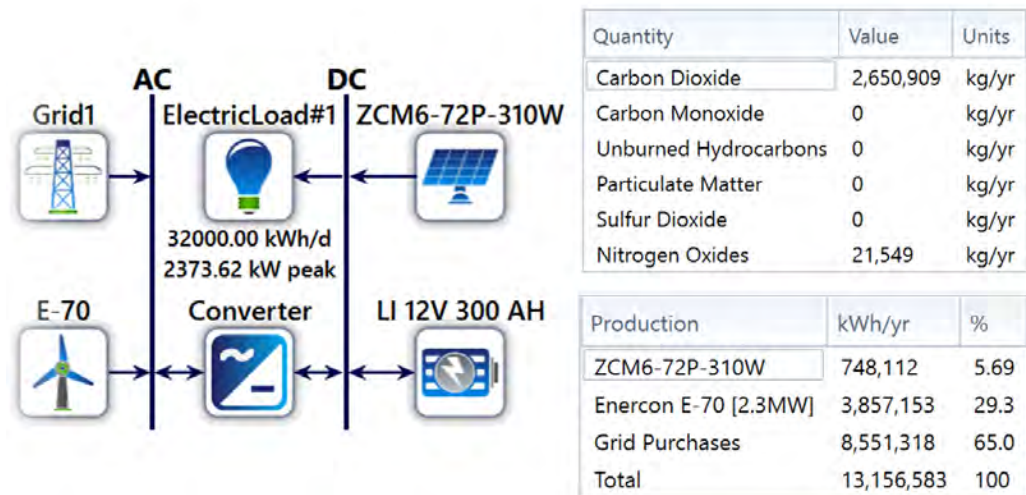


Figure A.20: Power setup schematic, emissions data and yearly energy production by source for the grid connected wind, PV and battery one hectare system.

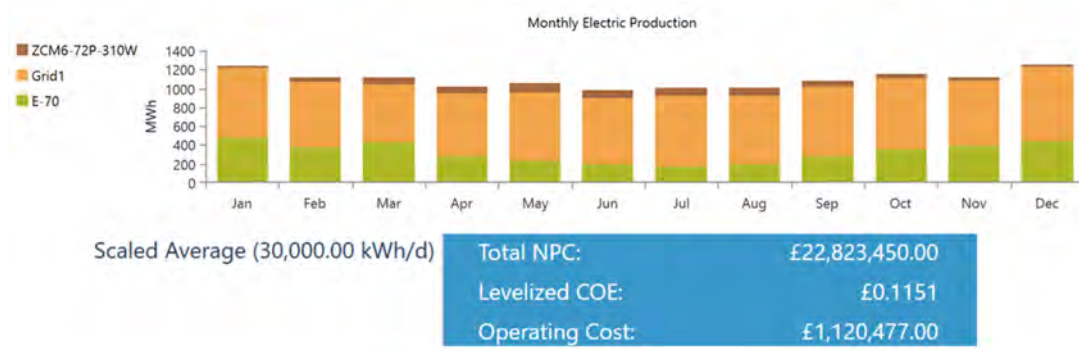


Figure A.21: Monthly electric production by energy source, NPC, LCOE and operating costs for the grid connected wind, PV and battery one hectare system.

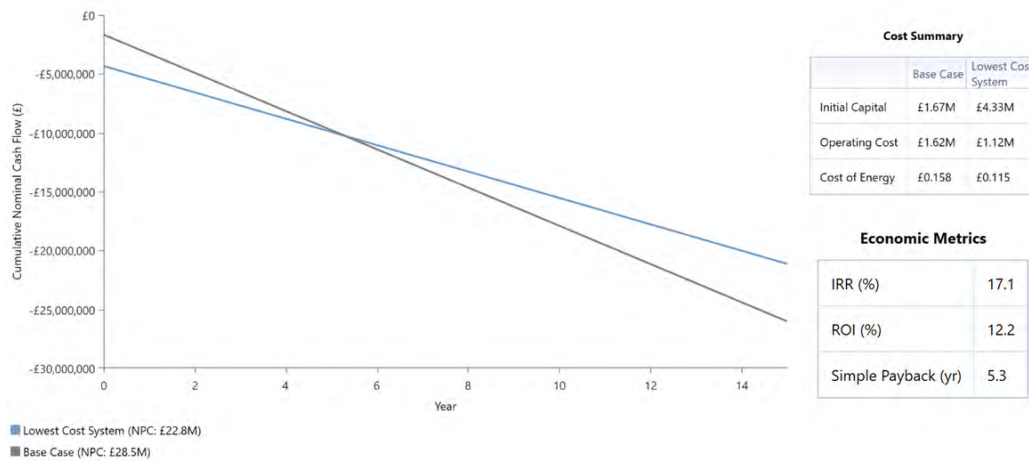


Figure A.22: Economic analysis of the grid connected wind turbine, PV and battery one hectare system in comparison to the base grid system throughout the 15 year project length.

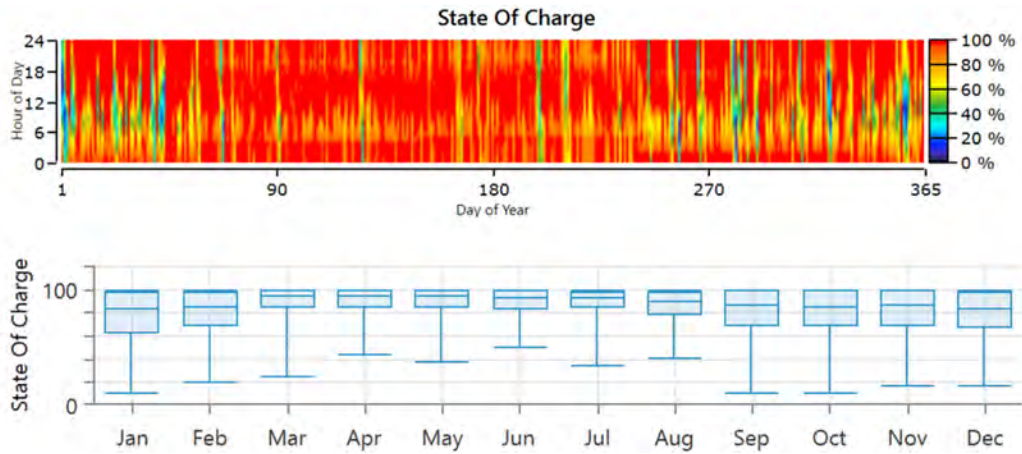


Figure A.23: Battery charge data for the off-grid wind turbine, PV and battery one hectare system.

Month	Energy Purchased (kWh)	Energy Sold (kWh)	Net Energy Purchased (kWh)	Peak Load (kW)	Energy Charge £	Demand Charge £
January	1,167,395	968,702	198,693	4,478	£60,429.22	£27,858.79
February	1,108,944	717,860	391,083	4,478	£72,038.78	£27,858.79
March	995,880	742,965	252,915	4,478	£87,811.58	£27,858.79
April	1,139,032	377,255	761,777	4,478	£122,524.5	£27,858.79
May	1,341,095	317,357	1,023,738	4,478	£152,903.6	£27,858.79
June	1,346,913	242,873	1,104,040	4,478	£160,477.2	£27,858.79
July	1,434,296	192,986	1,241,309	4,478	£173,694.7	£27,858.79
August	1,371,438	213,559	1,157,879	4,478	£167,732.7	£27,858.79
September	1,275,632	445,223	830,409	4,478	£111,989.3	£27,858.79
October	1,229,416	622,366	607,050	4,478	£99,323.34	£27,858.79
November	1,081,898	687,333	394,565	4,478	£85,225.37	£27,858.79
December	1,238,737	925,666	313,072	4,478	£73,690.42	£27,858.79
Annual	14,730,676	6,454,144	8,276,531	4,478	£1,367,841	£334,305.4

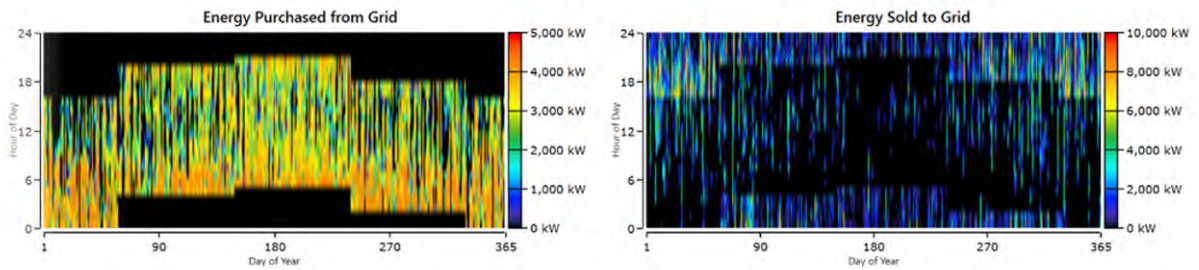


Figure A.24: Grid energy purchase and sell back information for the grid connected wind and battery two hectare system.

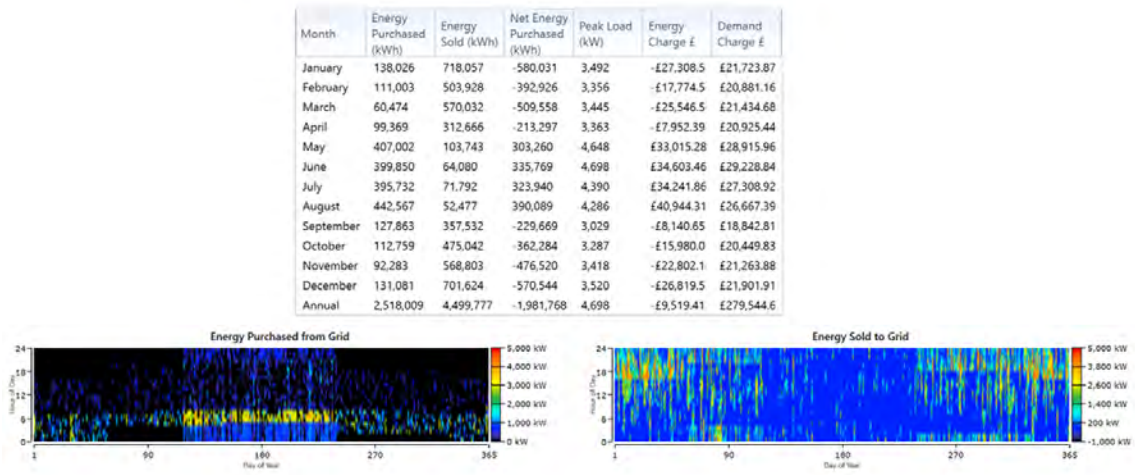


Figure A.25: Grid energy purchase and sell back information for the grid connected biomass CHP, wind and battery two hectare system with biogas 1.

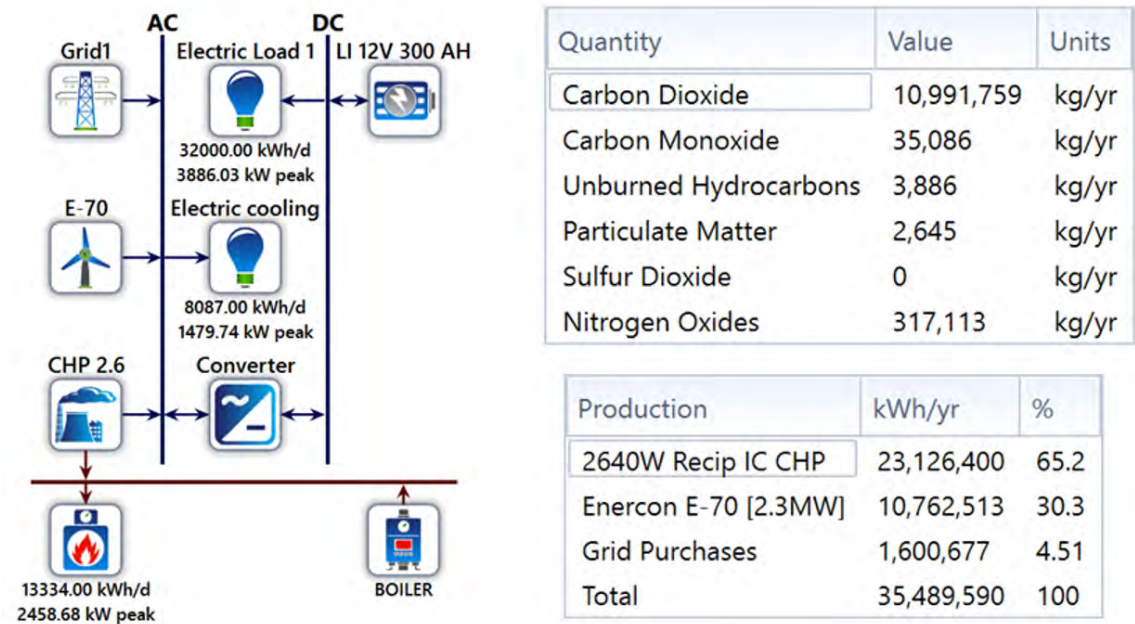


Figure A.26: Power setup schematic, emissions data and yearly electric production by source for the grid connected biomass CHP, wind and battery one hectare system with biogas 2.

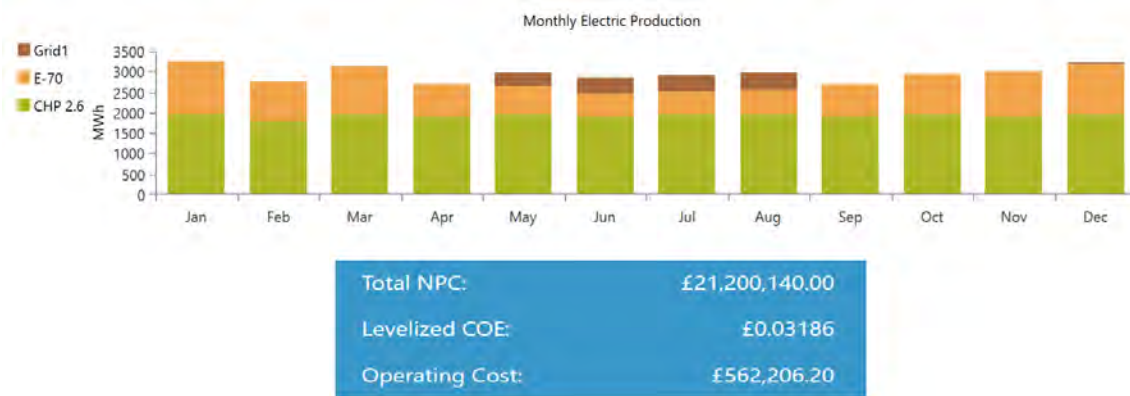


Figure A.27: Monthly electric production by energy source, NPC, LCOE and operating costs for the grid connected biomass CHP, wind and battery one hectare system with biogas 2.

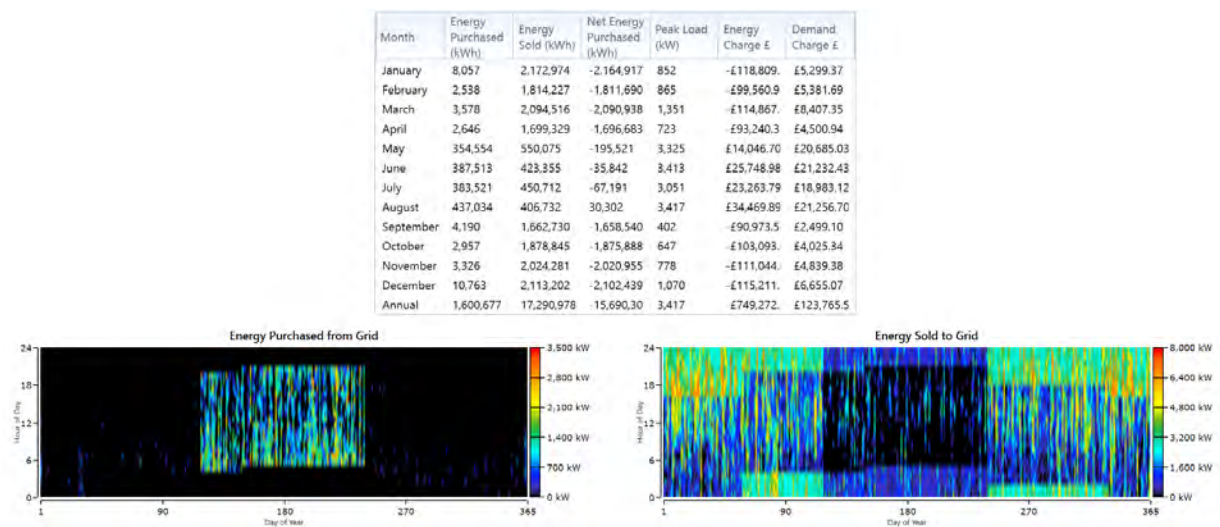


Figure A.28: Grid energy purchase and sell back information for the grid connected biomass CHP, wind and battery two hectare system with biogas 2.

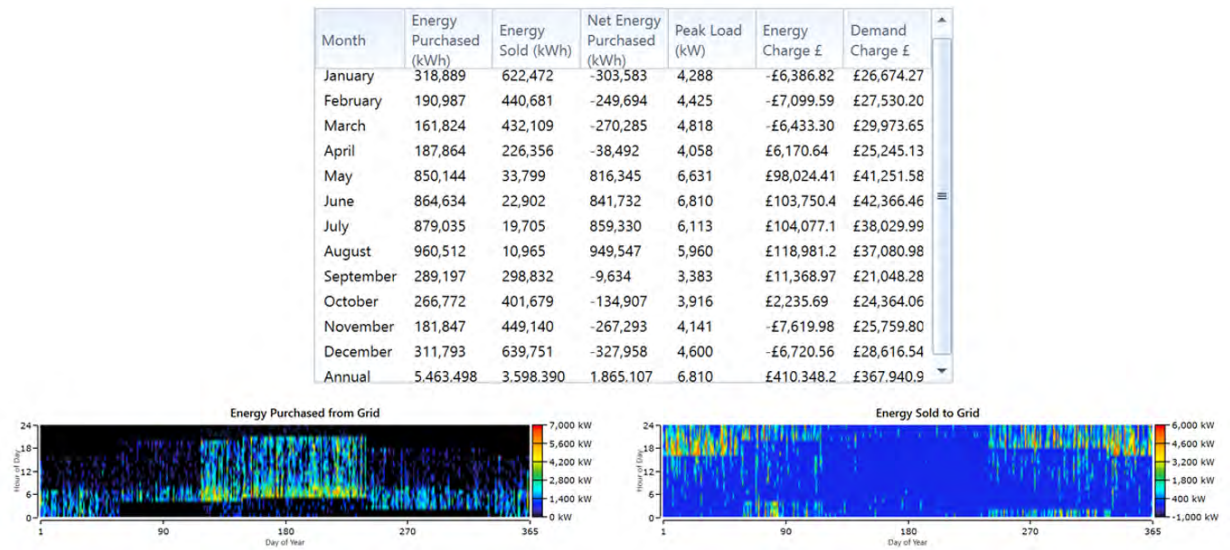


Figure A.29: Grid energy purchase and sell back information for the grid connected biomass CHP, wind and battery two hectare system.